History for Manuscript Number: RINENG-D-22-00804 oktarina heriyani (INDONESIA): "Perforated concave rectangular winglet pair vortex generators enhance the heat transfer of air flowing through heated tubes inside a channel"

Close

Correspondence History

Correspondence Date	Letter	Recipient	Revision
Oct 14, 2022	Editor Decision - Accept	oktarina heriyani, S.Si., M.T	1
Sep 23, 2022	Author Submits Revision Confirmation	oktarina heriyani, S.Si., M.T	1
Sep 23, 2022	PDF Built and Requires Approval	oktarina heriyani, S.Si., M.T	1
Sep 21, 2022	Author Revision Reminder - Before Due Date	oktarina heriyani, S.Si., M.T	1
Sep 18, 2022	Author Revision Reminder - Before Due Date	oktarina heriyani, S.Si., M.T	1
Sep 14, 2022	Author Revision Reminder - Before Due Date	oktarina heriyani, S.Si., M.T	1
Sep 11, 2022	Author Revision Reminder - Before Due Date	oktarina heriyani, S.Si., M.T	1
Sep 10, 2022	Author Requests Deadline Extension on Revision	noreply_EMsupport@elsevier.com	1
Sep 07, 2022	Author Revision Reminder - Before Due Date	oktarina heriyani, S.Si., M.T	1
Aug 24, 2022	Editor Decision - Revise	oktarina heriyani, S.Si., M.T	0
Jul 21, 2022	Author Notice of Manuscript Number	oktarina heriyani, S.Si., M.T	0
Jul 12, 2022	Author Submits New Manuscript Confirmation	oktarina heriyani, S.Si., M.T	0
Jul 12, 2022	PDF Built and Requires Approval	oktarina heriyani, S.Si., M.T	0

Close

Date: Jul 12, 2022
To: "oktarina heriyani" oktarina@uhamka.ac.id
From: "Results in Engineering" support@elsevier.com
Subject: Your PDF %ARTICLE_TITLE% has been built and requires approval

Dear Miss heriyani,

The PDF for your submission, "Perforated concave rectangular winglet pair vortex generators enhance the heat transfer of air flowing through heated tubes inside a channel" is ready for viewing.

This is an automatic email sent when your PDF is built. You may have already viewed and approved your PDF while on-line, in which case you do not need to return to view and approve the submission

Please go to https://www.editorialmanager.com/rineng/ to approve your submission.

Username: ********
If you do not know your confidential password, you may reset it by clicking this link: ********

Your submission must be approved in order to complete the submission process and send the manuscript to the Results in Engineering editorial office.

Please view the submission before approving it to be certain that your submission remains free of any errors.

Thank you for your time and patience.

Editorial Office Staff
Results in Engineering
https://www.editorialmanager.com/rineng/

#AU_RINENG#

To ensure this email reaches the intended recipient, please do not delete the above code

---

Date: Jul 12, 2022
To: "oktarina heriyani" oktarina@uhamka.ac.id
From: "Results in Engineering" support@elsevier.com
Subject: Submission Confirmation for %ARTICLE_TITLE%

Dear Miss heriyani,

Your submission entitled "Perforated concave rectangular winglet pair vortex generators enhance the heat transfer of air flowing through heated tubes inside a channel" has been received by journal Results in Engineering

You will be able to check on the progress of your paper by logging on to Editorial Manager as an author. The URL is https://www.editorialmanager.com/rineng/.

Your manuscript will be given a reference number once an Editor has been assigned.

Thank you for submitting your work to this journal.

Kind regards,

Results in Engineering

#AU_RINENG#

To ensure this email reaches the intended recipient, please do not delete the above code

---

Date:	Jul 21, 2022
To:	"oktarina heriyani" oktarina@uhamka.ac.id
cc:	"Mohammad Djaeni" moh.djaeni@live.undip.ac.id, "Aldila Kurnia Putri" aldilakurniaputri@gmail.com, "Syaiful Syaiful" syaiful.undip2011@gmail.com
From:	"Results in Engineering" support@elsevier.com
Subject:	A manuscript number has been assigned to %ARTICLE_TITLE%

Dear Miss heriyani,

Your submission entitled "Perforated concave rectangular winglet pair vortex generators enhance the heat transfer of air flowing through heated tubes inside a channel" has been been assigned the following manuscript number: RINENG-D-22-00804.

You will be able to check on the progress of your paper by logging on to Editorial Manager as an author. The URL is https://www.editorialmanager.com/rineng/.

Thank you for submitting your work to this journal.

Kind regards,

Antonio García, Ph.D
Editor in Chief
Results in Engineering

#AU_RINENG#

To ensure this email reaches the intended recipient, please do not delete the above code

---

In compliance with data protection regulations, you may request that we remove your personal registration details at any time. (Use the following URL: https://www.editorialmanager.com/rineng/login.asp?a=r). Please contact the publication office if you have any questions.

Date: Aug 24, 2022
To: "oktarina heriyani" oktarina@uhamka.ac.id
From: "Results in Engineering" support@elsevier.com
Subject: Your Submission

Ref.: Ms. No. RINENG-D-22-00804
Perforated concave rectangular winglet pair vortex generators enhance the heat transfer of air flowing through heated tubes inside a channel
Results in Engineering

Dear Miss heriyani,

Reviewers have now commented on your paper. You will see that they are advising that you revise your manuscript. If you are prepared to undertake the work required, I would be pleased to reconsider my decision.

For your guidance, reviewers' comments are appended below.

If you decide to revise the work, please submit a list of changes or a rebuttal against each point which is being raised when you submit the revised manuscript.

Please resubmit your revised manuscript by Sep 14, 2022.

To submit a revision, go to https://www.editorialmanager.com/rineng/ and log in as an Author. You will see a menu item call Submission Needing Revision. You will find your submission record there.

Yours sincerely

Ezio Mancaruso, Ph.D
Associate Editor
Results in Engineering

Comments from the Editors and Reviewers:

Your article would appear to be of interest to a wide engineering research community and in order to promote its visibility even more, may we recommend that you view the past published articles in Results in Engineering and if you find any relevant publications, CITE the article from this Journal.

Reviewer 1: Following are the few observations:
1. Author should add figure of location of thermocouple.
2. Heaters are placed after test section? How the heating of air takes place?
3. Details of perforations on rectangular and concave winglet is missing. pl add.
4. Provide details of validation of set up and heat loss analysis.
5. Mention pitch kept between two pins/winglet.
6. At lower Re both inline and staggered arrangement gives same result, while deviatio 3 observed after Re 8000. Author has to justify.
7. Provide more clarification about 1,2 & 3 pairs.
8. Compare the PRWP and PCRWP with without perforation.
9. Discuss how number of pairs contribute in improving TEF

Reviewer 2: This paper presented experimental results of the heat transfer, pressure drop and thermal performance characteristics of the perforated concave rectangular winglet pair vortex generators on plates in rectangular ducts to increase the heat transfer through the six heated tubes to the air stream. Perforated concave rectangular winglets were compared with perforated rectangular winglet pairs vortex generator mounted on rectangular plates. The subject of the article falls within the scope of the Results in Engineering. In my view, unless the paper is rewritten in a proper way, I think it is inadequate to be published in a scientific journal in its present state. I would like to provide the following comment:

1. There are many spelling and grammar mistakes in this paper, and many sentences are not easy to follow. The grammar and structure of sentences in this paper need to be modified carefully, such as the title of the article. The language of this paper need to be improved by a native English speaker.
2. The velocity ranges studied are given in the Abstract, whereas the Reynolds number ranges studied should be given.
3. Please review the keywords and add a few, for instance heat transfer, thermal performance.
4. The method section can be expanded.
5. The arrangement of vortex generators is given in Figure 2, but Figure 2 is not sufficient for a clear understanding of the construction of vortex generators. Additional figures should be drawn which clearly show the construction of vortex generators and the in-line and staggered arrangement.
6. Thermal characteristics are given in terms of the convective heat transfer coefficient (h), friction characteristics are given in terms of pressure drop. Why are thermal characteristics not given in terms of Nusselt number (Nu) and friction characteristics in terms of coefficient of friction (f)?
7. It is not specified how the hydraulic diameter (Dh) is calculated. How the Reynolds number (Re) was calculated is not specified.
8. No correlation (Nu-Re), (f-Re) is given.
9. Error analysis is given, but uncertainty analysis is not done.

Reviewer 3: In connection with climate change and an increase in the average annual temperature on Earth, there is a new danger of the negative impact of high temperatures on human life.
In this case, the improvement of air conditioning systems, including the search for the best thermal enhancement factor, cost-benefit ratio, etc., takes on a new sense, which is one of the main targets of this article. The topic is timely and of great practical significance to environmental protection, enhancing safety, and people's life comfort.
The manuscript is well-structured and includes all necessary parts.
Two key strengths of the paper are a good introduction section and an analysis and discussion of the results. Both research objectives and content are clear. The key scientific issues to be solved are moderate. The research experimental method is reasonable.

There are also several shortages worthy to be mentioned:
1. Seriously revise the formulas
a) If you use an italic font in formulas, use an italic font in their descriptions. For example, in formula (1), the Nusselt number (Nu) and friction factor (f); in formula (3), heat transfer coefficient (h). It may confuse the reader.
b) The Nusselt numbers in formula (1) and formula (2) have different designations. It may confuse the reader.
c) What are Nusselt number and friction factor with subscript 0 in formula (1)?
d) In formula (5), a pressure drop is the lowercase letter Δp, but in formula (6), a pressure drop is uppercase ΔP. Are these different pressures?
2. What is the error of pressure drop measurement with the Fluke 922 Airflow Micromanometer described in section "3.2 Effect of perforated vortex generators on pressure drop"? Did it cover the necessary range of pressures to be investigated? Could micromanometer error have affected the conclusions of the section? Because the pressure drop values of 4.58 Pa, 5 Pa and 5.4 Pa are close to each other.
3. The measurement error in the section "3.3 Effect of perforated VGs on thermal enhancement factor" and "Effects of perforated VGs on the cost-benefit ratio" is not clear. Can you show the error bar or describe it in the description?

4. In my humble opinion, the section "3.5 Flow visualisation" is better presented first in section "3. Results and Discussion".

As a result, the article appears to be a qualified research paper. The results presented are consistent with the aims and scope of the journal. But now the article needs a major revision with correction of formulas and clarification of measurement errors.

#AU_RINENG#

To ensure this email reaches the intended recipient, please do not delete the above code

---

Date: Sep 23, 2022
To: "oktarina heriyani" oktarina@uhamka.ac.id
From: "Results in Engineering" support@elsevier.com
Subject: Submission Confirmation for %MS_NUMBER%

Ref.: Ms. No. RINENG-D-22-00804R1
Perforated concave rectangular winglet pair vortex generators enhance the heat transfer of air flowing through heated tubes inside a channel

Dear Miss heriyani,

Results in Engineering has received your revised submission.

You may check the status of your manuscript by logging onto Editorial Manager at (https://www.editorialmanager.com/rineng/).

Kind regards,

#AU_RINENG#

To ensure this email reaches the intended recipient, please do not delete the above code

---

In compliance with data protection regulations, you may request that we remove your personal registration details at any time. (Use the following URL: https://www.editorialmanager.com/rineng/login.asp?a=r). Please contact the publication office if you have any questions.

Date: Oct 14, 2022
To: "oktarina heriyani" oktarina@uhamka.ac.id
From: "Ezio Mancaruso" ezio.mancaruso@stems.cnr.it
Subject: Your Submission

Ref.: Ms. No. RINENG-D-22-00804R1
Perforated concave rectangular winglet pair vortex generators enhance the heat transfer of air flowing through heated tubes inside a channel
Results in Engineering

Dear Miss heriyani,

I am pleased to tell you that your work has now been accepted for publication in Results in Engineering.

It was accepted on Oct 14, 2022

Comments from the Editor and Reviewers can be found below.

Thank you for submitting your work to this journal.

With kind regards

Ezio Mancaruso, Ph.D
Associate Editor
Results in Engineering

Comments from the Editors and Reviewers:

Reviewer 2: Dear Editor,

I reviewed the revised manuscript.

The authors have made most of the corrections I have asked of them. Therefore, the manuscript can be accepted for publication.

Kind regards,

Reviewer 3: The authors responded to all questions of interest, provided missing data, and corrected deficiencies. After the review, I recommend the article for publication in the journal.

Eligible for a waiver?

If your manuscript was transferred from an Elsevier subscription journal and submitted in this open

access journal before 31 December 2022, you do not have to pay the article publishing charge (APC). We will waive the APC.

How to get your APC waived?
Please use this webform to contact our support team:
https://service.elsevier.com/app/contact/supporthub/publishing/

You can then expect the following:
1. You will receive a voucher code upon successful validation.
2. You will receive an email with a link to the Rights and Access form.
3. Enter the voucher code in the Rights and Access form, in the Publishing options step and complete the form.

Important note:
Please complete the Rights and Access Form within 14 days of receipt of the link to the form. An open access invoice will be sent to you if you don't complete the Rights and Access form.

#AU_RINENG#

To ensure this email reaches the intended recipient, please do not delete the above code

---

Author's Response To Reviewer Comments

Close

Dear Editors and Reviewer
Thank you for your letter and for the reviewers' comments concerning our manuscript entitled "Perforated concave rectangular winglet pair vortex generators enhance the heat transfer of air flowing through heated tubes inside a channel" (Manuscript Number: Rineng-D-22-00804R1). The comments are all valuable and very helpful to revise and improve our paper, as well as significant guidelines for our research. We have learned comments carefully and have made the correction that we hope you meet with your approval. We have included the parts requested to be revised in the manuscript. Revised portions are marked in red in the revised paper. The main correction in papers and responses to reviewing comments is flowing.
Reviewer 1: Following are the few observations:
Author should add figure of location of thermocouple.

Thank you very much for the proposal. I've revised Figure 1 because I made a mistake in captioning the figure. One thermocouple is placed in the air inlet area, six thermocouples on the back surface of the tubes, and 15 on the outlet side of the wire, as observed in Figure 1.

Heaters are placed after test section? How the heating of air takes place?

Thanks for the question. The heater is connected to six tubes with each tube getting the same power. The total heating power of 40 W is induced in the six tubes by a regulator. Heating air flowing through the tubes occurs by convection. So that the air at the outlet side becomes hotter than that from the inlet side.

Details of perforations on rectangular and concave winglet is missing. pl add.
Thank you for the correction. I have added in the paper the detailed geometry of the perforated rectangular winglet (PRW) and perforated concave rectangular winglet (PCRW) vortex generators (VGs), as shown in Figure 2.

Perforated RWP Perforated CRWP

VGs have dimensions of the same length and width of 30 mm and have 36 holes. The bore diameter on the VGs is 2.5 mm. The distance between the holes is 5 mm from the center of the holes.

Provide details of validation of set up and heat loss analysis.
Set up validation
Thank you for your suggestion. The current study is a follow-up investigation of the w[illegible] of Yafid et al [1]. The experimental set-up of this study is similar to that of Yafid et al. experiment. The difference between the current study and the experiment of Yafid et al. is a test object where the current study uses concave rectangular winglet (CRW) VGs, while the work of Yafid et al. uses concave delta winglet (CDW) VGs. Whitaker et al. [2] studied the heat transfer characteristics of airflow through a single cylinder in a rectangular duct. To confirm the results of the experiment

Yafid et al. are valid, the same experimental set-up is determined. The Nu value from the experiment of Yafid et al. compared with Nu values from the experiments of Whitaker et al. in the Reynolds number range of 2,143 to 11,763, as shown in the figure below.

From the figure, it can be observed that Nu from the experimental results of Yafid et al. have the same trend as the experiments of Whitaker et al.

b. Heat Loss analysis
Heat loss analysis is carried out by taking into account the convection heat transfer from the six tubes to the surrounding fluid flow. Calculation of the heat transfer rate is carried out for two types of flow, namely laminar flow and turbulent flow.
The calculation of heat loss in this experiment is determined by calculating the difference between the induced electric power and the total heat through convection from the surface of the tubes to the fluid. In this experiment, six tubes in a wind tunnel are heated by a heater with a power of 40 W. In this work, the velocity of the inlet fluid is varied from 0.4 to 2 m/s at intervals of 0.2 m/s or in the Reynolds number range from 2,143 to 11,763. Based on the Reynolds number range, two types of flow are determined, namely laminar and turbulent. Therefore, the heat loss was determined from the correlation between laminar at 0.4 m/s and turbulent for other velocities.
The described formulas Nu, h, and q were used to determine the heat loss in the conduit of the six tubes.

$$Nu=(q\ D_h)/(A_{tube}\ [\![\Delta T]\!]_{LMTD}\ k) \quad (2)$$

$$h=q/(A_{tube}\ [\![\Delta T]\!]_{LMTD}\ ) \quad (3)$$

$$q=\dot{m}\ c_p\ (T_{out}-T_{in}\ ) \quad (4)$$

Where D_h, A_tube, $[\![\Delta T]\!]_{LMTD}$, $\dot{m}$, c_p, T_out, T_in, are hydraulic diameter, tube surface area, log mean temperature difference, mass flow rate, specific heat, outlet temperature, and inlet temperature.

$$D_h=\ [\![4A]\!]_c/P \quad (5)$$

$$[\![\Delta T]\!]_{LMTD}= ((\bar{T}_{tube}-\bar{T}_{out}\ )-(\bar{T}_{tube}-\bar{T}_{in}\ ))/\ln[(\bar{T}_{tube}-\bar{T}_{out}\ )-(\bar{T}_{tube}-\bar{T}_{in}\ )] \quad (6)$$

Where A_c dan T_tube are channel surface area and tube temperature, respectively.
The experimental data for hydraulic diameter D_h,, tube surface area A_tube, channel surface area A_c, and air specific heat c_p are 0.09223 m, 0.02338908 m2, 0.01056 m2, and 1.007 J/kgK, respectively. The following is a table for calculating the heat loss baseline.

Table 1 Heat Loss Baseline

baseline v (m/s)	Re	Mass flow rate (kg/s)	Density (kg/m3)	Dynamics viscous (kg/ms)	k	Pr	T inlet (C)	T outlet (C)	T tube (C)	ΔT LMTD	ΔT (T tube - T inlet)	Nu	h (W/mK)	q conv (W)	q input (W)	q loss (W)
0.4	2165	0.004757	1.13	1.9.E-05	0.03	0.73	29	33	50	19	21	155	45	19.48	40	20.52
0.6	3291	0.00719	1.13	1.9.E-05	0.03	0.73	28	31	46	16	18	174	50	18.98	40	21.02
0.8	4413	0.009618	1.14	1.9.E-05	0.03	0.03	28	30	44	15	16	192	50	19.19	40	20.81
1	5545	0.012056	1.14	1.9.E-05	0.03	0.73	28	30	43	14	15	214	55	19.84	40	20.16
1.2	6661	0.014477	1.14	1.9.E-05	0.03	0.73	28	29	43	14	15	228	61	21.15	40	18.85
1.4	7826	0.016958	1.15	1.9.E-05	0.03	0.73	28	29	41	12	13	247	70	20.30	40	19.70
1.6	8965	0.019407	1.15	1.9.E-05	0.03	0.73	27	29	40	12	13	263	75	21.03	40	18.97
1.8	10110	0.021863	1.15	1.9.E-05	0.03	0.73	27	28	39	12	12	296	84	22.54	40	17.46
2	11272	0.024341	1.15	1.9.E-05	0.03	0.73	27	28	38	11	11	342	97	24.17	40	15.83

In the table 1, it can be seen that the greater the velocity with the increase in Re number, the

lower the heat loss. It can be seen that the heat flow from the heater does not only spread into the tube, but convection occurs to the outside of the tube. Heat output increases with increasing Re. That is, the higher the flow velocity, the greater the turbulence through the silinder and the higher the turbulence intensity. An increase in turbulence intensity between a cold airflow and a hot cylinder with constant surface temperature is caused by the airflow velocity [3]. In row-tube arrays, this recirculation area increases for the second and subsequent columns. A lower air velocity in the circulation region indicates less airflow in that region participating in the local heating process [4]. The heat loss of all conditions in this experiment is shown in table 2 below.

Table 2 Calculation of heat loss for the whole case

type VGs	q conv (W)	q input (W)	q loss (W)
Baseline	20.74	40	19.26
PCRWPI1	25.15	40	14.85
PCRWPI2	27.55	40	12.45
PCRWPI3	27.61	40	12.39
PCRWPS1	26.43	40	13.57
PCRWPS2	26.43	40	13.57
PCRWPS3	27.94	40	12.06
PRWPI1	24.09	40	15.91
PRWPI2	27.25	40	12.75
PRWPI3	28.82	40	11.18
PRWPS1	23.94	40	16.06
PRWPS2	26.37	40	13.63
PRWPS3	28.12	40	11.88

Table 2 shows that the lowest heat loss occurs when three sets of PCRWPs are staggered. The placement of the VGs can increase heat transfer in square ducts as the VGs create longitudinal vortices that increase vortex strength in the wake region downstream of the tube. Longitudinal vortices make the overall temperature field more uniform, improve heat mixing and boundary layer modification, and improve heat transfer performance. A higher number of vortex generators creates more longitudinal vortices and greatly increases heat transfer [5], [3].

Mention pitch kept between two pins/winglet.
Thank you for the question. I've added Figure 3 (in the paper) showing the pitch between VGs for both inline and staggered configurations.

CRWP in-line CRWP staggered

RWP in-line RWP staggered

CRWP in-line CRWP staggered

RWP in-line RWP staggered

At lower Re both inline and staggered arrangement gives the same result, while deviation is observed after Re 8000. The author has to justify.

Thank you for your suggestion. In Figure 7(a) (in the paper), the convection heat transfer coefficient for the case of PRW VGs in-line has the same value as that of PCRW VGs in-line or staggered in a pair of VGs. In one pair of VGs, the longitudinal vortex is generated after the flow hits the VGs and weakens (He et al., 2013). This is in contrast to two and three pairs of VGs where the longitudinal vortex produced after striking the first VGs has amplified again when the flow strikes the second VGs and so on. Therefore, the value of the heat transfer coefficient in the case of a pair of PRW VGs has the same value as that of PCRW VGs at Reynolds numbers above 8,000.

Provide more clarification about 1,2 & 3 pairs.
Thank you for your suggestion. This study describes the cases of PCRW and PRW VGs for one, two, and three pairs. I have added explanations for cases one, two, and three pairs of perforated VGs to the paper.
For PRW and PCRW VGs in-line configurations with one, two, and three pairs are shown in Figures 4. For one pair, the VGs are placed on the left and right sides of the first row of tubes. VGs are placed on the first and third row tubes for two pairs. As for the three pairs, VGs are placed on the first, third, and fifth row tubes.

one pair PCRW inlline two pairs PCRW inline

three pairs PCRW inline

one pair PRW inline two pairs PRW inline

three pairs PRW inline
Figure 4. VGs pairs in-line configurations

For PRW and PCRW VGs staggered configurations with one, two, and three pairs are shown in Figures 5. For one pair, the VGs are placed on the right side of the first row tube and the left side of the second row tube. VGs are placed on the right side of the first, third row tubes and on the left side of the second and fourth tubes for two pairs. As for the three pairs, the VGs are placed on the right side of the first, third, fifth row of tubes and on the left side of the second, fourth and sixth tubes.

one pair PCRW staggered two pairs PCRW staggered

three pairs PCRW staggered

one pair PRW staggered two pairs PRW staggered

three pairs PRW staggered

Figure 5. VGs pairs staggered configurations

Compare the PRWP and PCRWP with without perforation.
Thank you for your request. In this study, an experiment was conducted to compare PRW VGs and PCRW VGs in improving heat transfer in a rectangular channel, as shown in Figures 7 to 9.

Comparison of convection heat transfer coefficient values.
Figure 7 provides a comparison of the convection heat transfer coefficients for PRW and PCRW. It can be seen that there was an increase in the convection heat transfer coeeficient with a rise in Re due to an increase in flow vortices and high turbulence intensity in the channel [6], a' 3 side a reduction in the wage region and stagnation area for each increase in flow velocity [7]. The increase in heat transfer for staggered VGs was better than in-line for PCRW VGs with any number of pairs at the highest Re (11,000). The results in Figure 7 show that the PCRWP VGs worked better than the PRWP VGs, and the staggered arrangement of the former with three pairs gave the highest yield, of 153.5 W/m2.K, as shown in Figure 7(c). Meanwhile, two PCRW pairs (137.33

W/m2.K, Figure 7(b)) were better than one (132.25 W/m2.K, Figure 7(a)) because VGs with a concave surface destabilise the centrifugal force of the fluid flow, which strengthens the flow vortices. This makes the mixing of the hot fluid near the wall with the cold fluid of the main flow more robust [8].

Pressure drop comparison
In general, the highest pressure drop was observed using PCRWP VGs with staggered configuration for all Reynolds numbers except for one pair of VGs, as shown in Figure 8. The highest pressure drop was found in PRWP VGs with in-line configuration at Reynolds numbers greater than 8,000. The pressure drop on the staggered VGs was found to be higher than that of the in-line due to the shorter distance between the VGs of the staggered configuration than that of the in-line [5].

TEF comparison
TEF is the thermal-hydraulic performance which is the ratio of the increase in heat transfer to the pressure drop ratio. In general, the highest TEF was observed in the use of PCRWP VGs with staggered configuration, as depicted in Figure 9. PCRW creates wider flow vortices that can reduce the wake area behind the cylinder. Reducing the wake area can reduce the recirculation zone. This affects the increased heat transfer from the back of the cylinder to the stream [3]. A large radius, high intensity antrior-posterior vortex can reduce the wake area. A reduction in the wake area increases the flow velocity behind the tube and reduces the recirculation area, resulting in an increased heat transfer in this area [9], [10].

CBR comparison
A low value of CBR means a more economical value from the use of VGs. In general, CBR on the use of PCRWP VGs with staggered configuration is the best, as informed in Figure 10. The lowest CBR value results were obtained with three pairs of staggered type VGs PCRW. Three pairs of VGs lower CBR than one and two VG pairs. This is because the installation of three pairs VGs results in a higher Nusselt number increase than one and two pairs VGs, resulting in a lower pressure drop increase and therefore a lower CBR. These results show that lower CBR improves thermal performance relative to resistivity [11].

Discuss how number of pairs contribute in improving TEF

Thank you for your question. Figure 9 shows the effect of the number of pairs and configuration of VGs on TEF, this is also found in Ref. (He et al., 2013), (Sun et al., 2020), and (Ranjan et al., 2022).

One pair

Two pairs

Three pairs
From the experimental results, as shown in Figure 9, the TEF with three pairs of VGs for both inline and staggered was the highest. The TEF for the case of 3 pairs of PCRWs was 5.02% greater than that of one and two pairs of PRWP VGs. The main reason is because the concave surface of the PCR causes the flow to be thrown away due to the centrifugal force which results in a stronger flow vorticity [12]. Larger and stronger flow vortices can reduce the recirculation zone which has an impact on increasing heat transfer from the rear surface of the tube to the flow [10]. The presence of flow that is formed in each gap between the VGA and the tube causes the TEF in the staggered configuration to be greater than that of the in-line [13]. The increase in TEF for the three-pair case with the staggered configuration was 1.50% and 4.91% greater than that of the inline PCRWP and PRWP, respectively.

Reference
[1] Y. Effendi, A. Prayogo, Syaiful, M. Djaeni, and E. Yohana, "Effect of perforated concave delta winglet vortex generators on heat transfer and flow resistance through the heated tubes in the channel," Experimental Heat Transfer, vol. 35, no. 5, pp. 553–576, 2022, doi:

10.1080/08916152.2021.1919245.
[2] S. Whitaker, "Forced Convection Heat Transfer Correlations for Flow In Pipes, Past Flat Plates, Single e Cylinders, Single Spheres, and for Flow In Packed Beds and Tube Bundles," Reprillted from AIChE JOURNAL, 1972.
[3] M. Awais and A. A. Bhuiyan, "Enhancement of thermal and hydraulic performance of compact finned-tube heat exchanger using vortex generators (VGs): A parametric study," International Journal of Thermal Sciences, vol. 140, pp. 154–166, Jun. 2019, doi: 10.1016/J.IJTHERMALSCI.2019.02.041.
[4] A. J. Modi and M. K. Rathod, "Experimental investigation of heat transfer enhancement and pressure drop of fin-and-circular tube heat exchangers with modified rectangular winglet vortex generator," Int J Heat Mass Transf, vol. 189, p. 122742, Jun. 2022, doi: 10.1016/J.IJHEATMASSTRANSFER.2022.122742.
[5] Y. L. He, P. Chu, W. Q. Tao, Y. W. Zhang, and T. Xie, "Analysis of heat transfer and pressure drop for fin-and-tube heat exchangers with rectangular winglet-type vortex generators," Appl Therm Eng, vol. 61, no. 2, pp. 770–783, Nov. 2013, doi: 10.1016/J.APPLTHERMALENG.2012.02.040.
[6] M. Pranita Hendraswari, M. S. Tony, and M. F. Soetanto, "Heat Transfer Enhancement inside Rectangular Channel by Means of Vortex Generated by Perforated Concave Rectangular Winglets," 2021, doi: 10.3390/fluids6010043.
[7] Syaiful, A. R. Siwi, T. S. Utomo, Yurianto, and R. Wulandari, "Numerical analysis of heat and fluid flow characteristics of airflow inside rectangular channel with presence of perforated concave delta winglet vortex generators," International Journal of Heat and Technology, vol. 37, no. 4, pp. 1059–1070, 2019, doi: 10.18280/IJHT.370415.
[8] A. Sinha, H. Chattopadhyay, A. K. Iyengar, and G. Biswas, "Enhancement of heat transfer in a fin-tube heat exchanger using rectangular winglet type vortex generators," Int J Heat Mass Transf, vol. 101, pp. 667–681, Oct. 2016, doi: 10.1016/J.IJHEATMASSTRANSFER.2016.05.032.
[9] A. Gupta, A. Roy, S. Gupta, and M. Gupta, "Numerical investigation towards implementation of punched winglet as vortex generator for performance improvement of a fin-and-tube heat exchanger," Int J Heat Mass Transf, vol. 149, p. 119171, Mar. 2020, doi: 10.1016/J.IJHEATMASSTRANSFER.2019.119171.
[10] Y. Li, Z. Qian, and Q. Wang, "Numerical investigation of thermohydraulic performance on wake region in finned tube heat exchanger with section-streamlined tube," Case Studies in Thermal Engineering, vol. 33, p. 101898, May 2022, doi: 10.1016/J.CSITE.2022.101898.
[11] M. W. Tian, S. Khorasani, H. Moria, S. Pourhedayat, and H. S. Dizaji, "Profit and efficiency boost of triangular vortex-generators by novel techniques," Int J Heat Mass Transf, vol. 156, p. 119842, 2020, doi: 10.1016/j.ijheatmasstransfer.2020.119842.
[12] H. Naik and S. Tiwari, "Thermodynamic performance analysis of an inline fin-tube heat exchanger in presence of rectangular winglet pairs," Int J Mech Sci, vol. 193, no. September 2020, p. 106148, 2021, doi: 10.1016/j.ijmecsci.2020.106148.
[13] L. O. Salviano, D. J. Dezan, and J. I. Yanagihara, "Thermal-hydraulic performance optimization of inline and staggered fin-tube compact heat exchangers applying longitudinal vortex generators," Appl Therm Eng, vol. 95, pp. 311–329, Feb. 2016, doi: 10.1016/J.APPLTHERMALENG.2015.11.069.

Reviewer 2: This paper presented experimental results of the heat transfer, pressure drop and thermal performance characteristics of the perforated concave rectangular winglet pair vortex generators on plates in rectangular ducts to increase the heat transfer through the six heated tubes to the air stream. Perforated concave rectangular winglets were compared with perforated rectangular winglet pairs vortex generator mounted on rectangular plates. The subject of the article falls within the scope of the Results in Engineering. In my view, unless the paper is re 3 ten in a proper way, I think it is inadequate to be published in a scientific journal in its present state. I would like to provide the following comment:
There are many spelling and grammar mistakes in this paper, and many sentences are not easy to follow. The grammar and structure of sentences in this paper need to be modified carefully, such as the title of the article. The language of this paper need to be improved by a native English speaker.

Thank you for your suggestion. To improve grammar and structure, I have sent this paper to elsevier service for proof reading.

The velocity ranges studied are given in the Abstract, whereas the Reynolds number ranges studied should be given.
Thank you for your correction. In this experiment, the intake air velocity is in the range of 0.4 to 2 m/s at intervals of 0.2 m/s or in the Reynolds number range of 2.143 to 11.763. I have included the Reynolds number range in the abstract.

Please review the keywords and add a few, for instance heat transfer, thermal performance.
Thank you for your suggestion. The keywords for this study are vortex generators, heat transfer, thermal-hydraulic performance, economic benefit. I've added keywords in the paper.

The method section can be expanded.
Thank you for your suggestion. I have improved this research method in the paper.
Based on Fig. 1, the rectangular channel is equipped with a blower (50 Hz, Wipro with a rated voltage of 220V), an inverter (Mitsubishi Electric type FR-D700 with an accuracy of 0.01), straightener, hot wire anemometer (Lutron type AM-4204 with an accuracy of 0.1), wattmeter (Lutron DW-6060 with an accuracy ± 1.0), central processing unit (CPU), micromanometer, thermocouple (K type with a temperature interval of -200 −1250℃ and an accuracy ± 0.5) where one thermocouple was placed in the air inlet area, six thermocouples on the back surface of the tubes and 15 on the outlet side of the wire, data acquisition (Advantech USB-4718 type with an accuracy of 0.001) and heater regulator. The heater was connected to six tubes with a diameter of 19.05 mm and height of 65.8 mm, with each tube having the same power. Total heating power of 40 W was applied to the six tubes using a regulator. The heating air flowing through the tubes occurs via convection. Thus, the air at the outlet side becomes hotter than that at the inlet side. A pressure micromanometer (Fluke type 922, with an accuracy of ± 0.05) was used to monitor the flow pressure drop. Two pitot tubes, each set 26 cm ahead of the inlet of the test specimen and 2.5 cm behind it, were connected to a micromanometer to measure the pressure drop. The pressure drop measurements were recorded 30 times for 5 sekon at each speed variation. Furthermore, flow visualisation was performed by directing the smoke from vaporised fluid in the fluid vaporator into the mainflow.

The arrangement of vortex generators is given in Figure 2, but Figure 2 is not sufficient for a clear understanding of the construction of vortex generators. Additional figures should be drawn which clearly show the construction of vortex generators and the in-line and staggered arrangement.
Thank you for your suggestion. The following shows the construction of vortex generators inline and staggered (figure 2, 4 and 5 in the paper).

Figure 2. Geometry of the VGs
For PRW and PCRW VGs in-line configurations with one, two, and three pairs are shown in Figures 4. For one pair, the VGs are placed on the left and right sides of the first row of tubes. VGs are placed on the first and third row tubes for two pairs. As for the three pairs, VGs are placed on the first, third, and fifth row tubes.

one pair PCRW inlline two pairs PCRW inline

three pairs PCRW inline

3

one pair PRW inline two pairs PRW inline

three pairs PRW inline
Figure 4. VGs pairs in-line configurations

For PRW and PCRW VGs staggered configurations with one, two, and three pairs are shown in Figures 5. For one pair, the VGs are placed on the right side of the first row tube and the left side of the second row tube. VGs are placed on the right side of the first, third row tubes and on the left side of the second and fourth tubes for two pairs. As for the three pairs, the VGs are placed on the right side of the first, third, fifth row of tubes and on the left side of the second, fourth and sixth tubes.

one pair PCRW staggered two pairs PCRW staggered

three pairs PCRW staggered

one pair PRW staggered two pairs PRW staggered

three pairs PRW staggered

Figure 5. VGs pairs staggered configurations

Thermal characteristics are given in terms of the convective heat transfer coefficient (h), friction characteristics are given in terms of pressure drop. Why are thermal characteristics not given in terms of Nusselt number (Nu) and friction characteristics in terms of coefficient of friction (f)?

Thank you for your correction. h versus Re and P vs Re are used instead of Nu - Re and f - Re in this experiment because, in the TEF calculation, the value of Nu represents the value of h resulting from the equation in formula 3 (in the paper), thus

$h=(N_u\ k)/D_h$ (3)

Figure 7 (in the paper) that h rises as Re rises shows that the Nu increases as Re rises, where h rises as Re rises [1]. While f in this experiment represents the ΔP as shown in the following formula

$f=(2\ \Delta P\ D_h)/(\rho\ V^2\ (L+6D))$ (8)

Formula 8 states that the friction factor (f) in the flow rate is determined by using the pressure drop (ΔP) characteristic where increasing the Reynolds number in figure 8 will decrease the friction factor [2].
The following are examples of several studies that use h as a representative of Nu and (ΔP) as a representative of f.
The experimental results of Yafid et al indicate that perforated VGs can increase the heat transfer rate and decrease the pressure drop using the parameters h, ΔP, and TEF as shown in the following graph[3].

Al Asadi et al represents heat transfer coefficient and pressure drop to show the results of their investigation that the addition of span wise gap variations can increase heat transfer performance and reduce pressure drop [4], as shown in the figure below.

3

Increased heat transfer in heat sinks, Zhang et al described the micro gap by pairing more VGs which resulted in a larger heat transfer coefficient and a reduced pressure drop value [5], as shown in the figure below.

Hosseinirad et al showed that the increase in heat transfer coefficient and pressure drop vs. Reynold number had a tendency to increase with the increase in Re to evaluate heat transfer [6]. There is an increase in heat transfer with an increase in Re which is indicated by an increase in the heat transfer coefficient and an increase in pressure drop along with an increase in Re.

It is not specified how the hydraulic diameter (Dh) is calculated. How the Reynolds number (Re) was calculated is not specified.

Thank you for your corrections. The calculation of the hydraulic diameter in this experiment uses a rectangular air duct with a side length of a = 0.165 m and a side width of b = 0.064 m with the resulting Dh of 0.0106 from the following formula.
$D_h=(4A_c)/p=4ab/2(a+b) =2ab/(a+b)$ (5)

The result of Dh is used to calculate Re with the formula
$Re=(\rho u_{in} D_h)/\mu$ (7)
With u_in of 0.4 – 2 m/s with an interval of 0.2 m/s, on the physical properties of air at a pressure of 1 atm and is the viscosity of the fluid so that Re used in this experiment ranges from 2,143 – 11,763.
No correlation (Nu-Re), (f-Re) is given.

Thank you for the correction. In this experiment, Nu – Re and f – Re are not shown but use h vs Re and ΔP vs Re because the Nu value represents the value of h that arises in this experiment as in equation 4 (in the manuscript)

$h=(N_u k)/D_h$ (3)

While f in this experiment represents the ΔP as shown in the following formula

$f=(2 \Delta P D_h)/(\rho V^2 (L+6D))$ (8)

The formula states that the friction factor (f) in the flow rate is determined by using the pressure drop (ΔP) characteristic where increasing the Reynolds number in figure 8 will decrease the friction factor [2].

Error analysis is given, but uncertainty analysis is not done.

Thank you for the correction. In the following, uncertainty analysis calculation data will be shown for the temperature at base line conditions with a velocity of 0.4 m/s as shown in Table 3 below.
Table 3 Base-line test temperature data at a speed of 0.4 m/s

T (Tube1)	T (Tube2)	T (Tube3)	T (Tube4)	T (Tube5)	T (Tube6)
49.19093	51.21368	48.32313	49.76915	47.80219	51.27142
49.1834	51.17728	48.3156	49.79053	47.7657	51.2639
49.14545	51.16826	48.30655	49.7526	47.7856	51.25489
49.12105	51.17277	48.28214	49.72821	47.76118	51.2594
49.15297	51.20465	48.28515	49.73122	47.73524	51.2624
49.09966	51.15141	48.28967	49.73573	47.76871	51.26691
49.09815	51.14991	48.23029	49.73423	47.73826	51.29428
49.08912	51.14089	48.25019	49.66739	47.72922	51.22751

From these data, it is found that $\bar{T}_{Tube}$ can be calculated by the equation as
$\bar{T}_{Tube}=(\bar{T}_{Tube1}+\bar{T}_{Tube2}+\bar{T}_{Tube3}+\bar{T}_{Tube4}+\bar{T}_{Tube5}+\bar{T}_{Tube6})/6=49.56℃$ (11)
Then, the average standard deviation is obtained by the following formula.

$s_{tube}=\sqrt{((\Sigma_{i=1}^{N}(T_{tubei}-\bar{T}_{tube})^2)/N(N-1))}=0.029$ (12)
Therefore, the average T_tube can be written as 49.5 ± 0.029℃. $\bar{T}_{out}$ calculation results

obtained 32.95℃. The average standard deviation was calculated using the following equation:
s_Tout=√((Σ_(i=1)^N▒(T_outi-T ̄_out)^2)/N(N-1))=0,051 (13)
Furthermore, the average value of T_out can be written as 32.95 ± 0.051℃. Using the same equation, the standard deviation of T_in was found to be 0.033. Thus, the average T_in value was 29.75 ± 0.016℃.
The value of q at a speed of 0.4 m/s was found to be 19.48 W. To determine of the standard deviation of q, the following equation was used:
〖RSS〗_q=√((〖s(ΔT〗 _out)∂q/(∂T_out))^2+(〖s(ΔT〗 _in)∂q/(∂T_in))^2) (14)
∂q/(∂T_out)=(∂(m·c_p·T_out-m·c_p·T_in))/(∂T_out)=m·c·p
∂q/(∂T_in)=(∂(m·c_p·T_out-m·c_p·T_in))/(∂T_in)=-(m·c·p)
where 〖s(ΔT〗 _out)=0.051℃ and 〖s(ΔT〗 _in)=0.033℃, ensuring, that 〖RSS〗_q= ± 0.290 W. Therefore, the heat transfer rate q becomes 19.48 ± 0.290 W. The value of 〖ΔT〗 _lmtd at a speed of 0.4 m/s was found to be 18.56℃. To determine the value of the standard deviation of 〖ΔT〗 _lmtd we used the following equation:
〖RSS〗_(〖ΔT〗 _lmtd) =√((〖s(ΔT〗 _tube)∂(〖ΔT〗 _lmtd)/(∂T_tube))^2+(〖s(ΔT〗 _out)∂(〖ΔT〗 _lmtd)/(∂T_out))^2+(〖s(ΔT〗 _in)∂(〖ΔT〗 _lmtd)/(∂T_in))^2) (15)
∂(〖ΔT〗 _lmtd)/(∂T_tube)=∂(((T_tube-T_out)-(T_tube-T_in))/ln 〖(T_tube-T_out)/(T_tube-T_in)〗)/(∂T_tube)
∂(〖ΔT〗 _lmtd)/(∂T_out)=∂(((T_tube-T_out)-(T_tube-T_in))/ln 〖(T_tube-T_out)/(T_tube-T_in)〗)/(∂T_out)
∂(〖ΔT〗 _lmtd)/(∂T_in)=∂(((T_tube-T_out)-(T_tube-T_in))/ln 〖(T_tube-T_out)/(T_tube-T_in)〗)/(∂T_in)
where 〖s(ΔT〗 _tube)=0,029℃, 〖s(ΔT〗 _out)=0,051℃ and 〖s(ΔT〗 _in)=0,033℃; we get 〖RSS〗_(〖ΔT〗 _lmtd) of ± 0.043, ensuring, that the obtained 〖ΔT〗 _lmtd is 8.56 ± 0.043.
The value of Nu at a speed of 0.4 m/s was found to be 155.31. The standard deviation of Nu was obtained using following equation
〖RSS〗_Nu=√((s(q)∂Nu/∂Q)^2+ 〖s(ΔT〗 _lmtd)∂Nu/(∂ 〖ΔT〗 _lmtd)) (16)
∂Nu/∂q=∂(q·D_h. 〖At〗 ^(-1)· 〖 〖ΔT〗 _lmtd〗 ^(-1)·k^(-1))/∂q=D_h/((At)(〖ΔT〗 _lmtd)(k))
∂Nu/(∂ 〖ΔT〗 _lmtd)=∂(q· 〖D_h·At〗 ^(-1)· 〖 〖ΔT〗 _lmtd〗 ^(-1).k^(-1))/(∂ 〖ΔT〗 _lmtd)=(q.D_h)/((At)(〖ΔT〗 _lmtd)^2 (k))
With the values of s(q)=0.290 W and 〖s(ΔT〗 _lmtd)=0.043, the obtained 〖RSS〗_Nu was ± 2.889 W/(m2℃). Therefore, the value of 〖RSS〗_Nu is 155.31 ± 2.889 W/m2℃.
The value of h at a speed of 0.4 m/s was found to be 44.86. To determine the standard deviation of Nu the following equation is used
〖RSS〗_h=√((s(Nu)∂h/Nu)^2) (17)
∂h/∂Nu=∂(h.D_h.k^(-1))/∂h=k/D_h
Furthermore, the value of_D_h is 0.092 m and k at T_f= 40.24 is 0.026. So the value of h at a speed of 0.4 m/s is:
〖RSS〗_h=√((s(Nu)∂h/Nu)^2)= 0,83
Thus, the number h at a speed of 0.4 m/s is 44.86 ± 0.83. So, the error h for the baseline at a speed of 0.4 m/s is
Error= 〖RSS〗_h/h×100 (18)
Error=0.83/44.86×100=1.51%
From the test in the baseline case with a speed of 2.0 m/s, the results of the pressure drop are listed in Table 4, which show that the average P can be calculated as follows:
(ΔP) ̄=(〖ΔP〗 _1+ 〖ΔP〗 _2+ 〖ΔP〗 _3+⋯+ 〖ΔP〗 _30)/30=3.51 Pa (19)
The average standard deviation of the pressure drop can then be calculated using the equation
s=√((Σ_(i=1)^N▒(〖ΔP〗 _i-(ΔP) ̄)^2)/N(N-1))=8.9×10^(-5) (20)
Baseline case for the pressure drop value at a speed of 2.0 m/s is 3.51±8.9×10^(-5) Pa. Then, the error in the form of percentage can be calculated using the following equation:
(8.9×10^(-5))/3.51×100=0.71
Table 4 Baseline pressure drop data at a speed of 2.0 m/s

ΔP (Pa)
Data to 2.0 m/s Data to 2.0 m/s
1 0.013 16 0.012
2 0.013 17 0.013
3 0.013 18 0.012

4 0.013 19 0.012
5 0.012 20 0.013
6 0.013 21 0.013
7 0.013 22 0.012
8 0.012 23 0.013
9 0.013 24 0.012
10 0.013 25 0.013
11 0.013 26 0.013
12 0.013 27 0.013
13 0.012 28 0.013
14 0.012 29 0.012
15 0.013 30 0.012

The equal calculation approach changed into used for all data. Therefore, the overall error outputs for the pressure-drop vortex generator with placement variations (in-line and staggered), Re and amount of VG sets (one, two and three) are listed in Table 5.

Table 5. Overall Pressure Drop (ΔP)

Vortex Generator Variations	Overall Error P (perforated)
1 PRWP in-line	2.94%
2 PRWP in-line	2.87%
3 PRWP in-line	1.98%
1 PRWP staggered	2.88%
2 PRWP staggered	2.34%
3 PRWP staggered	1.36%
1 PCRWP in-line	2.72%
2 PCRWP in-line	1.80%
3 PCRWP in-line	1.80%
1PCRWPstaggered	2.43%
2PCRWPstaggered	1.91%
3 PCRWP staggered	0.97%

The average TEF results from the experimental results can be calculated as follows.

$$\overline{(TEF)}=([\![TEF]\!]_1+ [\![TEF]\!]_2+ [\![TEF]\!]_3+\cdots+ [\![TEF]\!]_12)/12=1.12 \quad (21)$$

Then, the average standard deviation of the TEF can be calculated with the equation

$$s=\sqrt{((\Sigma_{i=1}^{N}([\![TEF]\!]_i-\overline{(TEF)})^2)/N(N-1))}=1.07 \quad (22)$$

Therefore, the TEF value was 1.12 ± 1.07. Then, the error in the form of percentage can be calculated using the following equation:

$$1.07/1.12\times100=0.94\%$$

The overall error results for the TEF vortex generator with placement variations (in-line and staggered), Re and amount of VG sets (one, two and three) are are listed inTable 6.

Table 6. Overall error TEF

Variasi Vortex Generator	Overall Error TEF (Berlubang)
1 RWP in-line	0.47 %
2 RWP in-line	0.47%
3 RWP in-line	0.43%
1 RWP staggered	0.47%
2 RWP staggered	0.47%
3 RWP staggered	0.43%
1 CRWP in-line	0.45%
2 CRWP in-line	0.45%
3 CRWP in-line	0.42%
1 CRWP staggered	0.45%
2 CRWP staggered	0.45%
3 CRWP staggered	0.41%

First, find the average CBR of the experimental results with the following formula.
$(CBR)\bar{}=([\![CBR]\!] _1+ [\![CBR]\!] _2+ [\![CBR]\!] _3+\cdots+ [\![CBR]\!] _12)/12=2.14$ (23)

The average standard deviation of the pressure drop CBR can then be calculated using the following equation:
$s=\sqrt{((\Sigma_{i=1)^N\blacksquare([\![CBR]\!] _i-(CBR)\bar{})^2)/N(N-1))}=1.60$ (24)
The CBR value is 2.14 ± 1.60. Then the error in the form of percentage can be calculated using thefollowing equation:
$1.60/2.14\times100=0.63\%$
The overall error results for the CBR vortex generator with placement variations (in-line and staggered), Re and amount of VG sets (one, two and three) are listed in Table 7
Table 7. Overall error CBR

Variasi Vortex Generator (Berlubang)	Overall Error CBR
1 RWP in-line	0.32%
2 RWP in-line	0.29%
3 RWP in-line	0.45%
1 RWP staggered	0.32%
2 RWP staggered	0.31%
3 RWP staggered	0.45%
1 CRWP in-line	0.4%
2 CRWP in-line	0.42%
3 CRWP in-line	0.56%
1 CRWP staggered	0.43%
2 CRWP staggered	0.42%
3 CRWP staggered	0.66%

Reference
[1] S. Caliskan, S. Şevik, and Ö. Özdilli, "Heat transfer enhancement by a sinusoidal wavy plate having punched triangular vortex generators," International Journal of Thermal Sciences, vol. 181, p. 107769, Nov. 2022, doi: 10.1016/J.IJTHERMALSCI.2022.107769.
[2] A. J. Modi and M. K. Rathod, "Comparative study of heat transfer enhancement and pressure drop for fin-and-circular tube compact heat exchangers with sinusoidal wavy and elliptical curved rectangular winglet vortex generator," Int J Heat Mass Transf, vol. 141, pp. 310–326, Oct. 2019, doi: 10.1016/J.IJHEATMASSTRANSFER.2019.06.088.
[3] Y. Effendi, A. Prayogo, Syaiful, M. Djaeni, and E. Yohana, "Effect of perforated concave delta winglet vortex generators on heat transfer and flow resistance through the heated tubes in the channel," Experimental Heat Transfer, vol. 35, no. 5, pp. 553–576, 2022, doi: 10.1080/08916152.2021.1919245.
[4] M. T. Al-Asadi, F. S. Alkasmoul, and M. C. T. Wilson, "Benefits of spanwise gaps in cylindrical vortex generators for conjugate heat transfer enhancement in micro-channels," Appl Therm Eng, vol. 130, pp. 571–586, Feb. 2018, doi: 10.1016/J.APPLTHERMALENG.2017.10.157.
[5] J. F. Zhang, Y. K. Joshi, and W. Q. Tao, "Single phase laminar flow and heat transfer characteristics of microgaps with longitudinal vortex generator array," Int J Heat Mass Transf, vol. 111, pp. 484–494, Aug. 2017, doi: 10.1016/J.IJHEATMASSTRANSFER.2017.03.036.
[6] E. Hosseinirad, M. Khoshvaght-Aliabadi, and F. Hormozi, "Evaluation of heat transfer and pressure drop in a mini-channel using transverse rectangular vortex-generators with various non-uniform heights," Appl Therm Eng, vol. 161, p. 114196, Oct. 2019, doi: 10.1016/J.APPLTHERMALENG.2019.114196.

Reviewer 3: In connection with climate change and an increase in the average annual temperature on Earth, there is a new danger of the negative impact of high temperatures on human life.
In this case, the improvement of air conditioning systems, including the search for the best thermal enhancement factor, cost-benefit ratio, etc., takes on a new sense, which is one of the main targets of this article. The topic is timely and of great practical significance to environmental protection, enhancing safety, and people's life comfort.
The manuscript is well-structured and includes all necessary parts.
Two key strengths of the paper are a good introduction section and an analysis and discussion of the results. Both research objectives and content are clear. The key scientific issues to be solved are moderate. The research experimental method is reasonable.

There are also several shortages worthy to be mentioned:
Seriously revise the formulas
If you use an italic font in formulas, use an italic font in their descriptions. For example, in formula (1), the Nusselt number (Nu) and friction factor (f); in formula (3), heat transfer coefficient (h). It may confuse the reader.

Thank you for the corrections. For formula and description fonts, improvements have been made where all formula and description fonts are italicized consistently.

The Nusselt numbers in formula (1) and formula (2) have different designations. It may confuse the reader.

Thanks for the correction. Consistent improvements have been made to writing the Nu symbol on paper.

What are Nusselt number and friction factor with subscript 0 in formula (1)?

Thanks for the corrections. The subscript 0 for Nusselt number and friction factor is meant for the baseline condition. This additional explanation has been added to the paper. The following is an explanation of formula 1.

TEF= ((Nu/ 〖Nu〗 _0))/(f/f_0)^(1/3) (1)

Di mana: 〖Nu〗 _0= Nusselt number pada kondisi baseline
f_0 = friction factor pada kondisi baseline

In formula (5), a pressure drop is the lowercase letter Δp, but in formula (6), a pressure drop is uppercase ΔP. Are these different pressures?

Thank you for the corrections. I'm so sorry for the error in writing the pressure drop symbol which is inconsistent. Improvements in writing pressure drop have been made with upperca 3 for the formula on the paper.

What is the error of pressure drop measurement with the Fluke 922 Airflow Micromanometer described in section "3.2 Effect of perforated vortex generators on pressure drop"? Did it cover the

necessary range of pressures to be investigated? Could micromanometer error have affected the conclusions of the section? Because the pressure drop values of 4.58 Pa, 5 Pa and 5.4 Pa are close to each other.

Thanks for the question. Pressure measurement errors with the Fluke 922 Airflow Micromanometer are explained in the uncertainty analysis section with the calculation results as below.
From the test in the baseline case with a speed of 2.0 m/s, the results of the pressure drop are listed in Table 4, which show that the average P can be calculated as follows:
$(\Delta P)\bar{}=(\ ⟦\Delta P⟧\ _1+\ ⟦\Delta P⟧\ _2+\ ⟦\Delta P⟧\ _3+\cdots+\ ⟦\Delta P⟧\ _30)/30=3.51$ Pa (19)
The average standard deviation of the pressure drop can then be calculated using the equation
$s=\sqrt{((\Sigma\_(i=1)^N▒(\ ⟦\Delta P⟧\ _i-(\Delta P)\bar{})^2\ )/N(N-1)\ )}=8.9\times10^{-5}$ (20)
Baseline case for the pressure drop value at a speed of 2.0 m/s is $3.51\pm8.9\times10^{-5}$ Pa. Then, the error in the form of percentage can be calculated using the following equation:
$(8.9\times10^{-5})/3.51\times100=0.71$

Table 4 Baseline pressure drop data at a speed of 2.0 m/s
ΔP (Pa)
Data to 2.0 m/s Data to 2.0 m/s
1 0.013 16 0.012
2 0.013 17 0.013
3 0.013 18 0.012
4 0.013 19 0.012
5 0.012 20 0.013
6 0.013 21 0.013
7 0.013 22 0.012
8 0.012 23 0.013
9 0.013 24 0.012
10 0.013 25 0.013
11 0.013 26 0.013
12 0.013 27 0.013
13 0.012 28 0.013
14 0.012 29 0.012
15 0.013 30 0.012

The equal calculation approach changed into used for all data. Therefore, the overall error outputs for the pressure-drop vortex generator with placement variations (in-line and staggered), Re and amount of VG sets (one, two and three) are listed in Table 5.
Table 5. Overall Pressure Drop (ΔP)
Vortex Generator Variations Overall Error P
(perforated)
1 PRWP in-line 2.94%
2 PRWP in-line 2.87%
3 PRWP in-line 1.98%
1 PRWP staggered 2.88%
2 PRWP staggered 2.34%
3 PRWP staggered 1.36%
1 PCRWP in-line 2.72%
2 PCRWP in-line 1.80%
3 PCRWP in-line 1.80%
1 PCRWP staggered 2.43%
2 PCRWP staggered 1.91%
3 PCRWP staggered 0.97%

The results of the measurement error calculation are still below the maximum accuracy limit of the tool by 5% so that it does not affect the conclusion section.

The measurement error in the section "3.3 Effect of perforated VGs on thermal enhancement

factor" and "Effects of perforated VGs on the cost-benefit ratio" is not clear. Can you show the error bar or describe it in the description?

Thanks for the question. The measurement error for the thermal increase factor and the cost benefit ratio has been added to the explanation in the paper in the data uncertainty section, as follows.
error bar TEF
The average TEF results from the experimental results can be calculated as follows.
$\overline{(TEF)}=(〖TEF〗 _1+ 〖TEF〗 _2+ 〖TEF〗 _3+⋯+ 〖TEF〗 _12)/12=1.12$ (21)
Then, the average standard deviation of the TEF can be calculated with the equation
$s=√((∑_{i=1}^{N}(〖TEF〗 _i-\overline{(TEF)})^2)/N(N-1))=1.07$ (22)
Therefore, the TEF value was 1.12 ± 1.07. Then, the error in the form of percentage can be calculated using the following equation:
1.07/1.12×100=0.94%
The overall error results for the TEF vortex generator with placement variations (in-line and staggered), Re and amount of VG sets (one, two and three) are are listed inTable 6.
Table 6. Overall error TEF

Variasi Vortex Generator	Overall Error TEF
(Berlubang)	
1 RWP in-line	0.47 %
2 RWP in-line	0.47%
3 RWP in-line	0.43%
1 RWP staggered	0.47%
2 RWP staggered	0.47%
3 RWP staggered	0.43%
1 CRWP in-line	0.45%
2 CRWP in-line	0.45%
3 CRWP in-line	0.42%
1 CRWP staggered	0.45%
2 CRWP staggered	0.45%
3 CRWP staggered	0.41%

b error bar CBR
First, find the average CBR of the experimental results with the following formula.
$\overline{(CBR)}=(〖CBR〗 _1+ 〖CBR〗 _2+ 〖CBR〗 _3+⋯+ 〖CBR〗 _12)/12=2.14$ (23)

The average standard deviation of the pressure drop CBR can then be calculated using the following equation:
$s=√((∑_{i=1}^{N}(〖CBR〗 _i-\overline{(CBR)})^2)/N(N-1))=1.60$ (24)
The CBR value is 2.14 ± 1.60. Then the error in the form of percentage can be calculated using thefollowing equation:
1.60/2.14×100=0.63%
The overall error results for the CBR vortex generator with placement variations (in-line and staggered), Re and amount of VG sets (one, two and three) are listed in Table 7.
Table 7. Overall error CBR

Variasi Vortex Generator	Overall Error CBR
(Berlubang)	
1 RWP in-line	0.32%
2 RWP in-line	0.29%
3 RWP in-line	0.45%
1 RWP staggered	0.32%
2 RWP staggered	0.31%
3 RWP staggered	0.45%
1 CRWP in-line	0.4%
2 CRWP in-line	0.42%
3 CRWP in-line	0.56%
1 CRWP staggered	0.43%

2 CRWP staggered 0.42%
3 CRWP staggered 0.66%

In my humble opinion, the section "3.5 Flow visualisation" is better presented first in section "3. Results and Discussion".
Thanks for the suggestions. The discussion of section 3.5 on visualization has been moved to the earlier section to 3.1 in the paper.

We tried our best to improve the manuscript and made some changes in the revised paper, and here we did not list the specific changes but marked in red in revised paper. We appreciate for Editors and Reviewrs' warm work earnestly, and hope that the correction will meet with approval. Once again, thank you very much for your comments and suggestions.

Yours Sincerely
Oktarina Heriyani

Close

Results in Engineering

Perforated concave rectangular winglet pair vortex generators enhance the heat transfer of air flowing through heated tubes inside a channel

--Manuscript Draft--

Manuscript Number:	RINENG-D-22-00804R1
Full Title:	Perforated concave rectangular winglet pair vortex generators enhance the heat transfer of air flowing through heated tubes inside a channel
Short Title:	PCRWP VGs enhance the heat transfer of air flowing through heated tubes inside a channel
Article Type:	Research paper
Section/Category:	Mechanical Engineering
Keywords:	perforated; rectangular winglet; concave; pressure drop; Vortex generator
Corresponding Author:	oktarina heriyani, S.Si., M.T Diponegoro University Faculty of Engineering jakarta timur, DKI Jakarta INDONESIA
Corresponding Author Secondary Information:	
Corresponding Author's Institution:	Diponegoro University Faculty of Engineering
Corresponding Author's Secondary Institution:	
First Author:	oktarina heriyani, S.Si., M.T
First Author Secondary Information:	
Order of Authors:	oktarina heriyani, S.Si., M.T
	Mohammad Djaeni, Prof., Dr., S.T., M.Eng
	Aldila Kurnia Putri
	Syaiful Syaiful, S.T., M.T., Ph.D
Order of Authors Secondary Information:	
Abstract:	A significant increase in the rate heat transfer in a heat exchanger system is made possible by increasing the convection heat-transfer coefficient using a passive method. The addition of vortex generators (VGs) to the fins and tubes of a heat exchanger is currently the most effective passive method. However, the increase in heat was accompanied by an increase in pressure drop. Therefore, in this study, we installed perforated concave rectangular winglet pair vortex generators (PCRWP VGs) on plates in rectangular ducts to increase the heat transfer through the six heated tubes to the air stream by lowering the enhancement in the pressure drop. We attempted to determine the best cost-benefit ratio (CBR) with a fluid flow velocity difference of 0.4 –2 m/s at intervals of 0.2 m/s (Reynolds number (Re) of 2,143 to 11,763) in the channel. The PCRWP VGs were composed of in-line and staggered configurations. The results showed a lower CBR (3.56) for the in-line configuration than for the staggered configuration. Moreover, the lowest CBR was accompanied by an increase in thermal performance (TEF) of 1.29.
Suggested Reviewers:	Serge Russeil serge.russeil@imt-nord-europe.fr his research focuses on vortex generators
	Yasser Amini aminiyasser@pgu.ac.id his research is focused on heat exchangers
	Atila Abir Igci atila.igci@bozok.edu.tr

	his research is focused on vortex generators
Response to Reviewers:	Dear Editors and Reviewer Thank you for your letter and for the reviewers' comments concerning our manuscript entitled "Perforated concave rectangular winglet pair vortex generators enhance the heat transfer of air flowing through heated tubes inside a channel" (Manuscript Number: Rineng-D-22-00804R1). The comments are all valuable and very helpful to revise and improve our paper, as well as significant guidelines for our research. We have learned comments carefully and have made the correction that we hope you meet with your approval. We have included the parts requested to be revised in the manuscript. Revised portions are marked in red in the revised paper. The main correction in papers and responses to reviewing comments is flowing. Reviewer 1: Following are the few observations: Author should add figure of location of thermocouple. Thank you very much for the proposal. I've revised Figure 1 because I made a mistake in captioning the figure. One thermocouple is placed in the air inlet area, six thermocouples on the back surface of the tubes, and 15 on the outlet side of the wire, as observed in Figure 1. Heaters are placed after test section? How the heating of air takes place? Thanks for the question. The heater is connected to six tubes with each tube getting the same power. The total heating power of 40 W is induced in the six tubes by a regulator. Heating air flowing through the tubes occurs by convection. So that the air at the outlet side becomes hotter than that from the inlet side. Details of perforations on rectangular and concave winglet is missing. pl add. Thank you for the correction. I have added in the paper the detailed geometry of the perforated rectangular winglet (PRW) and perforated concave rectangular winglet (PCRW) vortex generators (VGs), as shown in Figure 2. Perforated RWPPerforated CRWP VGs have dimensions of the same length and width of 30 mm and have 36 holes. The bore diameter on the VGs is 2.5 mm. The distance between the holes is 5 mm from the center of the holes. Provide details of validation of set up and heat loss analysis. Set up validation Thank you for your suggestion. The current study is a follow-up investigation of the work of Yafid et al [1]. The experimental set-up of this study is similar to that of Yafid et al. experiment. The difference between the current study and the experiment of Yafid et al. is a test object where the current study uses concave rectangular winglet (CRW) VGs, while the work of Yafid et al. uses concave delta winglet (CDW) VGs. Whitaker et al. [2] studied the heat transfer characteristics of airflow through a single cylinder in a rectangular duct. To confirm the results of the experiment Yafid et al. are valid, the same experimental set-up is determined. The Nu value from the experiment of Yafid et al. compared with Nu values from the experiments of Whitaker et al. in the Reynolds number range of 2,143 to 11,763, as shown in the figure below. From the figure, it can be observed that Nu from the experimental results of Yafid et al. have the same trend as the experiments of Whitaker et al. b. Heat Loss analysis Heat loss analysis is carried out by taking into account the convection heat transfer

from the six tubes to the surrounding fluid flow. Calculation of the heat transfer rate is carried out for two types of flow, namely laminar flow and turbulent flow.
The calculation of heat loss in this experiment is determined by calculating the difference between the induced electric power and the total heat through convection from the surface of the tubes to the fluid. In this experiment, six tubes in a wind tunnel are heated by a heater with a power of 40 W. In this work, the velocity of the inlet fluid is varied from 0.4 to 2 m/s at intervals of 0.2 m/s or in the Reynolds number range from 2,143 to 11,763. Based on the Reynolds number range, two types of flow are determined, namely laminar and turbulent. Therefore, the heat loss was determined from the correlation between laminar at 0.4 m/s and turbulent for other velocities.
The described formulas Nu, h, and q were used to determine the heat loss in the conduit of the six tubes.

$$Nu=(q\ D_h)/(A_{tube}\ \langle\!\langle \Delta T \rangle\!\rangle_{LMTD}\ k) \quad (2)$$

$$h=q/(A_{tube}\ \langle\!\langle \Delta T \rangle\!\rangle_{LMTD}) \quad (3)$$

$$q=\dot{m}\ c_p\ (T_{out}-T_{in}) \quad (4)$$

Where D_h, A_tube, $\langle\!\langle \Delta T \rangle\!\rangle_{LMTD}$, $\dot{m}$, c_p, T_out, T_in, are hydraulic diameter, tube surface area, log mean temperature difference, mass flow rate, specific heat, outlet temperature, and inlet temperature.

$$D_h=\ \langle\!\langle 4A \rangle\!\rangle_c/P \quad (5)$$

$$\langle\!\langle \Delta T \rangle\!\rangle_{LMTD}=\ ((\bar{T}_{tube}-\bar{T}_{out})-(\bar{T}_{tube}-\bar{T}_{in}))/\ln[(\bar{T}_{tube}-\bar{T}_{out})-(\bar{T}_{tube}-\bar{T}_{in})] \quad (6)$$

Where A_c dan T_tube are channel surface area and tube temperature, respectively. The experimental data for hydraulic diameter D_h,, tube surface area A_tube, channel surface area A_c, and air specific heat c_p are 0.09223 m, 0.02338908 m2, 0.01056 m2, and 1.007 J/kgK, respectively. The following is a table for calculating the heat loss baseline.

Table 1 Heat Loss Baseline

baseline	v (m/s)	Re	Mass flow rate (kg/s)	Density (kg/m3)	Dynamics viscous (kg/ms)	kPrT inlet (C)	T outlet (C)	T tube (C)	T LMTD	T tube - T inlet)	Nuh (W/mK)	q conv (W)	q input (W)	q loss (W)
	0.42	1650.00	47571.13	1.9E-05	0.03	0.732933501921	1554519.48	4020.52						
	0.63	2910.00	71911.13	1.9E-05	0.03	0.732831461618	1745018.98	4021.02						
	0.84	4130.00	96181.14	1.9E-05	0.03	0.032830441516	1925019.19	4020.81						
	1.05	5450.01	20561.14	1.9E-05	0.03	0.732830431415	2145519.84	4020.16						
	1.26	6610.01	44771.14	1.9E-05	0.03	0.732829431415	2286121.15	4018.85						
	1.47	8260.01	69581.15	1.9E-05	0.03	0.732829411213	2477020.30	4019.70						
	1.68	9650.01	94071.15	1.9E-05	0.03	0.732729401213	2637521.03	4018.97						
	1.81	01100.02	18631.15	1.9E-05	0.03	0.732728391212	2968422.54	4017.46						
	2	112720.02	43411.15	1.9E-05	0.03	0.732728381111	3429724.17	4015.83						

In the table 1, it can be seen that the greater the velocity with the increase in Re number, the lower the heat loss. It can be seen that the heat flow from the heater does not only spread into the tube, but convection occurs to the outside of the tube. Heat output increases with increasing Re. That is, the higher the flow velocity, the greater the turbulence through the silinder and the higher the turbulence intensity. An increase in turbulence intensity between a cold airflow and a hot cylinder with constant surface temperature is caused by the airflow velocity [3]. In row-tube arrays, this recirculation area increases for the second and subsequent columns. A lower air velocity in the circulation region indicates less airflow in that region participating in the local heating process [4]. The heat loss of all conditions in this experiment is shown in table 2 below.

Table 2 Calculation of heat loss for the whole case

type	VGs	q conv (W)	q input (W)	q loss (W)
Baseline	20.74	4019.26		
PCRWPI	125.15	4014.85		
PCRWPI	227.55	4012.45		

PCRWPI327.614012.39
PCRWPS126.434013.57
PCRWPS226.434013.57
PCRWPS327.944012.06
PRWPI124.094015.91
PRWPI227.254012.75
PRWPI328.824011.18
PRWPS123.944016.06
PRWPS226.374013.63
PRWPS328.124011.88
Table 2 shows that the lowest heat loss occurs when three sets of PCRWPs are staggered. The placement of the VGs can increase heat transfer in square ducts as the VGs create longitudinal vortices that increase vortex strength in the wake region downstream of the tube. Longitudinal vortices make the overall temperature field more uniform, improve heat mixing and boundary layer modification, and improve heat transfer performance. A higher number of vortex generators creates more longitudinal vortices and greatly increases heat transfer [5], [3].

Mention pitch kept between two pins/winglet.
Thank you for the question. I've added Figure 3 (in the paper) showing the pitch between VGs for both inline and staggered configurations.

CRWP in-lineCRWP staggered

RWP in-lineRWP staggered

CRWP in-lineCRWP staggered

RWP in-lineRWP staggered

At lower Re both inline and staggered arrangement gives the same result, while deviation is observed after Re 8000. The author has to justify.

Thank you for your suggestion. In Figure 7(a) (in the paper), the convection heat transfer coefficient for the case of PRW VGs in-line has the same value as that of PCRW VGs in-line or staggered in a pair of VGs. In one pair of VGs, the longitudinal vortex is generated after the flow hits the VGs and weakens (He et al., 2013). This is in contrast to two and three pairs of VGs where the longitudinal vortex produced after striking the first VGs has amplified again when the flow strikes the second VGs and so on. Therefore, the value of the heat transfer coefficient in the case of a pair of PRW VGs has the same value as that of PCRW VGs at Reynolds numbers above 8,000.

Provide more clarification about 1,2 & 3 pairs.
Thank you for your suggestion. This study describes the cases of PCRW and PRW VGs for one, two, and three pairs. I have added explanations for cases one, two, and three pairs of perforated VGs to the paper.
For PRW and PCRW VGs in-line configurations with one, two, and three pairs are shown in Figures 4. For one pair, the VGs are placed on the left and right sides of the first row of tubes. VGs are placed on the first and third row tubes for two pairs. As for the three pairs, VGs are placed on the first, third, and fifth row tubes.

one pair PCRW inllinetwo pairs PCRW inline

three pairs PCRW inline

one pair PRW inlinetwo pairs PRW inline

three pairs PRW inline
Figure 4. VGs pairs in-line configurations

For PRW and PCRW VGs staggered configurations with one, two, and three pairs are shown in Figures 5. For one pair, the VGs are placed on the right side of the first row tube and the left side of the second row tube. VGs are placed on the right side of the first, third row tubes and on the left side of the second and fourth tubes for two pairs. As for the three pairs, the VGs are placed on the right side of the first, third, fifth row of tubes and on the left side of the second, fourth and sixth tubes.

one pair PCRW staggeredtwo pairs PCRW staggered

three pairs PCRW staggered

one pair PRW staggeredtwo pairs PRW staggered

three pairs PRW staggered

Figure 5. VGs pairs staggered configurations

Compare the PRWP and PCRWP with without perforation.
Thank you for your request. In this study, an experiment was conducted to compare PRW VGs and PCRW VGs in improving heat transfer in a rectangular channel, as shown in Figures 7 to 9.

Comparison of convection heat transfer coefficient values.
Figure 7 provides a comparison of the convection heat transfer coefficients for PRW and PCRW. It can be seen that there was an increase in the convection heat transfer coeeficient with a rise in Re due to an increase in flow vortices and high turbulence intensity in the channel [6], alongside a reduction in the wage region and stagnation area for each increase in flow velocity [7]. The increase in heat transfer for staggered VGs was better than in-line for PCRW VGs with any number of pairs at the highest Re (11,000). The results in Figure 7 show that the PCRWP VGs worked better than the PRWP VGs, and the staggered arrangement of the former with three pairs gave the highest yield, of 153.5 W/m2.K, as shown in Figure 7(c). Meanwhile, two PCRW pairs (137.33 W/m2.K, Figure 7(b)) were better than one (132.25 W/m2.K, Figure 7(a)) because VGs with a concave surface destabilise the centrifugal force of the fluid flow, which strengthens the flow vortices. This makes the mixing of the hot fluid near the wall with the cold fluid of the main flow more robust [8].

Pressure drop comparison
In general, the highest pressure drop was observed using PCRWP VGs with staggered configuration for all Reynolds numbers except for one pair of VGs, as shown in Figure 8. The highest pressure drop was found in PRWP VGs with in-line configuration at Reynolds numbers greater than 8,000. The pressure drop on the staggered VGs was found to be higher than that of the in-line due to the shorter distance between the VGs of the staggered configuration than that of the in-line [5].

TEF comparison
TEF is the thermal-hydraulic performance which is the ratio of the increase in heat transfer to the pressure drop ratio. In general, the highest TEF was observed in the use of PCRWP VGs with staggered configuration, as depicted in Figure 9. PCRW creates wider flow vortices that can reduce the wake area behind the cylinder. Reducing the wake area can reduce the recirculation zone. This affects the increased heat transfer from the back of the cylinder to the stream [3]. A large radius, high intensity antrior-posterior vortex can reduce the wake area. A reduction in the wake area increases the flow velocity behind the tube and reduces the recirculation area, resulting in an increased heat transfer in this area [9], [10].

CBR comparison
A low value of CBR means a more economical value from the use of VGs. In general, CBR on the use of PCRWP VGs with staggered configuration is the best, as informed in Figure 10. The lowest CBR value results were obtained with three pairs of staggered type VGs PCRW. Three pairs of VGs lower CBR than one and two VG pairs. This is because the installation of three pairs VGs results in a higher Nusselt number increase than one and two pairs VGs, resulting in a lower pressure drop increase and therefore a lower CBR. These results show that lower CBR improves thermal performance relative to resistivity [11].

Discuss how number of pairs contribute in improving TEF

Thank you for your question. Figure 9 shows the effect of the number of pairs and configuration of VGs on TEF, this is also found in Ref. (He et al., 2013), (Sun et al., 2020), and (Ranjan et al., 2022).

One pair

Two pairs

Three pairs
From the experimental results, as shown in Figure 9, the TEF with three pairs of VGs for both inline and staggered was the highest. The TEF for the case of 3 pairs of PCRWs was 5.02% greater than that of one and two pairs of PRWP VGs. The main reason is because the concave surface of the PCR causes the flow to be thrown away due to the centrifugal force which results in a stronger flow vorticity [12]. Larger and stronger flow vortices can reduce the recirculation zone which has an impact on increasing heat transfer from the rear surface of the tube to the flow [10]. The presence of flow that is formed in each gap between the VGA and the tube causes the TEF in the staggered configuration to be greater than that of the in-line [13]. The increase in TEF for the three-pair case with the staggered configuration was 1.50% and 4.91% greater than that of the inline PCRWP and PRWP, respectively.

Reference
[1]Y. Effendi, A. Prayogo, Syaiful, M. Djaeni, and E. Yohana, “Effect of perforated concave delta winglet vortex generators on heat transfer and flow resistance through the heated tubes in the channel,” Experimental Heat Transfer, vol. 35, no. 5, pp. 553–576, 2022, doi: 10.1080/08916152.2021.1919245.
[2]S. Whitaker, “Forced Convection Heat Transfer Correlations for Flow In Pipes, Past Flat Plates, Single e Cylinders, Single Spheres, and for Flow In Packed Beds and Tube Bundles,” Reprillted from AIChE JOURNAL, 1972.
[3]M. Awais and A. A. Bhuiyan, “Enhancement of thermal and hydraulic performance of compact finned-tube heat exchanger using vortex generators (VGs): A parametric study,” International Journal of Thermal Sciences, vol. 140, pp. 154–166, Jun. 2019, doi: 10.1016/J.IJTHERMALSCI.2019.02.041.
[4]A. J. Modi and M. K. Rathod, “Experimental investigation of heat transfer enhancement and pressure drop of fin-and-circular tube heat exchangers with modified rectangular winglet vortex generator,” Int J Heat Mass Transf, vol. 189, p. 122742, Jun. 2022, doi: 10.1016/J.IJHEATMASSTRANSFER.2022.122742.
[5]Y. L. He, P. Chu, W. Q. Tao, Y. W. Zhang, and T. Xie, “Analysis of heat transfer and pressure drop for fin-and-tube heat exchangers with rectangular winglet-type vortex generators,” Appl Therm Eng, vol. 61, no. 2, pp. 770–783, Nov. 2013, doi: 10.1016/J.APPLTHERMALENG.2012.02.040.
[6]M. Pranita Hendraswari, M. S. Tony, and M. F. Soetanto, “Heat Transfer Enhancement inside Rectangular Channel by Means of Vortex Generated by Perforated Concave Rectangular Winglets,” 2021, doi: 10.3390/fluids6010043.
[7]Syaiful, A. R. Siwi, T. S. Utomo, Yurianto, and R. Wulandari, “Numerical analysis of heat and fluid flow characteristics of airflow inside rectangular channel with presence of perforated concave delta winglet vortex generators,” International Journal of Heat and Technology, vol. 37, no. 4, pp. 1059–1070, 2019, doi: 10.18280/IJHT.370415.
[8]A. Sinha, H. Chattopadhyay, A. K. Iyengar, and G. Biswas, “Enhancement of heat transfer in a fin-tube heat exchanger using rectangular winglet type vortex generators,” Int J Heat Mass Transf, vol. 101, pp. 667–681, Oct. 2016, doi: 10.1016/J.IJHEATMASSTRANSFER.2016.05.032.

[9]A. Gupta, A. Roy, S. Gupta, and M. Gupta, “Numerical investigation towards implementation of punched winglet as vortex generator for performance improvement of a fin-and-tube heat exchanger,” Int J Heat Mass Transf, vol. 149, p. 119171, Mar. 2020, doi: 10.1016/J.IJHEATMASSTRANSFER.2019.119171.
[10]Y. Li, Z. Qian, and Q. Wang, “Numerical investigation of thermohydraulic performance on wake region in finned tube heat exchanger with section-streamlined tube,” Case Studies in Thermal Engineering, vol. 33, p. 101898, May 2022, doi: 10.1016/J.CSITE.2022.101898.
[11]M. W. Tian, S. Khorasani, H. Moria, S. Pourhedayat, and H. S. Dizaji, “Profit and efficiency boost of triangular vortex-generators by novel techniques,” Int J Heat Mass Transf, vol. 156, p. 119842, 2020, doi: 10.1016/j.ijheatmasstransfer.2020.119842.
[12]H. Naik and S. Tiwari, “Thermodynamic performance analysis of an inline fin-tube heat exchanger in presence of rectangular winglet pairs,” Int J Mech Sci, vol. 193, no. September 2020, p. 106148, 2021, doi: 10.1016/j.ijmecsci.2020.106148.
[13]L. O. Salviano, D. J. Dezan, and J. I. Yanagihara, “Thermal-hydraulic performance optimization of inline and staggered fin-tube compact heat exchangers applying longitudinal vortex generators,” Appl Therm Eng, vol. 95, pp. 311–329, Feb. 2016, doi: 10.1016/J.APPLTHERMALENG.2015.11.069.

Reviewer 2: This paper presented experimental results of the heat transfer, pressure drop and thermal performance characteristics of the perforated concave rectangular winglet pair vortex generators on plates in rectangular ducts to increase the heat transfer through the six heated tubes to the air stream. Perforated concave rectangular winglets were compared with perforated rectangular winglet pairs vortex generator mounted on rectangular plates. The subject of the article falls within the scope of the Results in Engineering. In my view, unless the paper is rewritten in a proper way, I think it is inadequate to be published in a scientific journal in its present state. I would like to provide the following comment:
There are many spelling and grammar mistakes in this paper, and many sentences are not easy to follow. The grammar and structure of sentences in this paper need to be modified carefully, such as the title of the article. The language of this paper need to be improved by a native English speaker.
Thank you for your suggestion. To improve grammar and structure, I have sent this paper to elsevier service for proof reading.

The velocity ranges studied are given in the Abstract, whereas the Reynolds number ranges studied should be given.
Thank you for your correction. In this experiment, the intake air velocity is in the range of 0.4 to 2 m/s at intervals of 0.2 m/s or in the Reynolds number range of 2.143 to 11.763. I have included the Reynolds number range in the abstract.

Please review the keywords and add a few, for instance heat transfer, thermal performance.
Thank you for your suggestion. The keywords for this study are vortex generators, heat transfer, thermal-hydraulic performance, economic benefit. I've added keywords in the paper.

The method section can be expanded.
Thank you for your suggestion. I have improved this research method in the paper. Based on Fig. 1, the rectangular channel is equipped with a blower (50 Hz, Wipro with a rated voltage of 220V), an inverter (Mitsubishi Electric type FR-D700 with an accuracy of 0.01), straightener, hot wire anemometer (Lutron type AM-4204 with an accuracy of 0.1), wattmeter (Lutron DW-6060 with an accuracy ± 1.0), central processing unit (CPU), micromanometer, thermocouple (K type with a temperature interval of -200 –1250°C and an accuracy ± 0.5) where one thermocouple was placed in the air inlet area, six thermocouples on the back surface of the tubes and 15 on the outlet side of the wire, data acquisition (Advantech USB-4718 type with an accuracy of 0.001) and heater regulator. The heater was connected to six tubes with a diameter of

19.05 mm and height of 65.8 mm, with each tube having the same power. Total heating power of 40 W was applied to the six tubes using a regulator. The heating air flowing through the tubes occurs via convection. Thus, the air at the outlet side becomes hotter than that at the inlet side.
A pressure micromanometer (Fluke type 922, with an accuracy of ± 0.05) was used to monitor the flow pressure drop. Two pitot tubes, each set 26 cm ahead of the inlet of the test specimen and 2.5 cm behind it, were connected to a micromanometer to measure the pressure drop. The pressure drop measurements were recorded 30 times for 5 sekon at each speed variation. Furthermore, flow visualisation was performed by directing the smoke from vaporised fluid in the fluid vaporator into the mainflow.

The arrangement of vortex generators is given in Figure 2, but Figure 2 is not sufficient for a clear understanding of the construction of vortex generators. Additional figures should be drawn which clearly show the construction of vortex generators and the in-line and staggered arrangement.
Thank you for your suggestion. The following shows the construction of vortex generators inline and staggered (figure 2, 4 and 5 in the paper).

Figure 2. Geometry of the VGs
For PRW and PCRW VGs in-line configurations with one, two, and three pairs are shown in Figures 4. For one pair, the VGs are placed on the left and right sides of the first row of tubes. VGs are placed on the first and third row tubes for two pairs. As for the three pairs, VGs are placed on the first, third, and fifth row tubes.

one pair PCRW inllinetwo pairs PCRW inline

three pairs PCRW inline

one pair PRW inlinetwo pairs PRW inline

three pairs PRW inline
Figure 4. VGs pairs in-line configurations

For PRW and PCRW VGs staggered configurations with one, two, and three pairs are shown in Figures 5. For one pair, the VGs are placed on the right side of the first row tube and the left side of the second row tube. VGs are placed on the right side of the first, third row tubes and on the left side of the second and fourth tubes for two pairs. As for the three pairs, the VGs are placed on the right side of the first, third, fifth row of tubes and on the left side of the second, fourth and sixth tubes.

one pair PCRW staggeredtwo pairs PCRW staggered

three pairs PCRW staggered

one pair PRW staggeredtwo pairs PRW staggered

three pairs PRW staggered

Figure 5. VGs pairs staggered configurations

Thermal characteristics are given in terms of the convective heat transfer coefficient (h), friction characteristics are given in terms of pressure drop. Why are thermal characteristics not given in terms of Nusselt number (Nu) and friction characteristics in terms of coefficient of friction (f)?

Thank you for your correction. h versus Re and P vs Re are used instead of Nu - Re and f - Re in this experiment because, in the TEF calculation, the value of Nu represents the value of h resulting from the equation in formula 3 (in the paper), thus

h=(N_u k)/D_h (3)

Figure 7 (in the paper) that h rises as Re rises shows that the Nu increases as Re rises, where h rises as Re rises [1]. While f in this experiment represents the ∆P as shown in the following formula

$f=(2\ \Delta P\ D_h)/(\rho\ V^2\ (L+6D))(8)$

Formula 8 states that the friction factor (f) in the flow rate is determined by using the pressure drop (∆P) characteristic where increasing the Reynolds number in figure 8 will decrease the friction factor [2].
The following are examples of several studies that use h as a representative of Nu and (∆P) as a representative of f.
The experimental results of Yafid et al indicate that perforated VGs can increase the heat transfer rate and decrease the pressure drop using the parameters h, ∆P, and TEF as shown in the following graph[3].

Al Asadi et al represents heat transfer coefficient and pressure drop to show the results of their investigation that the addition of span wise gap variations can increase heat transfer performance and reduce pressure drop [4], as shown in the figure below.

Increased heat transfer in heat sinks, Zhang et al described the micro gap by pairing more VGs which resulted in a larger heat transfer coefficient and a reduced pressure drop value [5], as shown in the figure below.

Hosseinirad et al showed that the increase in heat transfer coefficient and pressure drop vs. Reynold number had a tendency to increase with the increase in Re to evaluate heat transfer [6]. There is an increase in heat transfer with an increase in Re which is indicated by an increase in the heat transfer coefficient and an increase in pressure drop along with an increase in Re.

It is not specified how the hydraulic diameter (Dh) is calculated. How the Reynolds number (Re) was calculated is not specified.

Thank you for your corrections. The calculation of the hydraulic diameter in this experiment uses a rectangular air duct with a side length of a = 0.165 m and a side width of b = 0.064 m with the resulting Dh of 0.0106 from the following formula.
$D_h=(4A_c)/p=4ab/2(a+b) =2ab/(a+b)$ (5)

The result of Dh is used to calculate Re with the formula
$Re=(\rho u_{in} D_h)/\mu(7)$
With u_in of 0.4 – 2 m/s with an interval of 0.2 m/s, on the physical properties of air at a pressure of 1 atm and is the viscosity of the fluid so that Re used in this experiment ranges from 2,143 – 11,763.
No correlation (Nu-Re), (f-Re) is given.

Thank you for the correction. In this experiment, Nu – Re and f – Re are not shown but use h vs Re and ΔP vs Re because the Nu value represents the value of h that arises in this experiment as in equation 4 (in the manuscript)

$h=(N_u\ k)/D_h$ (3)

While f in this experiment represents the ∆P as shown in the following formula

$f=(2\ \Delta P\ D_h)/(\rho\ V^2\ (L+6D))(8)$

The formula states that the friction factor (f) in the flow rate is determined by using the pressure drop (∆P) characteristic where increasing the Reynolds number in figure 8 will

decrease the friction factor [2].

Error analysis is given, but uncertainty analysis is not done.

Thank you for the correction. In the following, uncertainty analysis calculation data will be shown for the temperature at base line conditions with a velocity of 0.4 m/s as shown in Table 3 below.
Table 3 Base-line test temperature data at a speed of 0.4 m/s
T (Tube1)T (Tube2)T (Tube3)T (Tube4)T (Tube5)T (Tube6)
49.1909351.2136848.3231349.7691547.8021951.27142
49.183451.1772848.315649.7905347.765751.2639
49.1454551.1682648.3065549.752647.785651.25489
49.1210551.1727748.2821449.7282147.7611851.2594
49.1529751.2046548.2851549.7312247.7352451.2624
49.0996651.1514148.2896749.7357347.7687151.26691
49.0981551.1499148.2302949.7342347.7382651.29428
49.0891251.1408948.2501949.6673947.7292251.22751

From these data, it is found that $\bar{T}\_Tube$ can be calculated by the equation as
$\bar{T}\_Tube=(\bar{T}\_Tube1+\bar{T}\_Tube2+\bar{T}\_Tube3+\bar{T}\_Tube4+\bar{T}\_Tube5+\bar{T}\_Tube6)/6=49.56℃$ (11)
Then, the average standard deviation is obtained by the following formula.

$s\_tube=\sqrt{((\sum\_(i=1)^N▒(T\_tubei-\bar{T}\_tube)^2)/N(N-1))}=0.029$(12)
Therefore, the average T_tube can be written as 49.5 ± 0.029℃. $\bar{T}\_out$ calculation results obtained 32.95℃. The average standard deviation was calculated using the following equation:
$s\_Tout=\sqrt{((\sum\_(i=1)^N▒(T\_outi-\bar{T}\_out)^2)/N(N-1))}=0,051$(13)
Furthermore, the average value of T_out can be written as 32.95 ± 0.051℃. Using the same equation, the standard deviation of T_in was found to be 0.033. Thus, the average T_in value was 29.75 ± 0.016℃.
The value of q at a speed of 0.4 m/s was found to be 19.48 W. To determine of the standard deviation of q, the following equation was used:
$〖RSS〗\_q=\sqrt{((〖s(\Delta T〗\_out)\partial q/(\partial T\_out))^2+(〖s(\Delta T〗\_in)\partial q/(\partial T\_in))^2 }$(14)
$\partial q/(\partial T\_out)=(\partial(m•c\_p•T\_out-m•c\_p•T\_in))/(\partial T\_out)=m•c•p$
$\partial q/(\partial T\_in)=(\partial(m•c\_p•T\_out-m•c\_p•T\_in))/(\partial T\_in)=-(m•c•p)$
where $〖s(\Delta T〗\_out)=0.051℃$ and $〖s(\Delta T〗\_in)=0.033℃$, ensuring, that $〖RSS〗\_q=$ ± 0.290 W. Therefore, the heat transfer rate q becomes 19.48 ± 0.290 W. The value of $〖\Delta T〗\_lmtd$ at a speed of 0.4 m/s was found to be 18.56℃. To determine the value of the standard deviation of $〖\Delta T〗\_lmtd$ we used the following equation:
$〖RSS〗\_(〖\Delta T〗\_lmtd) =\sqrt{((〖s(\Delta T〗\_tube)\partial(〖\Delta T〗\_lmtd)/(\partial T\_tube))^2+(〖s(\Delta T〗\_out)\partial(〖\Delta T〗\_lmtd)/(\partial T\_out))^2+(〖s(\Delta T〗\_in)\partial(〖\Delta T〗\_lmtd)/(\partial T\_in))^2 }$(15)
$\partial(〖\Delta T〗\_lmtd)/(\partial T\_tube)=\partial(((T\_tube-T\_out)-(T\_tube-T\_in))/ln 〖(T\_tube-T\_out)/(T\_tube-T\_in)〗)/(\partial T\_tube)$
$\partial(〖\Delta T〗\_lmtd)/(\partial T\_out)=\partial(((T\_tube-T\_out)-(T\_tube-T\_in))/ln 〖(T\_tube-T\_out)/(T\_tube-T\_in)〗)/(\partial T\_out)$
$\partial(〖\Delta T〗\_lmtd)/(\partial T\_in)=\partial(((T\_tube-T\_out)-(T\_tube-T\_in))/ln 〖(T\_tube-T\_out)/(T\_tube-T\_in)〗)/(\partial T\_in)$
where $〖s(\Delta T〗\_tube)=0,029℃$, $〖s(\Delta T〗\_out)=0,051℃$ and $〖s(\Delta T〗\_in)=0,033℃$; we get $〖RSS〗\_(〖\Delta T〗\_lmtd)$ of ± 0.043, ensuring, that the obtained $〖\Delta T〗\_lmtd$ is 8.56 ± 0.043.
The value of Nu at a speed of 0.4 m/s was found to be 155.31. The standard deviation of Nu was obtained using following equation
$〖RSS〗\_Nu=\sqrt{((s(q)\partial Nu/\partial Q)^2+ 〖s(\Delta T〗\_lmtd)\partial Nu/(\partial 〖\Delta T〗\_lmtd))}$(16)
$\partial Nu/\partial q=\partial(q•D\_h.〖At〗^(-1)• 〖〖\Delta T〗\_lmtd〗^(-1)•k^(-1))/\partial q=D\_h/((At)(〖\Delta T〗\_lmtd)(k))$
$\partial Nu/(\partial 〖\Delta T〗\_lmtd)=\partial(q• 〖D\_h•At〗^(-1)• 〖〖\Delta T〗\_lmtd〗^(-1).k^(-1))/(\partial 〖\Delta T〗\_lmtd)=(q.D\_h)/((At)(〖\Delta T〗\_lmtd)^2 (k))$
With the values of s(q)=0.290 W and $〖s(\Delta T〗\_lmtd)=0.043$, the obtained $〖RSS〗\_Nu$ was ± 2.889 W⁄(m2℃). Therefore, the value of $〖RSS〗\_Nu$ is 155.31 ± 2.889 W⁄m2℃.
The value of h at a speed of 0.4 m/s was found to be 44.86. To determine the standard deviation of Nu the following equation is used

〖RSS〗_h=√((s(Nu)∂h/Nu)^2)(17)
∂h/∂Nu=∂(h.D_h.k^(-1))/∂h=k/D_h
Furthermore, the value of_D_h is 0.092 m and k at T_f= 40.24 is 0.026. So the value of h at a speed of 0.4 m/s is:
〖RSS〗_h=√((s(Nu)∂h/Nu)^2)= 0,83
Thus, the number h at a speed of 0.4 m/s is 44.86 ± 0.83. So, the error h for the baseline at a speed of 0.4 m/s is
Error=〖RSS〗_h/h×100(18)
Error=0.83/44.86×100=1.51%
From the test in the baseline case with a speed of 2.0 m/s, the results of the pressure drop are listed in Table 4, which show that the average P can be calculated as follows:
(ΔP)¯=(〖ΔP〗_1+〖ΔP〗_2+〖ΔP〗_3+⋯+〖ΔP〗_30)/30=3.51 Pa(19)
The average standard deviation of the pressure drop can then be calculated using the equation
s=√((∑_(i=1)^N▒(〖ΔP〗_i-(ΔP)¯)^2)/N(N-1))=8.9×10^(-5)(20)
Baseline case for the pressure drop value at a speed of 2.0 m/s is 3.51±8.9×10^(-5) Pa. Then, the error in the form of percentage can be calculated using the following equation:
(8.9×10^(-5))/3.51×100=0.71
Table 4 Baseline pressure drop data at a speed of 2.0 m/s
ΔP (Pa)
Data to2.0 m/sData to2.0 m/s
10.013160.012
20.013170.013
30.013180.012
40.013190.012
50.012200.013
60.013210.013
70.013220.012
80.012230.013
90.013240.012
100.013250.013
110.013260.013
120.013270.013
130.012280.013
140.012290.012
150.013300.012

The equal calculation approach changed into used for all data. Therefore, the overall error outputs for the pressure-drop vortex generator with placement variations (in-line and staggered), Re and amount of VG sets (one, two and three) are listed in Table 5.
Table 5. Overall Pressure Drop (ΔP)
Vortex Generator VariationsOverall Error P
(perforated)
1 PRWP in-line2.94%
2 PRWP in-line2.87%
3 PRWP in-line1.98%
1 PRWP staggered2.88%
2 PRWP staggered2.34%
3 PRWP staggered1.36%
1 PCRWP in-line2.72%
2 PCRWP in-line1.80%
3 PCRWP in-line1.80%
1PCRWPstaggered2.43%
2PCRWPstaggered1.91%
3 PCRWP staggered0.97%

The average TEF results from the experimental results can be calculated as follows.
(TEF)¯=(〖TEF〗_1+〖TEF〗_2+〖TEF〗_3+⋯+〖TEF〗_12)/12=1.12 (21)
Then, the average standard deviation of the TEF can be calculated with the equation
s=√((∑_(i=1)^N▒(〖TEF〗_i-(TEF)¯)^2)/N(N-1))=1.07(22)
Therefore, the TEF value was 1.12 ± 1.07. Then, the error in the form of percentage can be calculated using the following equation:
1.07/1.12×100=0.94%

The overall error results for the TEF vortex generator with placement variations (in-line and staggered), Re and amount of VG sets (one, two and three) are are listed inTable 6.

Table 6. Overall error TEF

Variasi Vortex Generator (Berlubang)	Overall Error TEF
1 RWP in-line	0.47 %
2 RWP in-line	0.47%
3 RWP in-line	0.43%
1 RWP staggered	0.47%
2 RWP staggered	0.47%
3 RWP staggered	0.43%
1 CRWP in-line	0.45%
2 CRWP in-line	0.45%
3 CRWP in-line	0.42%
1 CRWP staggered	0.45%
2 CRWP staggered	0.45%
3 CRWP staggered	0.41%

First, find the average CBR of the experimental results with the following formula.
(CBR)¯=(〖CBR〗_1+〖CBR〗_2+〖CBR〗_3+⋯+〖CBR〗_12)/12=2.14 (23)

The average standard deviation of the pressure drop CBR can then be calculated using the following equation:
s=√((∑_(i=1)^N▒(〖CBR〗_i-(CBR)¯)^2)/N(N-1))=1.60(24)
The CBR value is 2.14 ± 1.60. Then the error in the form of percentage can be calculated using thefollowing equation:
1.60/2.14×100=0.63%
The overall error results for the CBR vortex generator with placement variations (in-line and staggered), Re and amount of VG sets (one, two and three) are listed in Table 7

Table 7. Overall error CBR

Variasi Vortex Generator (Berlubang)	Overall Error CBR
1 RWP in-line	0.32%
2 RWP in-line	0.29%
3 RWP in-line	0.45%
1 RWP staggered	0.32%
2 RWP staggered	0.31%
3 RWP staggered	0.45%
1 CRWP in-line	0.4%
2 CRWP in-line	0.42%
3 CRWP in-line	0.56%
1 CRWP staggered	0.43%
2 CRWP staggered	0.42%
3 CRWP staggered	0.66%

Reference

[1]S. Caliskan, S. Şevik, and Ö. Özdilli, “Heat transfer enhancement by a sinusoidal wavy plate having punched triangular vortex generators,” International Journal of Thermal Sciences, vol. 181, p. 107769, Nov. 2022, doi: 10.1016/J.IJTHERMALSCI.2022.107769.
[2]A. J. Modi and M. K. Rathod, “Comparative study of heat transfer enhancement and pressure drop for fin-and-circular tube compact heat exchangers with sinusoidal wavy and elliptical curved rectangular winglet vortex generator,” Int J Heat Mass Transf, vol. 141, pp. 310–326, Oct. 2019, doi: 10.1016/J.IJHEATMASSTRANSFER.2019.06.088.
[3]Y. Effendi, A. Prayogo, Syaiful, M. Djaeni, and E. Yohana, “Effect of perforated concave delta winglet vortex generators on heat transfer and flow resistance through the heated tubes in the channel,” Experimental Heat Transfer, vol. 35, no. 5, pp. 553–576, 2022, doi: 10.1080/08916152.2021.1919245.
[4]M. T. Al-Asadi, F. S. Alkasmoul, and M. C. T. Wilson, “Benefits of spanwise gaps in cylindrical vortex generators for conjugate heat transfer enhancement in micro-channels,” Appl Therm Eng, vol. 130, pp. 571–586, Feb. 2018, doi: 10.1016/J.APPLTHERMALENG.2017.10.157.
[5]J. F. Zhang, Y. K. Joshi, and W. Q. Tao, “Single phase laminar flow and heat

transfer characteristics of microgaps with longitudinal vortex generator array," Int J Heat Mass Transf, vol. 111, pp. 484–494, Aug. 2017, doi: 10.1016/J.IJHEATMASSTRANSFER.2017.03.036.
[6]E. Hosseinirad, M. Khoshvaght-Aliabadi, and F. Hormozi, "Evaluation of heat transfer and pressure drop in a mini-channel using transverse rectangular vortex-generators with various non-uniform heights," Appl Therm Eng, vol. 161, p. 114196, Oct. 2019, doi: 10.1016/J.APPLTHERMALENG.2019.114196.

Reviewer 3: In connection with climate change and an increase in the average annual temperature on Earth, there is a new danger of the negative impact of high temperatures on human life.
In this case, the improvement of air conditioning systems, including the search for the best thermal enhancement factor, cost-benefit ratio, etc., takes on a new sense, which is one of the main targets of this article. The topic is timely and of great practical significance to environmental protection, enhancing safety, and people's life comfort.
The manuscript is well-structured and includes all necessary parts.
Two key strengths of the paper are a good introduction section and an analysis and discussion of the results. Both research objectives and content are clear. The key scientific issues to be solved are moderate. The research experimental method is reasonable.

There are also several shortages worthy to be mentioned:
Seriously revise the formulas
If you use an italic font in formulas, use an italic font in their descriptions. For example, in formula (1), the Nusselt number (Nu) and friction factor (f); in formula (3), heat transfer coefficient (h). It may confuse the reader.

Thank you for the corrections. For formula and description fonts, improvements have been made where all formula and description fonts are italicized consistently.

The Nusselt numbers in formula (1) and formula (2) have different designations. It may confuse the reader.

Thanks for the correction. Consistent improvements have been made to writing the Nu symbol on paper.

What are Nusselt number and friction factor with subscript 0 in formula (1)?

Thanks for the corrections. The subscript 0 for Nusselt number and friction factor is meant for the baseline condition. This additional explanation has been added to the paper. The following is an explanation of formula 1.

TEF= ((Nu/〖Nu〗_0))/(f/f_0)^(1/3) (1)

Di mana: 〖Nu〗_0= Nusselt number pada kondisi baseline
f_0 = friction factor pada kondisi baseline

In formula (5), a pressure drop is the lowercase letter Δp, but in formula (6), a pressure drop is uppercase ΔP. Are these different pressures?

Thank you for the corrections. I'm so sorry for the error in writing the pressure drop symbol which is inconsistent. Improvements in writing pressure drop have been made with uppercase P for the formula on the paper.

What is the error of pressure drop measurement with the Fluke 922 Airflow Micromanometer described in section "3.2 Effect of perforated vortex generators on pressure drop"? Did it cover the necessary range of pressures to be investigated? Could micromanometer error have affected the conclusions of the section? Because the pressure drop values of 4.58 Pa, 5 Pa and 5.4 Pa are close to each other.

Thanks for the question. Pressure measurement errors with the Fluke 922 Airflow Micromanometer are explained in the uncertainty analysis section with the calculation results as below.
From the test in the baseline case with a speed of 2.0 m/s, the results of the pressure drop are listed in Table 4, which show that the average P can be calculated as follows:
(ΔP)¯=(〖ΔP〗 _1+ 〖ΔP〗 _2+ 〖ΔP〗 _3+⋯+ 〖ΔP〗 _30)/30=3.51 Pa(19)
The average standard deviation of the pressure drop can then be calculated using the equation
s=√((∑_(i=1)^N▒(〖ΔP〗 _i-(ΔP)¯)^2)/N(N-1))=8.9×10^(-5)(20)
Baseline case for the pressure drop value at a speed of 2.0 m/s is 3.51±8.9×10^(-5) Pa. Then, the error in the form of percentage can be calculated using the following equation:
(8.9×10^(-5))/3.51×100=0.71

Table 4 Baseline pressure drop data at a speed of 2.0 m/s
ΔP (Pa)
Data to2.0 m/sData to2.0 m/s
10.013160.012
20.013170.013
30.013180.012
40.013190.012
50.012200.013
60.013210.013
70.013220.012
80.012230.013
90.013240.012
100.013250.013
110.013260.013
120.013270.013
130.012280.013
140.012290.012
150.013300.012

The equal calculation approach changed into used for all data. Therefore, the overall error outputs for the pressure-drop vortex generator with placement variations (in-line and staggered), Re and amount of VG sets (one, two and three) are listed in Table 5.
Table 5. Overall Pressure Drop (ΔP)
Vortex Generator VariationsOverall Error P
(perforated)
1 PRWP in-line2.94%
2 PRWP in-line2.87%
3 PRWP in-line1.98%
1 PRWP staggered2.88%
2 PRWP staggered2.34%
3 PRWP staggered1.36%
1 PCRWP in-line2.72%
2 PCRWP in-line1.80%
3 PCRWP in-line1.80%
1 PCRWP staggered2.43%
2 PCRWP staggered1.91%

3 PCRWP staggered0.97%

The results of the measurement error calculation are still below the maximum accuracy limit of the tool by 5% so that it does not affect the conclusion section.

The measurement error in the section "3.3 Effect of perforated VGs on thermal enhancement factor" and "Effects of perforated VGs on the cost-benefit ratio" is not clear. Can you show the error bar or describe it in the description?

Thanks for the question. The measurement error for the thermal increase factor and the cost benefit ratio has been added to the explanation in the paper in the data uncertainty section, as follows.
error bar TEF
The average TEF results from the experimental results can be calculated as follows.
$(TEF)^{-}=(〖TEF〗_1+〖TEF〗_2+〖TEF〗_3+\cdots+〖TEF〗_12)/12=1.12$ (21)
Then, the average standard deviation of the TEF can be calculated with the equation
$s=\sqrt{((\sum_{i=1)^N(〖TEF〗_i-(TEF)^{-})^2)/N(N-1)}}=1.07$(22)
Therefore, the TEF value was 1.12 ± 1.07. Then, the error in the form of percentage can be calculated using the following equation:
1.07/1.12×100=0.94%
The overall error results for the TEF vortex generator with placement variations (in-line and staggered), Re and amount of VG sets (one, two and three) are are listed inTable 6.
Table 6. Overall error TEF

Variasi Vortex Generator (Berlubang)	Overall Error TEF
1 RWP in-line	0.47 %
2 RWP in-line	0.47%
3 RWP in-line	0.43%
1 RWP staggered	0.47%
2 RWP staggered	0.47%
3 RWP staggered	0.43%
1 CRWP in-line	0.45%
2 CRWP in-line	0.45%
3 CRWP in-line	0.42%
1 CRWP staggered	0.45%
2 CRWP staggered	0.45%
3 CRWP staggered	0.41%

b error bar CBR
First, find the average CBR of the experimental results with the following formula.
$(CBR)^{-}=(〖CBR〗_1+〖CBR〗_2+〖CBR〗_3+\cdots+〖CBR〗_12)/12=2.14$ (23)

The average standard deviation of the pressure drop CBR can then be calculated using the following equation:
$s=\sqrt{((\sum_{i=1)^N(〖CBR〗_i-(CBR)^{-})^2)/N(N-1)}}=1.60$(24)
The CBR value is 2.14 ± 1.60. Then the error in the form of percentage can be calculated using thefollowing equation:
1.60/2.14×100=0.63%
The overall error results for the CBR vortex generator with placement variations (in-line and staggered), Re and amount of VG sets (one, two and three) are listed in Table 7.
Table 7. Overall error CBR

Variasi Vortex Generator (Berlubang)	Overall Error CBR
1 RWP in-line	0.32%
2 RWP in-line	0.29%
3 RWP in-line	0.45%
1 RWP staggered	0.32%
2 RWP staggered	0.31%
3 RWP staggered	0.45%
1 CRWP in-line	0.4%
2 CRWP in-line	0.42%
3 CRWP in-line	0.56%
1 CRWP staggered	0.43%

	2 CRWP staggered0.42% 3 CRWP staggered0.66% In my humble opinion, the section "3.5 Flow visualisation" is better presented first in section "3. Results and Discussion". Thanks for the suggestions. The discussion of section 3.5 on visualization has been moved to the earlier section to 3.1 in the paper. We tried our best to improve the manuscript and made some changes in the revised paper, and here we did not list the specific changes but marked in red in revised paper. We appreciate for Editors and Reviewrs' warm work earnestly, and hope that the correction will meet with approval. Once again, thank you very much for your comments and suggestions. Yours Sincerely Oktarina Heriyani
Additional Information:	
Question	**Response**
Results in Engineering is an open access journal which charges an Article Publishing Charge (APC) to cover the cost associated with the publication process. All articles published Open Access will be immediately and permanently free on ScienceDirect for users to read, download, and use in accordance with the author's selected Creative Commons user license. **As an Author, I acknowledge I need to pay the Article Publishing Charge if my manuscript is accepted for publication.**	Yes
Please enter the **Word Count** of your manuscript	
Result in Engineering is an open access journal which charges an Article Publishing Charge (APC) to cover the cost associated with the publication process. All articles published Open Access will be immediately and permanently free on ScienceDirect for users to read, download, and use in accordance with the author's selected Creative Commons user license. **Please note that there is a fee if your manuscript is accepted for publication.**	Yes

CRediT author statement

Oktarina Heriyani: Conceptualization, Methodology, Investigation, Writing – Original Draft preparation.: **Mohammad Djaeni**: Supervision – Reviewing and Editing.: **Syaiful**: Conceptualization, Writing – Reviewing and Editing, Conceptualization.: ***Aldila Kurnia Putri****:* Visualization, Validation.

Declaration of interests

☒The authors declare that they have no known competing financial interests or personal relationships that could have appeared to influence the work reported in this paper.

☐The authors declare the following financial interests/personal relationships which may be considered as potential competing interests:

HIGHLIGHTS

- Perforated vortex generators installed to increase heat transfer and reduce pressure drop through six heated tubes to the air stream.
- Perforated concave rectangular winglets compared with perforated rectangular winglet pairs vortex generator mounted on rectangular plates were investigated experimentally.
- Perforated concave rectangular winglets improve thermal performance better than perforated rectangular winglet pairs vortex generators.
- The best thermal performance improvement is at the lowest cost benefit ratio.

Perforated concave rectangular winglet pair vortex generators enhance the heat transfer of air flowing through heated tubes inside a channel

Oktarina Heriyani[*12], Mohammad Djaeni[1], Syaiful[*1], Aldila Kurnia Putri[1]
[1]Mechanical Engineering Department, Engineering Faculty, University of Diponegoro, Semarang, Indonesia
[2]Mechanical Engineering Program, Engineering Faculty, University of Muhammadiyah Prof. DR. HAMKA, Jakarta, Indonesia

Abstract

A significant increase in the rate of heat transfer in a heat exchanger system is made possible by increasing the convection heat-transfer coefficient using a passive method. The addition of vortex generators (VGs) to the fins and tubes of the heat exchanger is currently the most effective passive method. However, the augment in heat is accompanied by an increase in pressure drop. Therefore, in this study, we installed perforated concave rectangular winglet pair vortex generators (PCRWP VGs) on plates in rectangular ducts to increase the heat transfer through the six heated tubes to the air stream with lowering the enhance in pressure drop. We sought to decide the best cost-benefit ratio (CBR) with the difference in fluid flow velocity from 0.4 to 2 m/s with 0.2 m/s intervals in the ducts. PCRWP VGs were composed using in-line and staggered configurations. The outcomes showed a lower CBR (3.56) for the in-line configuration than staggered. Moreover, the lowest CBR was accompanied by a thermal performance (TEF) increase of 1.29.

1. Introduction

The global energy demand is expected to triple in the next few years. The main driver is the increasing use of air conditioning (AC) machines, according to a statement by the International Energy Agency (IEA) [1]. Thus, promoting energy efficiency in air conditioners becomes important, which requires us to maximise their thermal performance. Improving the thermal performance of an air conditioner involves increasing the rate of heat transfer in its main component, the condenser. A condenser commonly used in air conditioners comprises a fin and tube, which function as a refrigerant cooling medium. However, the high thermal resistance (reaching 75%) of the fin air side of the condenser lowers the heat transfer rate in the heat exchanger [2]. That thermal resistance must be lowered to enhance the heat transfer rate.

One of the most commonly used active methods to increase the rate of heat transfer is adding vortex generators (VGs), which according to the research results of Mugisidi et al., increases the performance of a condenser [3]. The added VGs cause longitudinal vortices (LVs), damage the primary flow, make the second flow as large as the first, and increase the air mixing in the area [4,5]. The size of the LVs, shape of the flow, and mixing formed are influenced by the shape, geometry, and position of the VGs added to the fins and tubes of the heat exchanger [6].

Samidifat et al., in their research, showed that simple rectangular vortex generators (RVGs) can increase the heat transfer rate by 7%, although this causes a pressure drop in the heat exchanger system [7]. Meanwhile, modified RVGs with a concave shape on the front and rear surfaces decrease the heat transfer performance of the heat exchanger tube. A better option is RVGs with a double convex front surface and a single concave back surface, which can strengthen the primary vortex, thus increasing the rate of heat transfer from the plate to the fluid, as demonstrated in a study by Kashyap et al. [8]. Further research conducted by Kashyap et al. in the same year concluded that modifying the surface shape of RWVGs can create longitudinal eddies that interact with the boundary layer, increasing the rate of convection heat transfer [9]. The increase in the optimal heat transfer rate, based on their research, is 14.4. Beyond this, Song et al. attempted to compare changes in the rate of heat transfer in a heat

exchanger system paired with concave or convex curved, delta winglet VGs [10]. The results showed that the concave VGs could improve heat transfer better than the convex VGs. Yet, it is not only the difference in shape that affects the change in the heat transfer rate; changes in the geometry of VGs also play a role.

Research conducted by Zeeshan et al. showed that increasing the angle of attack increased the rate of heat transfer (to 37.01–64.54%) if a pair of rectangular winglet vortex generators (RWVGs) were placed at the back of the tube; yet, this did not reduce the pressure drop [11]. Beyond this, the number of pairs of RWVGs affected the increase in heat transfer, as discovered by Oheriyani et al., with a 15.17% better hydraulic thermal performance for three pairs of RWVGs compared to the baseline [12]. The more pairs of VGs placed in the crossflow, the higher the increase in the heat transfer rate, as found by Wang et al. [13]. A study by Sun et al. further discovered that increasing the number of RWVGs in the heat exchanger tube increased the heat transfer, with a maximum thermal enhancement factor (TEF) of 1.27 [14]. The TEF value of a V delta winglet VG, meanwhile, reached 1.82–3% higher than a V rectangular winglet VG, as revealed by Promvonge et al. [15]. These results were obtained with the optimal blockage ratio (BR)=0.15 and pitch ratio (PR)=1.0. Elsewhere, Skullong et al. modified the shapes of RWVGs with optimal BRs and PRs to achieve an optimum heat transfer performance and reduced pressure drop; their shape modification involved perforating RWVGs [16].

The positions of the holes in RWVGs do not significantly affect the increase in heat transfer, but it greatly affects the flow resistance of VGs. The heat transfer rate increases as the height (vertical position) of the hole increases. Width-wise, although there is an initial increase, the heat transfer rate decreases with increasing lateral distance [17]. An increase in the number of holes in RWVGs indicates an increase in fluid flow; this forces fluid to flow behind RWVGs, which increases the heat transfer [18]. The heat transfer rate increases during laminar flow when the Reynolds number (Re) increases, then decreases with an increase in Re during turbulent flow [19]. Positioning the tube in-line, with a pair of RWVGs in a common flow-down configuration, provides better performance than the common flow-up [20]. However, a staggered tube position is superior to this, resulting in a 25.85% higher heat-transfer performance than when a pair of RWVGs is not used [21].

In the existing studies, no detailed analyses of heat transfer were carried out from the surfaces of several cylinders heated and arranged in-line when using a perforated vortex generator. Therefore, this study focused on investigating the advantages of using perforated concave rectangular winglet pair vortex generators (PCRWP VGs) to increase the heat transfer of airflow through heated tubes arranged in-line in the ducts.

2. Experimental Approach

2.1 Experimental setup

This research was conducted experimentally with a test equipment scheme comprising a rectangular channel sized 370 x 18 x 8 cm. The duct was made of 1 cm-thick glass, as shown in Figure 1.

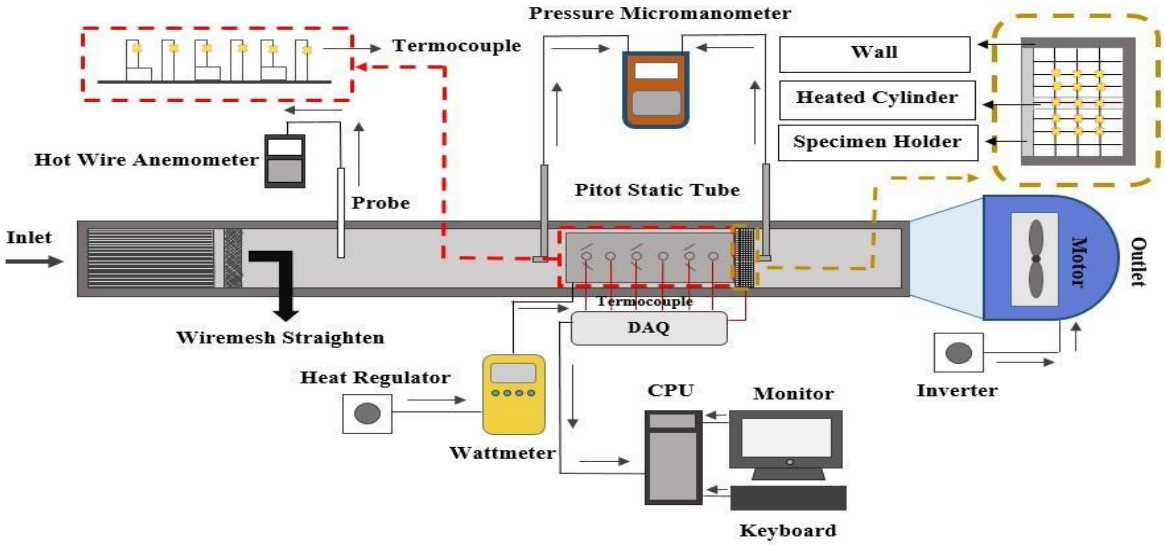

Figure 1 Experimental Tool Schematic

Based on Figure 1 is equipped with a blower (50 Hz, Wipro with a rated voltage of 220V), an inverter (Mitsubishi Electric type FR-D700 with an accuracy of 0.01), a straightener, a hot wire anemometer (Lutron type AM-4204 with an accuracy of 0.1), heater regulator, wattmeter (Lutron DW-6060 with an accuracy ± 1.0), thermocouple (K type with a temperature interval of -200 –1250 ℃ and an accuracy ± 0.5), data acquisition (Advantech USB-4718 type with an accuracy of 0.001), CPU, pressure micromanometer (Fluke type 922 with an accuracy of 0.05), and micromanometer.

The test in this experiment varied the inlet air velocity from 0.4 to 2 m/s with 0.2 m/s intervals. Air flowing at a constant heat rate of 40 W passed through six cylindrical tubes with a diameter of 19.05 mm and a height of 65.8 mm. The six cylindrical tubes were composed in-line with 60 mm between the centers of the cylinders.

The VGs used as test specimens were perforated rectangular winglet pair and perforated concave rectangular winglet pair types sized 30 x 30 mm. The VGs were be assembled on aluminium plates measuring 500 x 155 x 1 mm in one, two, or three pairs. Naik et al. verified the merits of using rectangular, winglet pair vortex generators with a CFD configuration to improve the heat transfer rate [22]. Thus, the VGs pairs were divided into in-line and staggered arrangements, with a common flow-down (CFD) configuration, as shown in Figure 2. We fixed our angle of attack at 15° since Lu and Zhai represented that reaps the best hydraulic thermal performance [23].

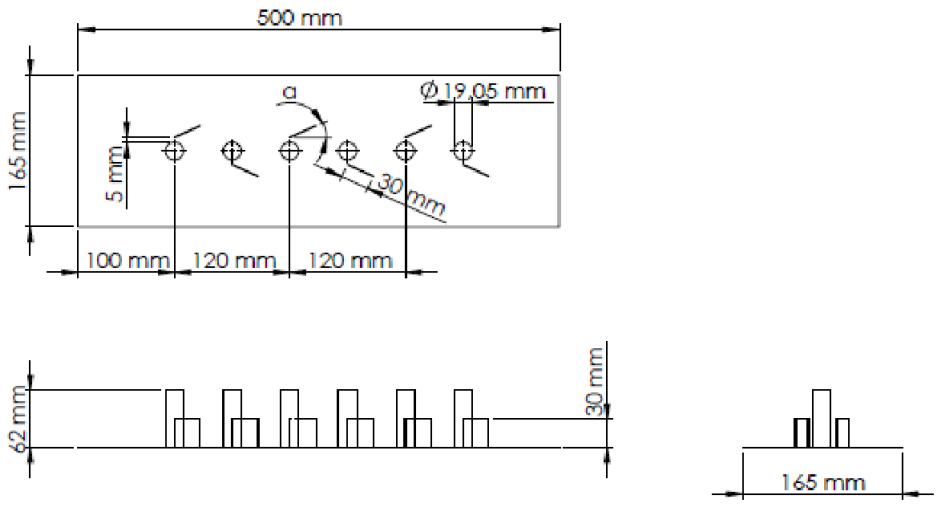
500 mm
a
Ø 19,05 mm
165 mm
5 mm
30 mm
100 mm
120 mm
120 mm
62 mm
30 mm
165 mm

(a)

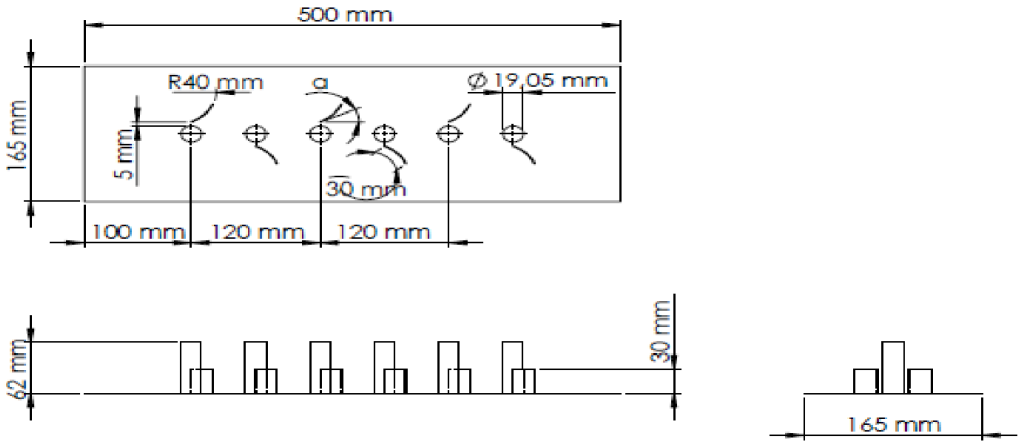
500 mm
R40 mm
a
Ø 19,05 mm
165 mm
5 mm
30 mm
100 mm
120 mm
120 mm
62 mm
30 mm
165 mm

(b)

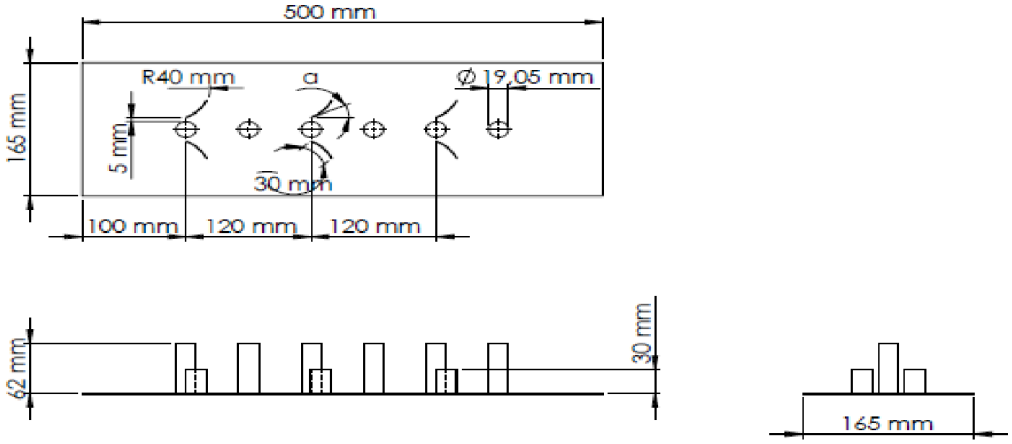
500 mm
R40 mm
a
Ø 19,05 mm
165 mm
5 mm
30 mm
100 mm
120 mm
120 mm
62 mm
30 mm
165 mm

(c)

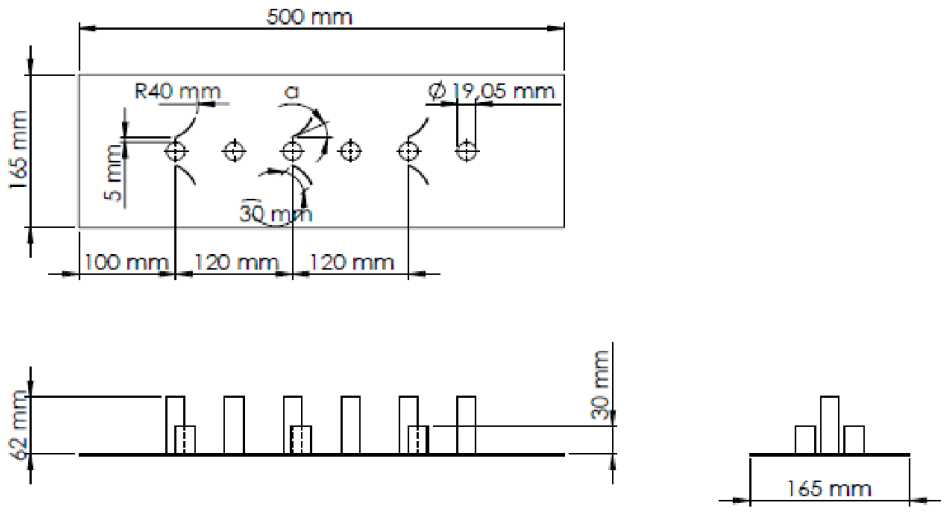

(d)

Figure 2 Arrangement of test specimens; rectangular winglet vortex generators with (a) staggered or (b) in-line arrangement; concave rectangular winglet vortex generators with (c) staggered or (d) in-line arrangement

2.2 Parameter definitions

The parameters in this study were derived from the equation used by Oneissi et al. to obtain the Thermal Enhancement Factor (TEF) [24], namely

$$TEF = \frac{\frac{Nu}{Nu_0}}{\left(\frac{f}{f_0}\right)^{\frac{1}{3}}} \quad (1)$$

The Nusselt number (Nu) and friction factor (f), based on the research of Zeeshan et al., were formulated via equations (2) and (3) [11]

$$N_u = \frac{Q}{A_t \Delta T_{LMTD}} \cdot \frac{D_h}{k} \quad (2)$$

where Q, A_t, ΔT_{LTMD}, D_h, and k are the convection heat transfer rate, surface area, log mean temperature difference, hydraulic diameter, and thermal conductivity, respectively.

$$f = \frac{2\,\Delta P\, D_h}{\rho\, V^2\, (L+6D)} \quad (3)$$

where $\rho, V,$ and L are the density of the air, velocity of the inlet airflow, and length of the test specimen plate, while the convection heat-transfer coefficient (h) is counted by the equation

$$h = \frac{N_u\, k}{D_h} \quad (4)$$

The further equation required to determine the cost-benefit ratio (CBR), defined as the ratio of pressure drop per variation in Nu number, as formulated by Tian et al. [25], is as follows

$$CBR = \frac{\%\Delta p}{\%Nu} \quad (5)$$

This concept investigates whether or not the method used to enhance the heat transfer rate is economically efficient. In the hydrodynamic test, the pressure drop (ΔP) P is measured by the pressure difference on the sides of the *inlet* (P_{inlet}) and *outlet* (P_{outlet}) of the test specimen in the tested part, using equation (6):

$$\Delta P = P_{inlet} - P_{outlet} \quad (6)$$

2.3 Validation

To ensure that the experimental procedure was sound, validation was done by comparing the current experiment with baseline conditions. Those were determined using the experimental results for the Nusselt number (Nu) from the works of Whitaker [26] and Syaiful et al. [27], which both showed the same trend, where Nu increased with an increasing Reynolds number (Re) from 2000 to 10,000.

3. Results and Discussion

3.1 Effect of perforated vortex generators on heat transfer

The increase in the convection heat transfer was due to the mixing of fluids caused by strong LVs [28]. The strength of the LVs is caused by the number of pairs of VGs. Increasing the number of pairs of VGs in the test specimen can increase the coefficient value of the convection heat transfer [29], as shown in Figure 3.

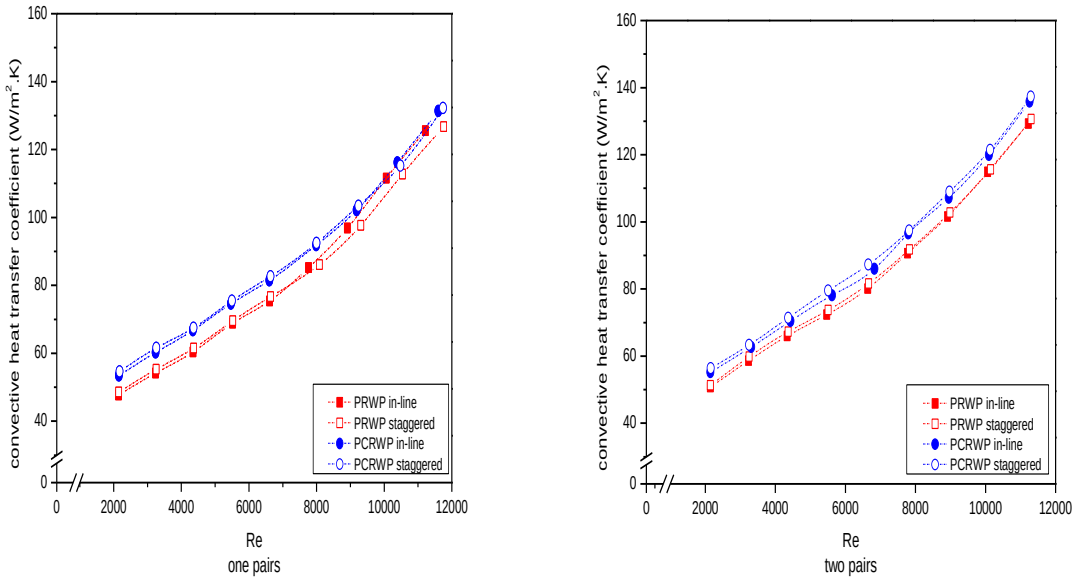

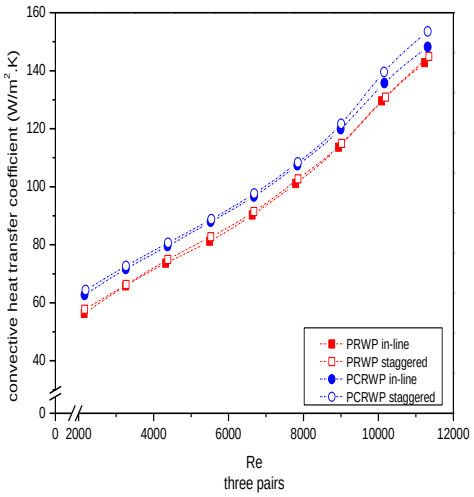

(c)

Figure 3 Graphs of convective heat-transfer coefficient against Reynolds number; (a) one, (b) two, (c) three pairs

In Figure 3, we can see the convective heat-transfer coefficient with respect to the Reynolds number (Re), analysed after installing PCRWP VGs or (non-concave) perforated, rectangular, winglet pair vortex generators (PRWP VGs), with one, two, and three pairs, arranged in-line or staggered. Based on Figure 3, it can be seen that there was an increase in the heat transfer with a rise in Re due to an increase in flow vortices and high turbulence intensity in the channel [30], alongside a reduction in the wage region and stagnation area [31] for each increase in flow velocity. The increase in heat transfer for staggered VGs was better than in-line for PCRW VGs with any number of pairs at the highest Re (11,000). The results in Figure 3 show that the PCRWP VGs worked better than the PRWP VGs, and the staggered arrangement of the former with three pairs gave the highest yield, of 153.5 W/m^2.K, as shown in Figure 3(c). Meanwhile, two PCRW pairs (137.33 W/m^2.K, Figure 3(b)) were better than one (132.25 W/m^2.K, Figure 3(a)) because VGs with a concave surface destabilise the centrifugal force of the fluid flow, which strengthens the flow vortices. This makes the mixing of the hot fluid near the wall with the cold fluid of the main flow more robust [32,33].

3.2 Effect of perforated vortex generators on pressure drop

The use of VGs can affect the increase in heat transfer, but there is often an accompanying increase in pressure drop, as shown in Figure 4 where an increase in pressure drop can be seen along with the increases in Re and pair numbers for both the VG types, PCRW and PRW. This was caused by the resistance to fluid flow against the walls of the VGs and the addition of the frontal area of VGs in the next pair arrangement [34]. The pressure drop in the staggered arrangement was lower than in the in-line one, while the PRW VGs type created a lower pressure drop than the PCRW VGs due to the latter reducing the frontal area hit by the airflow, resulting in a decrease in drag [35]. In addition, jet flow from the VG hole can reduce the stagnation flow, which can, in turn, reduce the pressure drop [36]. A significant decrease noted in the pressure drop was due to the VGS perforation used [37]. The best pressure drop value for one pair with a staggered arrangement was 4.58 Pa (see Figure 4(a)), while two pairs (5 Pa, Figure 4(b)) were better than three (5.4 Pa, Figure 4(c)).

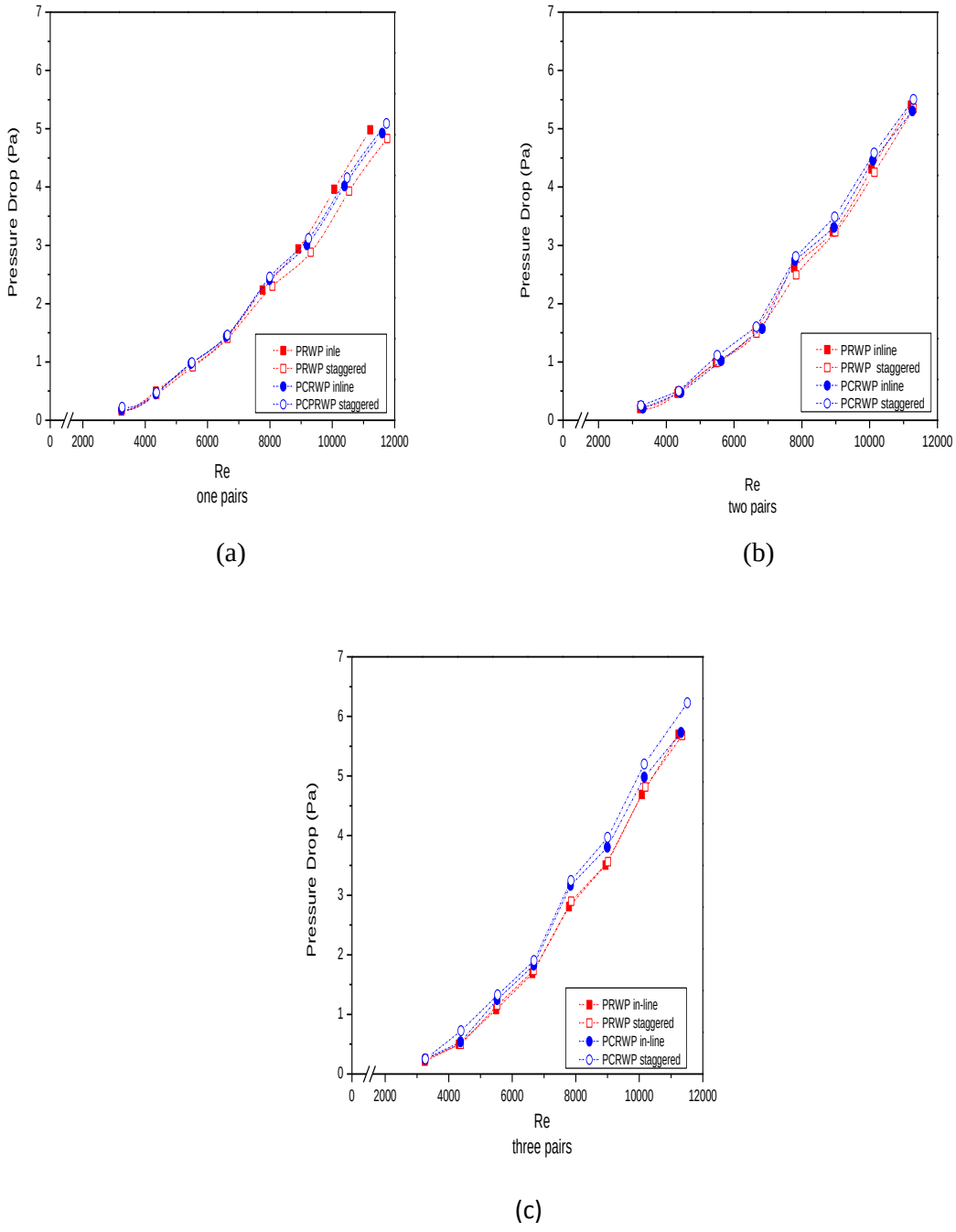

Figure 4 Graph of pressure drop against Reynolds number; (a) one, (b) two, (c) three pairs

3.3 Effect of perforated VGs on thermal enhancement factor

The TEF showed the hydraulic thermal performance while using VGs, which played a role in restructuring the incoming fluid flow pattern. The increase in TEF was due to the influence of complex overlapping structures, which meant the flow developed into a turbulent structure, greatly affecting the heat transfer increase [38]. The experimental TEF values are shown in Figure 5.

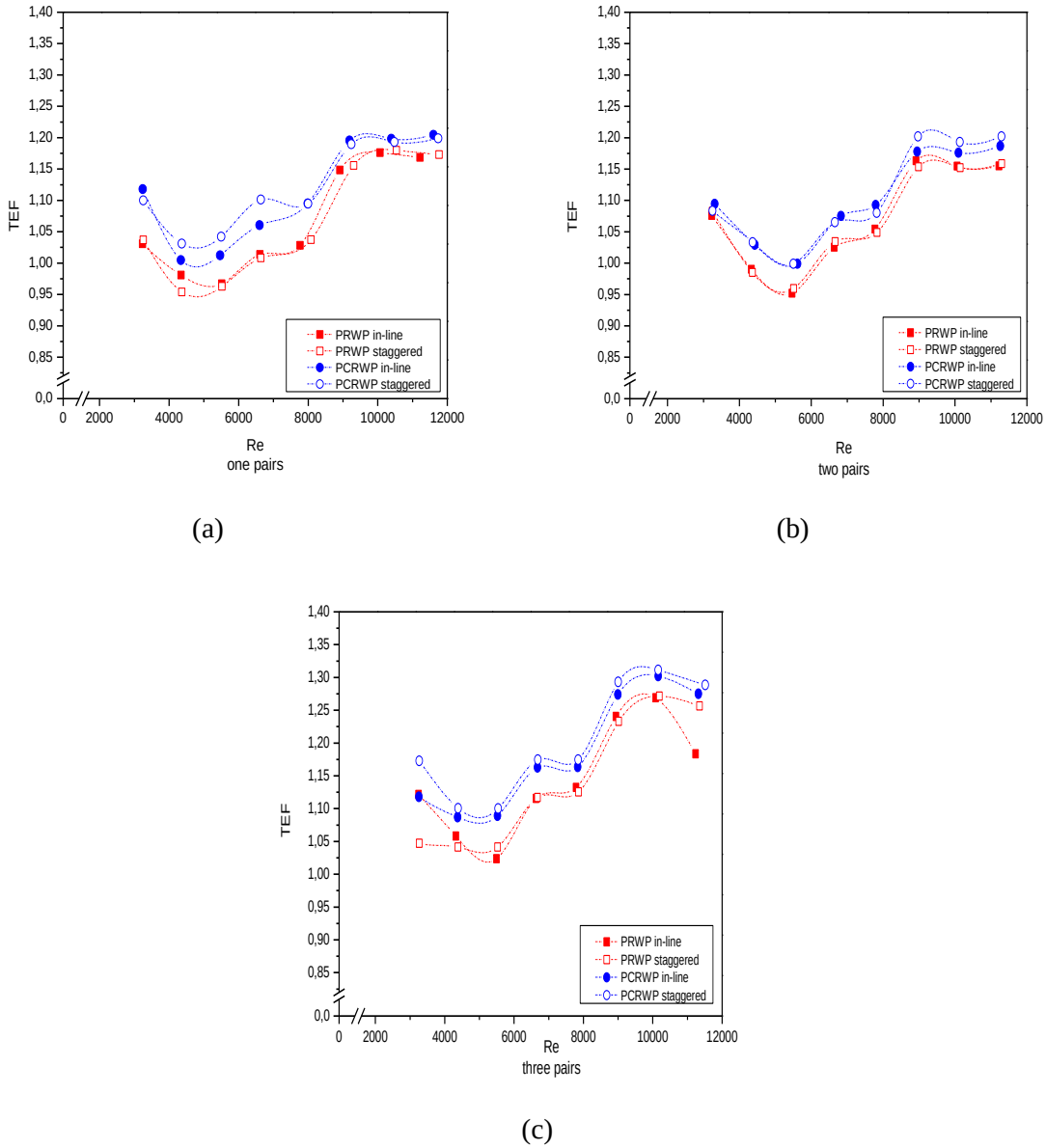

Figure 5 Graph of thermal enhancement factor against Reynolds number; (a) one, (b) two, (c) three pairs

It can be seen in Figure 5 that there was an increase in TEF with greater pairs of VGs used for both PCRW and PRW VGs. This happened because PCRW produced wider flow vortices, which reduced the wake region behind the cylinder, thereby reducing the recirculation zone, which impacted the heat transfer increase from the rear cylinder surface to the flow [39]. In this process, the large of longitudinal vortices with high intensities can reduce the wake area, which increases the flow velocity downstream of the tube and reduces the recirculation region, leading to an increased heat transfer rate in the region [40,41]. Based on Figure 5, the best TEF increase occurred at Re 8000–9000. The best TEF values with one, two, or three pairs occurred in the staggered arrangement with PCRW VGs, at 1.18, 1.20, and 1.29, respectively (see Figure 5).

3.4 Effects of perforated VGs on the cost-benefit ratio

Economic evaluation cannot be carried out based just on the TEF and the net profit from the transferred unit's heat load [42]. Instead, it must be determined by evaluating the economic value of the heat transfer improvement, by calculating the CBR, as shown in Figure 6.

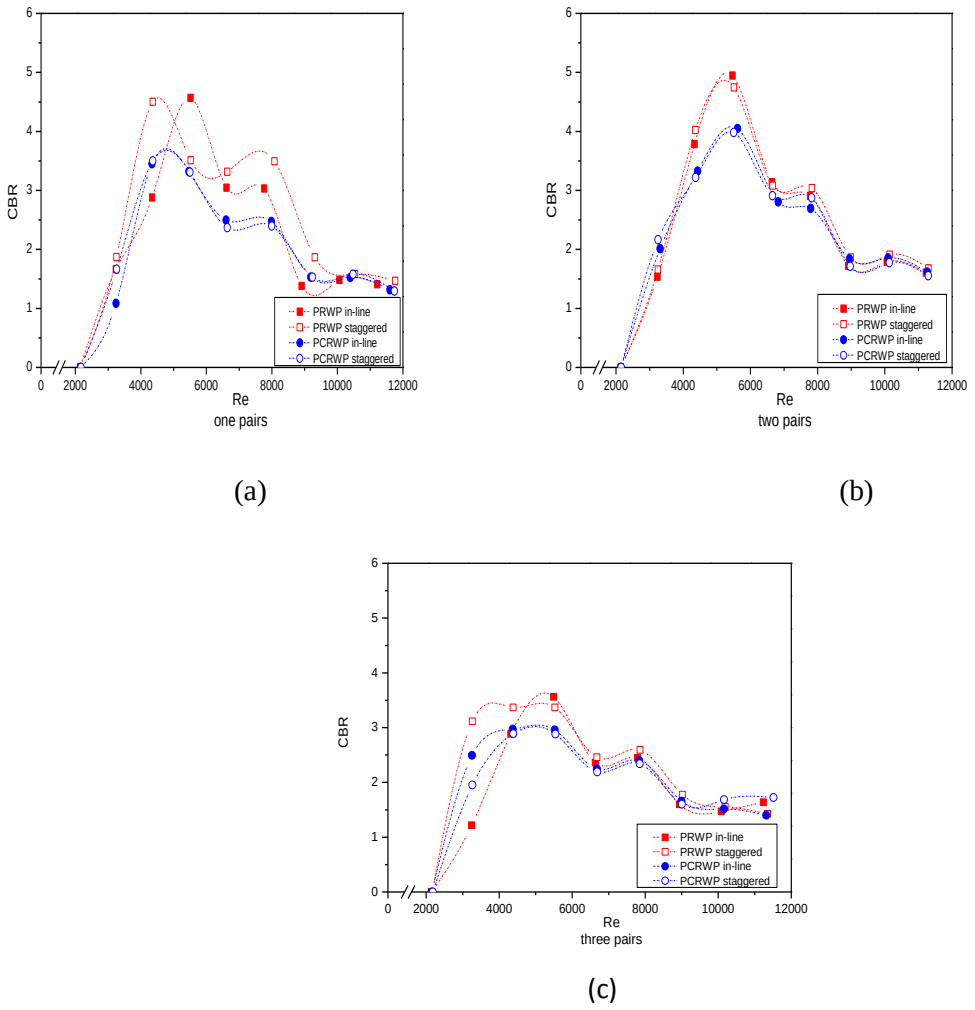

Figure 6 Graph of cost-benefit ratio against Reynolds number; (a) one, (b) two, (c) three pairs

Figure 6 is the result of the CBR calculation to compare the percentage raise in pressure drop with the percentage increase in the Nusselt number when using VGs. These results indicate that a lower CBR results in an improvement in thermal performance, which was higher than the drag force [25]. In Figure 6, the greatest increase in CBR values occurs with the PRW VGs, with an in-line arrangement, totalling 4.57, 4.95, or 3.56 for one, two, or three pairs, respectively. The lowest CBR value was measured when PCRW VGs, with a staggered arrangement and three pairs, were used. Three VG pairs showed a lower CBR than one and two pairs because they brought about the greatest increase in the Nusselt number, accompanied by a lower pressure drop increase, which lowered the CBR.

3.5 Flow visualisation

The flow visualisation test was carried out to observe the LV formed after the flow passed through the VGs in the rectangular channel. This test was conducted under low-light conditions to clarify the formed

LV. The laser beam was refracted by a cylindrical glass (diameter 5 mm), which produced a cross-sectional area perpendicular to the direction of flow. The smoke formed from the evaporation of the liquid was used to visualize the LV in the flow. The VGs used in this visualisation test were PRWP and PCRWP with an in-line arrangement, as can be seen in Figure 7.

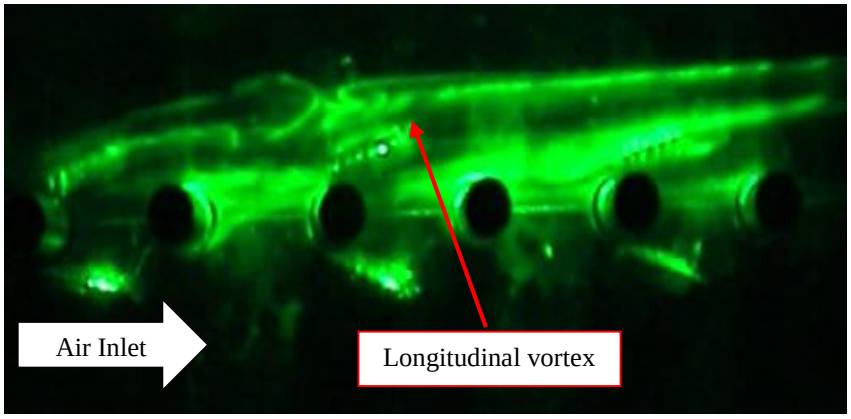

(a)

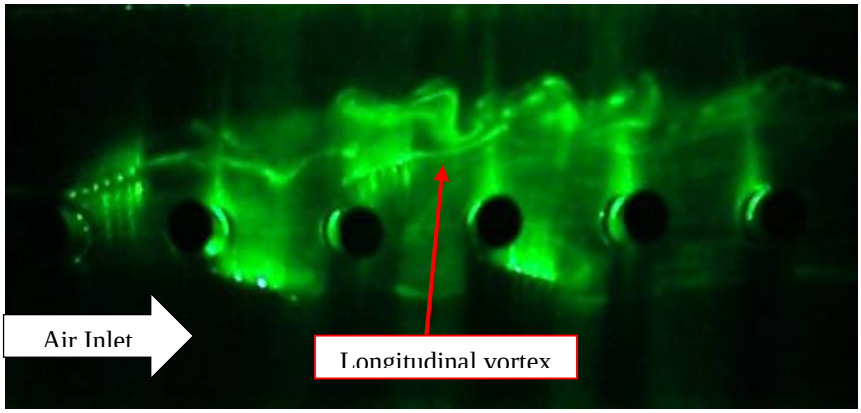

(b)

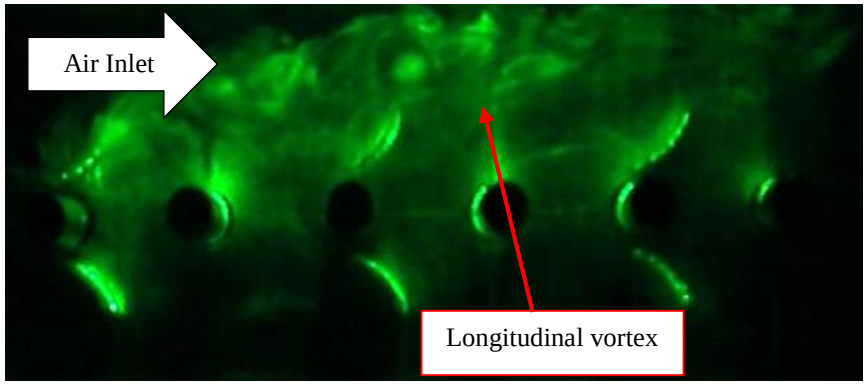

(c)

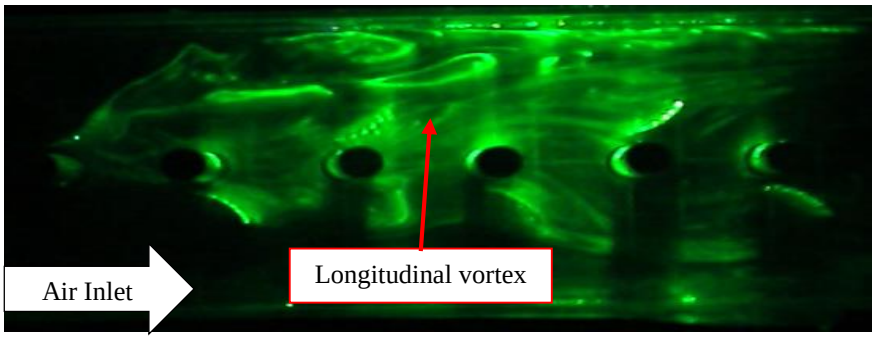

(d)

Figure 7 Visualisation of LV generated by (a) in-line (b) staggered PRWP (c) in-line (d) staggered PCRWP

In Figure 7 (c,d), the PCRWP VGs appear to produce LV in a wide flow area compared to the PRWP VGs in Figure 7 (a,b) downstream. The back region of the PCRWP VGs has a wider frontal surface area than the PRWP VGs. As a result, the mixing of near fluid the channel walls with the fluid in the mainstream is better, meaning the heat transfer rate is increased [32]. Downstream, the LV compression in the wake area increases the fluid flow velocity pass the cylindrical structure, thereby increasing the heat transfer rate from the channel surface to the fluid flow in the wake region [43]. The increase in heat transfer produced when using PCRWP VGs is better than with PRWP VGs.

3.6 Error analysis

The deviation (error) is the difference between the measured and actual values, which introduces uncertainty to a result. When using large amounts of data, scientific data-processing is necessary to determine the deviations (errors) that occurred during data collection, which may affect the results of analysis.

The deviation in the average pressure data was calculated using the following equation (7) [44, 45]

$$\overline{\Delta P} = \frac{\Delta P_1 + \Delta P_2 + \cdots + \Delta P_{30}}{30} \quad \textbf{(7)}$$

The next step calculated the mean standard deviation using equation (8) [44, 45]

$$S_{\Delta p} = \sqrt{\frac{\sum_{i=1}^{n} (\Delta P_i - \overline{\Delta P})^2}{N(N-1)}} \quad \textbf{(8)}$$

To calculate the overall error, equation (9) was used as follows [44, 45]

$$\%error_{\ \Delta P} = \left(\frac{S_{\Delta P}}{\overline{\Delta P}}\right) 100\% \quad \textbf{(9)}$$

The value of the overall error for VGs with holes was 0.97%, while the value of the overall error in the pressure drop for VGs with holes was 2.2%

Conclusion

Based on the experimental results for perforated concave rectangular winglet pair vortex generators (PCRWP VGs) use in increasing the heat transfer of airflow through heated tubes arranged in-line in

the duct, we conclude that using PCRWP VGs affects the convection heat transfer coefficient, pressure drop in achieving hydraulic thermal performance, and cost-benefit ratio. In our investigations, the best heat-transfer convection coefficient was 153.5 W/m^2.K for three pairs of PCRW VGs composed in a staggered manner. The greatest improvement in the pressure drop value (4.58 Pa), meanwhile, occurred for one pair of PCRW VGs arranged in a staggered manner, while the hydraulic thermal performance was best (1.29) in this experiment with three pairs of PCRW VGs composed in a staggered manner. Finally, the best CBR (3.56) was recorded again for three pairs of PCRW VGs composed in a staggered manner.

Acknowledgements

The authors would like to thank LEMLITBANG UHAMKA which has funded this research through internal grants from UHAMKA and UPPI UHAMKA what have contributed in facilitating translation and proof reading. The authors also thank the UNDIP thermofluidics laboratory, where the authors carried out this experiment.

Bibliography

[1] R. Sebayang, "AC Akan Jadi Pengkonsumsi Listrik Utama di Dunia," *CNBC Indonesia*. 2018.

[2] Z. Qian, Q. Wang, and J. Cheng, "Analysis of heat and resistance performance of plate fin-and-tube heat exchanger with rectangle-winglet vortex generator," *Int. J. Heat Mass Transf.*, vol. 124, pp. 1198–1211, 2018, doi: 10.1016/j.ijheatmasstransfer.2018.04.037.

[3] D. Mugisidi, O. Heriyani, P. H. Gunawan, and D. Apriani, "Performance improvement of a forced draught cooling tower using a vortex generator," *CFD Lett.*, vol. 13, no. 1, pp. 45–57, 2021, doi: 10.37934/cfdl.13.1.4557.

[4] A. J. Modi, N. A. Kalel, and M. K. Rathod, "Thermal performance augmentation of fin-and-tube heat exchanger using rectangular winglet vortex generators having circular punched holes," *Int. J. Heat Mass Transf.*, 2020, doi: 10.1016/j.ijheatmasstransfer.2020.119724.

[5] K. W. Song and T. Tagawa, "The optimal arrangement of vortex generators for best heat transfer enhancement in flat-tube-fin heat exchanger," *Int. J. Therm. Sci.*, 2018, doi: 10.1016/j.ijthermalsci.2018.06.011.

[6] C. Yu, H. Zhang, M. Zeng, R. Wang, and B. Gao, "Numerical study on turbulent heat transfer performance of a new compound parallel flow shell and tube heat exchanger with longitudinal vortex generator," *Appl. Therm. Eng.*, vol. 164, no. May 2019, p. 114449, 2020, doi: 10.1016/j.applthermaleng.2019.114449.

[7] M. Samadifar and D. Toghraie, "Numerical simulation of heat transfer enhancement in a plate-fin heat exchanger using a new type of vortex generators," *Appl. Therm. Eng.*, vol. 133, no. September 2017, pp. 671–681, 2018, doi: 10.1016/j.applthermaleng.2018.01.062.

[8] U. Kashyap, K. Das, and B. K. Debnath, "Effect of surface modification of a rectangular vortex generator on heat transfer rate from a surface to fluid," *Int. J. Therm. Sci.*, vol. 127, no. August 2017, pp. 61–78, 2018, doi: 10.1016/j.ijthermalsci.2018.01.004.

[9] U. Kashyap, K. Das, and B. K. Debnath, "Effect of surface modification of a rectangular vortex generator on heat transfer rate from a surface to fluid: An extended study," *Int. J. Therm. Sci.*, vol. 134, no. August, pp. 269–281, 2018, doi: 10.1016/j.ijthermalsci.2018.08.020.

[10] K. W. Song, T. Tagawa, Z. H. Chen, and Q. Zhang, "Heat transfer characteristics of concave and convex curved vortex generators in the channel of plate heat exchanger under laminar

flow," *Int. J. Therm. Sci.*, vol. 137, no. November 2018, pp. 215–228, 2019, doi: 10.1016/j.ijthermalsci.2018.11.002.

[11] M. Zeeshan, S. Nath, D. Bhanja, and A. Das, "Numerical investigation for the optimal placements of rectangular vortex generators for improved thermal performance of fin-and-tube heat exchangers," *Appl. Therm. Eng.*, 2018, doi: 10.1016/j.applthermaleng.2018.03.006.

[12] O. Heriyani, M. Djaeni, and . Syaiful, "Thermal-Hydraulic Performance Analysis by Means of Rectangular Winglet Vortex Generators in a Channel: An Experimental Study," *Eur. J. Eng. Technol. Res.*, vol. 6, no. 3, pp. 150–153, 2021, doi: 10.24018/ejers.2021.6.3.2424.

[13] C. Wang, Z. Wang, L. Wang, L. Luo, and B. Sundén, "Experimental study of fluid flow and heat transfer of jet impingement in cross-flow with a vortex generator pair," *Int. J. Heat Mass Transf.*, vol. 135, pp. 935–949, 2019, doi: 10.1016/j.ijheatmasstransfer.2019.02.024.

[14] Z. Sun, K. Zhang, W. Li, Q. Chen, and N. Zheng, "Investigations of the turbulent thermal-hydraulic performance in circular heat exchanger tubes with multiple rectangular winglet vortex generators," *Appl. Therm. Eng.*, 2020, doi: 10.1016/j.applthermaleng.2019.114838.

[15] P. Promvonge and S. Skullong, "Thermo-hydraulic performance in heat exchanger tube with V-shaped winglet vortex generator," *Appl. Therm. Eng.*, 2020, doi: 10.1016/j.applthermaleng.2019.114424.

[16] S. Skullong, P. Promthaisong, P. Promvonge, C. Thianpong, and M. Pimsarn, "Thermal performance in solar air heater with perforated-winglet-type vortex generator," *Sol. Energy*, vol. 170, no. June, pp. 1101–1117, 2018, doi: 10.1016/j.solener.2018.05.093.

[17] Z. Han, Z. Xu, and J. Wang, "Numerical simulation on heat transfer characteristics of rectangular vortex generators with a hole," *Int. J. Heat Mass Transf.*, vol. 126, pp. 993–1001, 2018, doi: 10.1016/j.ijheatmasstransfer.2018.06.081.

[18] A. J. Modi, N. A. Kalel, and M. K. Rathod, "Thermal performance augmentation of fin-and-tube heat exchanger using rectangular winglet vortex generators having circular punched holes," *Int. J. Heat Mass Transf.*, vol. 158, pp. 1–16, 2020, doi: 10.1016/j.ijheatmasstransfer.2020.119724.

[19] C. Luo, S. Wu, K. Song, L. Hua, and L. Wang, "Thermo-hydraulic performance optimization of wavy fin heat exchanger by combining delta winglet vortex generators," *Appl. Therm. Eng.*, 2019, doi: 10.1016/j.applthermaleng.2019.114343.

[20] H. Naik and S. Tiwari, "Thermodynamic performance analysis of an inline fin-tube heat exchanger in presence of rectangular winglet pairs," *Int. J. Mech. Sci.*, vol. 193, no. September 2020, p. 106148, 2021, doi: 10.1016/j.ijmecsci.2020.106148.

[21] H. Naik and S. Tiwari, "Thermal performance analysis of fin-tube heat exchanger with staggered tube arrangement in presence of rectangular winglet pairs," *Int. J. Therm. Sci.*, vol. 161, no. July 2020, p. 106723, 2021, doi: 10.1016/j.ijthermalsci.2020.106723.

[22] H. Naik and S. Tiwari, "Effect of winglet location on performance of fin-tube heat exchangers with inline tube arrangement," *Int. J. Heat Mass Transf.*, vol. 125, pp. 248–261, 2018, doi: 10.1016/j.ijheatmasstransfer.2018.04.071.

[23] G. Lu and X. Zhai, "Effects of curved vortex generators on the air-side performance of fin-and-tube heat exchangers," *Int. J. Therm. Sci.*, vol. 136, no. May 2018, pp. 509–518, 2019, doi: 10.1016/j.ijthermalsci.2018.11.009.

[24] M. Oneissi, C. Habchi, S. Russeil, T. Lemenand, and D. Bougeard, "Heat transfer enhancement of inclined projected winglet pair vortex generators with protrusions," *Int. J.*

Therm. Sci., vol. 134, no. August, pp. 541–551, 2018, doi: 10.1016/j.ijthermalsci.2018.08.032.

[25] M. W. Tian, S. Khorasani, H. Moria, S. Pourhedayat, and H. S. Dizaji, "Profit and efficiency boost of triangular vortex-generators by novel techniques," *Int. J. Heat Mass Transf.*, vol. 156, p. 119842, 2020, doi: 10.1016/j.ijheatmasstransfer.2020.119842.

[26] S. Whitaker, "Forced Convection Heat Transfer Correlations for Flow In Pipes, Past Flat Plates, Single," *AIChE J.*, vol. 18, no. 2, pp. 361–371, 1972.

[27] Syaiful, M. P. Hendraswari, M. S. K. T. Tony, and M. F. Soetanto, "Heat transfer enhancement inside rectangular channel by means of vortex generated by perforated concave rectangular winglets," *Fluids*, vol. 6, no. 1, Jan. 2021, doi: 10.3390/FLUIDS6010043.

[28] Syaiful, A. R. Siwi, T. S. Utomo, Yurianto, and R. Wulandari, "Numerical analysis of heat and fluid flow characteristics of airflow inside rectangular channel with presence of perforated concave delta winglet vortex generators," *Int. J. Heat Technol.*, vol. 37, no. 4, pp. 1059–1070, 2019, doi: 10.18280/IJHT.370415.

[29] M. Awais and A. A. Bhuiyan, "Enhancement of thermal and hydraulic performance of compact finned-tube heat exchanger using vortex generators (VGs): A parametric study," *Int. J. Therm. Sci.*, vol. 140, no. January, pp. 154–166, Jun. 2019, doi: 10.1016/j.ijthermalsci.2019.02.041.

[30] S. Gururatana, R. Prapainop, S. Chuepeng, and S. Skullong, "Development of heat transfer performance in tubular heat exchanger with improved NACA0024 vortex generator," *Case Stud. Therm. Eng.*, vol. 26, Aug. 2021, doi: 10.1016/J.CSITE.2021.101166.

[31] H. Ke *et al.*, "Thermal-hydraulic performance and optimization of attack angle of delta winglets in plain and wavy finned-tube heat exchangers," *Appl. Therm. Eng.*, vol. 150, pp. 1054–1065, Mar. 2019, doi: 10.1016/j.applthermaleng.2019.01.083.

[32] A. Arora, P. M. V. Subbarao, and R. S. Agarwal, "Development of parametric space for the vortex generator location for improving thermal compactness of an existing inline fin and tube heat exchanger," *Appl. Therm. Eng.*, vol. 98, pp. 727–742, Apr. 2016, doi: 10.1016/J.APPLTHERMALENG.2015.12.117.

[33] S. Gururatana and S. Skullong, "Heat transfer augmentation in a pipe with 3D printed wavy insert," *Case Stud. Therm. Eng.*, vol. 21, p. 100698, Oct. 2020, doi: 10.1016/J.CSITE.2020.100698.

[34] A. Sinha, H. Chattopadhyay, A. K. Iyengar, and G. Biswas, "Enhancement of heat transfer in a fin-tube heat exchanger using rectangular winglet type vortex generators," *Int. J. Heat Mass Transf.*, vol. 101, pp. 667–681, Oct. 2016, doi: 10.1016/j.ijheatmasstransfer.2016.05.032.

[35] A. J. Modi and M. K. Rathod, "Experimental investigation of heat transfer enhancement and pressure drop of fin-and-circular tube heat exchangers with modified rectangular winglet vortex generator," *Int. J. Heat Mass Transf.*, vol. 189, p. 122742, Jun. 2022, doi: 10.1016/J.IJHEATMASSTRANSFER.2022.122742.

[36] K. Boukhadia, H. Ameur, D. Sahel, and M. Bozit, "Effect of the perforation design on the fluid flow and heat transfer characteristics of a plate fin heat exchanger," *Int. J. Therm. Sci.*, vol. 126, no. December 2017, pp. 172–180, Apr. 2018, doi: 10.1016/j.ijthermalsci.2017.12.025.

[37] C.-H. Huang and L.-W. Liu, "Optimal position and perforated radius of punched vortex generators for heat sink," *Case Stud. Therm. Eng.*, vol. 32, p. 101916, Apr. 2022, doi: 10.1016/J.CSITE.2022.101916.

[38] Y. Menni *et al.*, "Effects of two-equation turbulence models on the convective instability in

finned channel heat exchangers," *Case Stud. Therm. Eng.*, vol. 31, p. 101824, Mar. 2022, doi: 10.1016/J.CSITE.2022.101824.

[39] M. Awais and A. A. Bhuiyan, "Enhancement of thermal and hydraulic performance of compact finned-tube heat exchanger using vortex generators (VGs): A parametric study," *Int. J. Therm. Sci.*, vol. 140, pp. 154–166, Jun. 2019, doi: 10.1016/J.IJTHERMALSCI.2019.02.041.

[40] A. Gupta, A. Roy, S. Gupta, and M. Gupta, "Numerical investigation towards implementation of punched winglet as vortex generator for performance improvement of a fin-and-tube heat exchanger," *Int. J. Heat Mass Transf.*, vol. 149, Mar. 2020, doi: 10.1016/J.IJHEATMASSTRANSFER.2019.119171.

[41] Y. Li, Z. Qian, and Q. Wang, "Numerical investigation of thermohydraulic performance on wake region in finned tube heat exchanger with section-streamlined tube," *Case Stud. Therm. Eng.*, vol. 33, p. 101898, May 2022, doi: 10.1016/J.CSITE.2022.101898.

[42] H. Chen, H. Ayed, R. Marzouki, F. Emami, I. Mahariq, and F. Jarad, "Thermal, hydraulic, exergetic and economic evaluation of a flat tube heat exchanger equipped with a plain and modified conical turbulator," *Case Stud. Therm. Eng.*, vol. 28, pp. 2214–157, Dec. 2021, doi: 10.1016/J.CSITE.2021.101587.

[43] C. K. Mangrulkar, A. S. Dhoble, S. Chamoli, A. Gupta, and V. B. Gawande, "Recent advancement in heat transfer and fluid flow characteristics in cross flow heat exchangers," *Renew. Sustain. Energy Rev.*, vol. 113, Oct. 2019, doi: 10.1016/J.RSER.2019.06.027.

[44] E. O. Doebelin and D. N. Manik, "Measurement Systems Application And Design : Ernest O. Doebelin : Free Download, Borrow, and Streaming : Internet Archive," pp. 531–532, 1966.

[45] R. J. Moffat, "Describing the Uncertainties in Experimental Results."

Perforated concave rectangular winglet pair vortex generators enhance the heat transfer of air flowing through heated tubes inside a channel

Oktarina Heriyani[*12], Mohammad Djaeni[1], Syaiful[*1], Aldila Kurnia Putri[1]
[1]Mechanical Engineering Department, Engineering Faculty, University of Diponegoro, Semarang, Indonesia
[2]Mechanical Engineering Program, Engineering Faculty, University of Muhammadiyah Prof. DR. HAMKA, Jakarta, Indonesia

Abstract

A significant increase in the rate heat transfer in a heat exchanger system is made possible by increasing the convection heat-transfer coefficient using a passive method. The addition of vortex generators (VGs) to the fins and tubes of a heat exchanger is currently the most effective passive method. However, the increase in heat was accompanied by an increase in pressure drop. Therefore, in this study, we installed perforated concave rectangular winglet pair vortex generators (PCRWP VGs) on plates in rectangular ducts to increase the heat transfer through the six heated tubes to the air stream by lowering the enhancement in the pressure drop. We attempted to determine the best cost-benefit ratio (*CBR*) with a fluid flow velocity difference of 0.4 –2 m/s at intervals of 0.2 m/s (Reynolds number (*Re*) of 2,143 to 11,763) in the channel. The PCRWP VGs were composed of in-line and staggered configurations. The results showed a lower *CBR* (3.56) for the in-line configuration than for the staggered configuration. Moreover, the lowest *CBR* was accompanied by an increase in thermal performance (*TEF*) of 1.29.

Keywords: Perforated; Rectangular winglet; Concave; Pressure drop; Vortex generator; Heat transfer; Thermal performance

1. Introduction

The global energy demand is expected to triple over the next few years. According to a statement by the International Energy Agency (IEA), the main driver is the increasing use of air conditioning (AC) machines [1]. Thus, promoting energy efficiency in air conditioners is important and requires maximising their thermal performance, which involves increasing the rate of heat transfer in its main component, i.e., the condenser. A condenser, commonly used in air conditioners, comprises a fin and a tube and functions as a refrigerant cooling medium. However, the high thermal resistance (75%) of the fin air side of the condenser lowers the heat-transfer rate in the heat exchanger[2]. Thus, the thermal resistance must be lowered to enhance the heat transfer rate.

A commonly used active methods to increase the rate of heat transfer involves adding vortex generators (VGs), which, according to the research results obtained by Mugisidi et al., increases the performance of a condenser[3]. The added VGs cause longitudinal vortices (LVs), damage the primary flow, make the second flow as large as the first and increase air mixing in the area[4][5]. The size of the LVs, shape of the flow, and mixing are influenced by the shape, geometry and position of the VGs added to the fins and tubes of the heat exchanger[6].

Samidifat et al. showed that simple rectangular vortex generators (RVGs) can increase the heat transfer rate by 7%; however, this causes a pressure drop in the heat exchanger system[7]. Meanwhile, modified RVGs with a concave shape on the front and rear surfaces decreased the heat transfer performance of the heat exchanger tube. A better option is to use RVGs with a double convex front surface and a single concave back surface, which can strengthen the primary vortex, increasing the rate of heat transfer from the plate to the fluid, as demonstrated in a study by Kashyap et al.[8]. Further research conducted by Kashyap et al. in the same year concluded that modifying the surface shape of rectangular winglet vortex generators (RWVGs) can create longitudinal eddies that interact with the boundary layer, thereby increasing the rate of convection heat transfer[9]. Based on their research, the

increase in the optimal heat transfer rate was 14.4. The optimal heat transfer performance was also obtained from the results of experiments conducted by Adnan et al. on rectangular ducts by adding delta and rectangular winglet VGs[10]. Concave curved delta winglet VGs were compared with convex curved delta winglet VGs by Song et al. to observe changes in the heat transfer rate[11].The results showed that the concave VGs improved the heat transfer better than the convex VGs. The differences in the shape of the VGs affects the change in the heat transfer rate and the change in the geometry of the VG, such as a new rib geometry in the cylinder channel[12].

Zeeshan et al. showed that increasing the angle of attack increased the rate of heat transfer (to 37.01–64.54%) if a pair of RWVGs were placed at the back of the tube even though this did not reduce the pressure drop[13]. A decrease in the value of the pressure drop also did not occur significantly, even though there was an increase in heat of 260% in heat, as per the results of the research conducted by Linardo et al. using the batched heat and channelled pipe (BHCP) approach[14]. The increase in heat transfer performance is influenced by the number of RWVG pairs based on the research results of Heriyani et al., where there is an increase in the hydraulic thermal performance evaluation criteria by 15.17% for three pairs of RWVG compared with the baseline [15]. Wang et al. found that the more pairs of VGs placed in the crossflow, the higher the increase in the heat transfer coefficient[16]. Sun et al. further discovered that increasing the number of RWVGs in the heat exchanger tube increased the heat transfer, with a maximum thermal enhancement factor (*TEF*) of 1.27 [17]. The *TEF* value of a V-delta winglet VG reached 1.82–3% higher than that of a V-rectangular winglet VG, as revealed by Promvonge et al.[18]. These results were obtained with an optimal blockage ratio (*BR*) of 0.15 and pitch ratio (*PR*) 1.0. Skullong et al. modified the shapes of RWVGs with optimal BRs and PRs to achieve an optimum heat transfer performance and reduced pressure drop; their shape modification involved perforating RWVGs [19].

The positions of the holes in the RWVGs did not significantly affect the increase in heat transfer; however, they significantly affected the flow resistance of the VGs. The heat-transfer rate increased as the height (vertical position) of the hole increased. Widthwise, although there is an initial increase, the heat transfer rate decreased with increasing lateral distance[20]. An increase in the number of holes in the RWVGs indicates an increase in fluid flow, which forces the fluid to flow behind the RWVGs, thereby increasing heat transfer[4]. The heat transfer rate increased during laminar flow when the Reynolds number (Re) increased and then decreased with an increase in Re during turbulent flow [20]. Positioning the tube in-line with a pair of RWVGs in a common flow-down configuration provides better performance than the common flow-up configuration. However, a staggered tube position is superior, resulting in a 25.85% higher heat-transfer performance than when a pair of RWVGs is not used[21].

In the existing studies, no detailed analyses of heat transfer were conducted on from the surfaces of several cylinders heated and arranged in-line when using a perforated vortex generator. Therefore, the focus herein is on investigating the advantages of using perforated concave rectangular winglet pair vortex generators (PCRWP VGs) to increase the heat transfer of the airflow through heated tubes arranged in-line in the ducts.

2. Experimental Approach

2.1 Experimental setup

This research was conducted experimentally with a test equipment scheme comprising a rectangular channel sized 370 x 18 x 8 cm. The duct was made of 1 cm thick glass, as shown in Fig. 1.

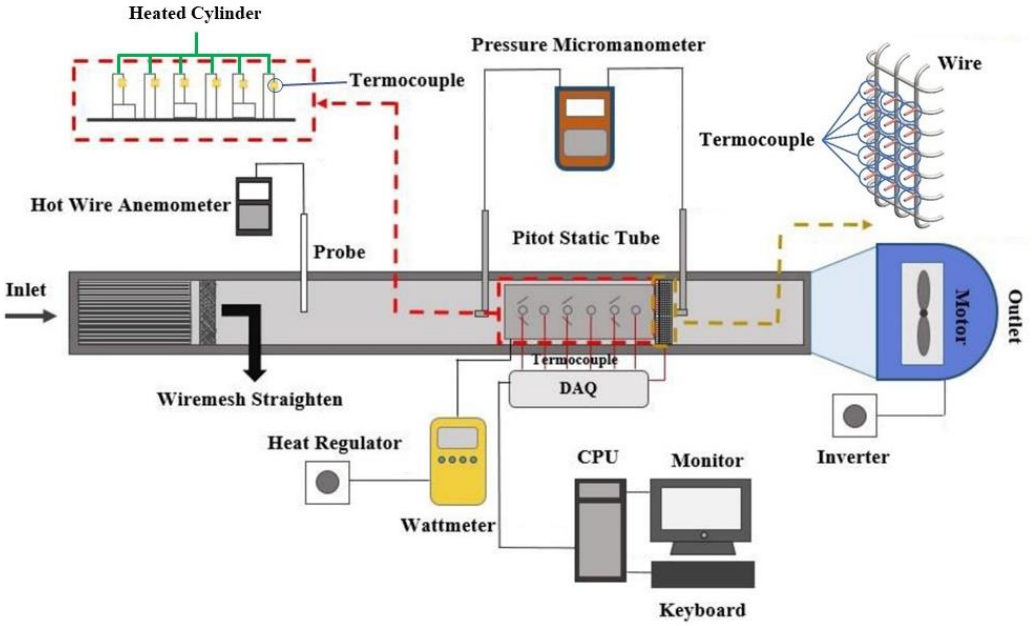

Fig. 1. Experimental tool schematic

Based on Fig. 1, the rectangular channel is equipped with a blower (50 Hz, Wipro with a rated voltage of 220V), an inverter (Mitsubishi Electric type FR-D700 with an accuracy of 0.01), straightener, hot wire anemometer (Lutron type AM-4204 with an accuracy of 0.1), wattmeter (Lutron DW-6060 with an accuracy ± 1.0), central processing unit (CPU), micromanometer, thermocouple (K type with a temperature interval of -200 –1250℃ and an accuracy ± 0.5) where one thermocouple was placed in the air inlet area, six thermocouples on the back surface of the tubes and 15 on the outlet side of the wire, data acquisition (Advantech USB-4718 type with an accuracy of 0.001) and heater regulator. The heater was connected to six tubes with a diameter of 19.05 mm and height of 65.8 mm, with each tube having the same power. Total heating power of 40 W was applied to the six tubes using a regulator. The heating air flowing through the tubes occurs via convection. Thus, the air at the outlet side becomes hotter than that at the inlet side.

A pressure micromanometer (Fluke type 922, with an accuracy of ± 0.05) was used to monitor the flow pressure drop. Two pitot tubes, each set 26 cm ahead of the inlet of the test specimen and 2.5 cm behind it, were connected to a micromanometer to measure the pressure drop. The pressure drop measurements were recorded 30 times for 5 sekon at each speed variation. Furthermore, flow visualisation was performed by directing the smoke from vaporised fluid in the fluid vaporator into the mainflow.

The VGs used as test specimens were perforated rectangular winglet pair (PRWP) and perforated concave rectangular winglet pair (PCRWP) vortex generators (VGs). Perforated is a term for holes in the VGs, as shown in Fig. 2. The VGs have dimensions of the same length and width of 30 mm, with

36 holes. The bore diameter on the VGs was 2.5 mm. The distance between the holes was 5 mm from the center.

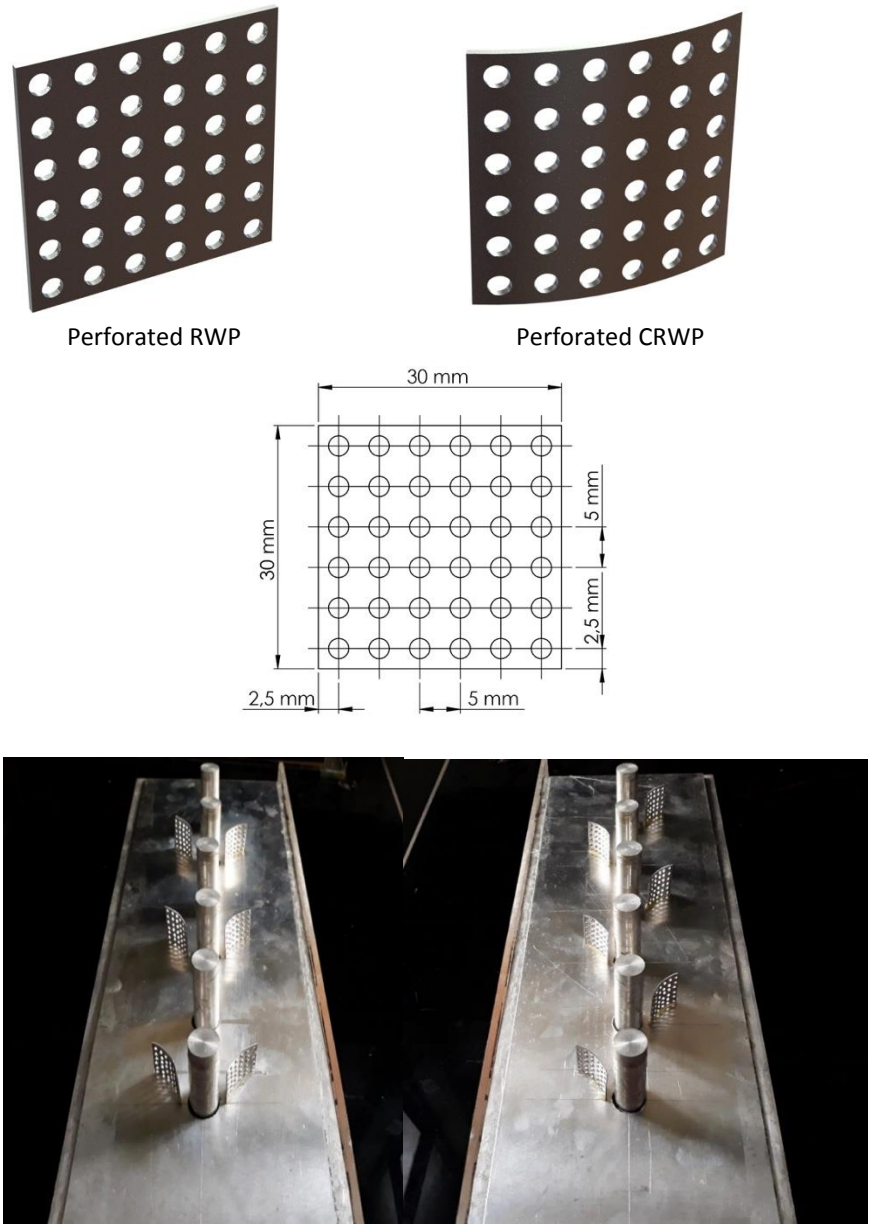

Fig. 2. Geometry of the VGs

The VGs are placed on an aluminium plate measuring 500 x 165 x 1 mm. The geometry and the pitch between VGs for both in-line and staggered configurations are shown in Fig 3, with an angle of attack (α) of 150[2]. The distance between the cylinders is 120 mm, with a cylinder diameter of 19.05 mm.

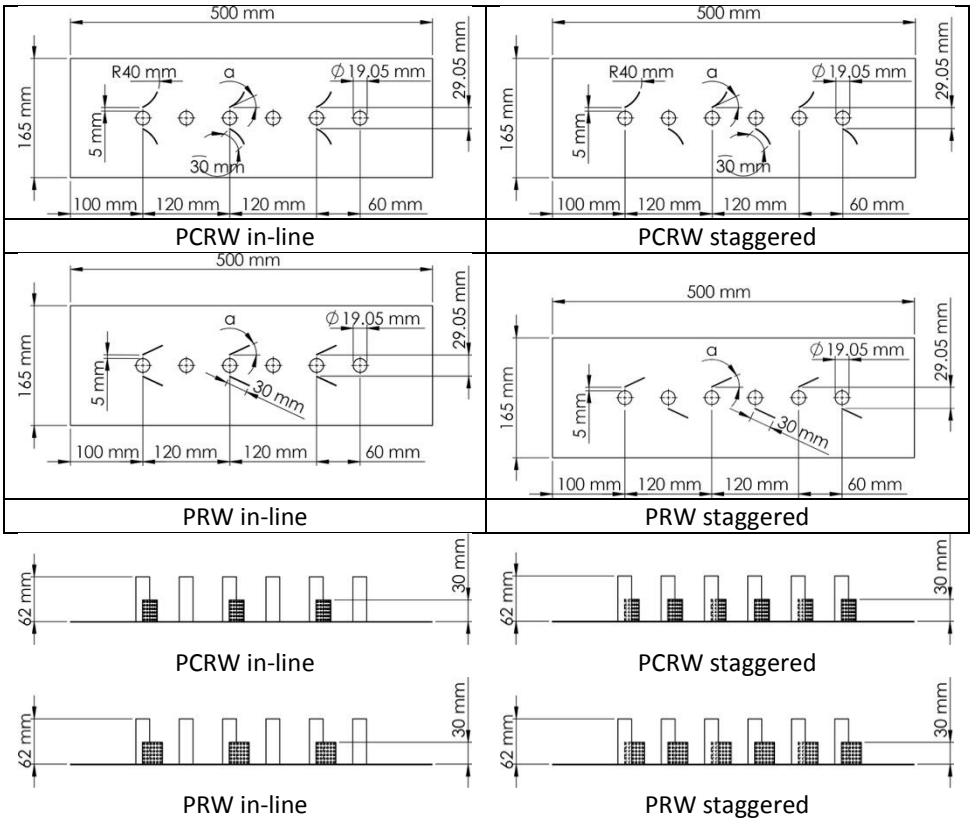

Fig. 3. Geometry and pitch of the VGs

The VGs configurations were arranged in-line and staggered on the plate. The perforated rectangular winglet (PRW) and perforated concave rectangular winglet (PCRW) VGs in-line configurations with one, two and three pairs are shown in Fig. 4. For each pair, the VGs were placed on the left and right sides of the first row of tubes. VGs were placed in the first- and third- row tubes for two pairs. For the three pairs, VGs were placed on the first-, third-, and fifth-row tubes.

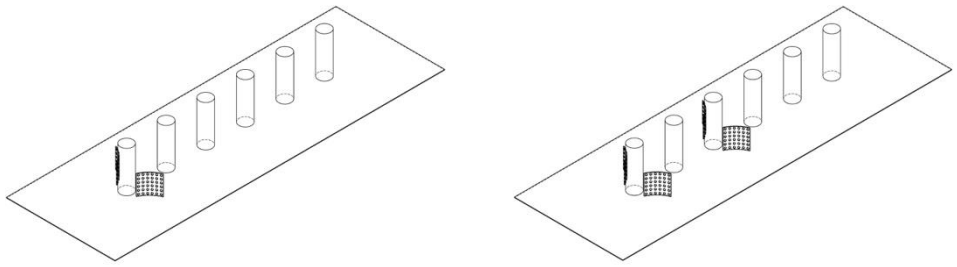

One pair PCRW in-line

Two pairs PCRW in-line

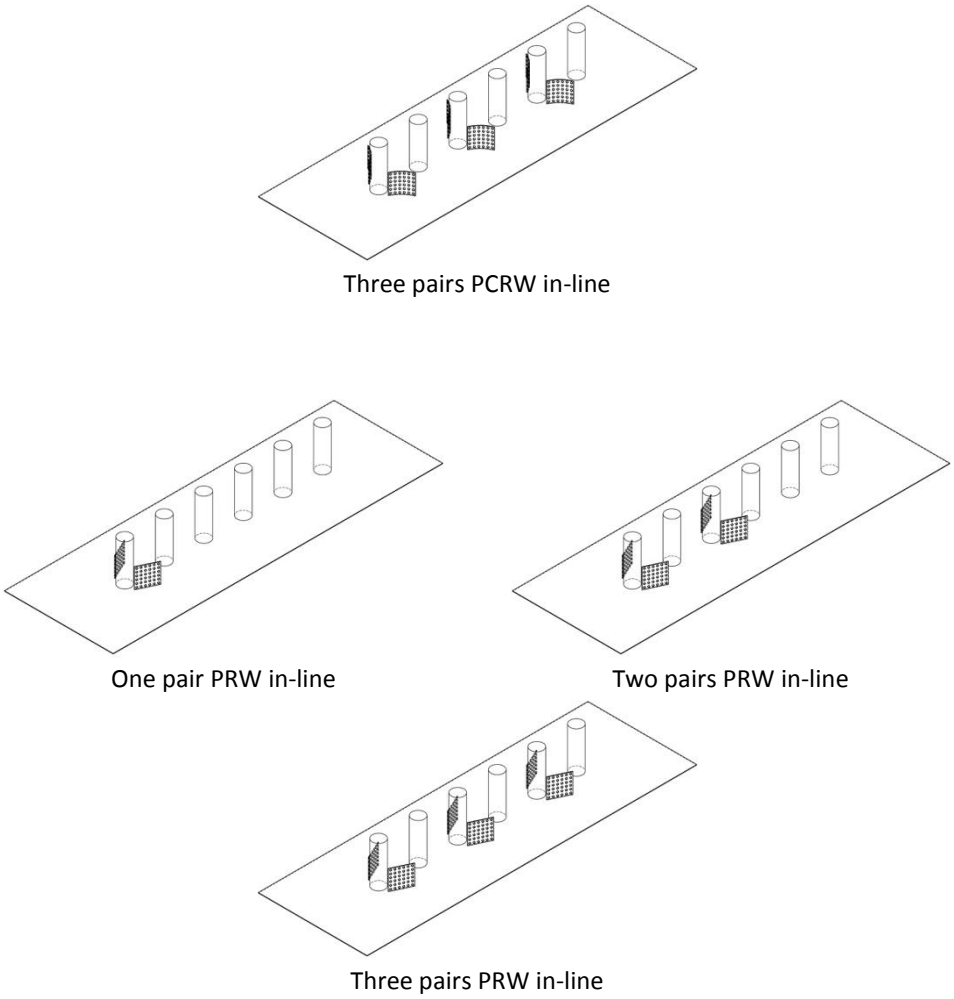

Fig. 4. VGs pairs in-line configurations

The PRW and PCRW VGs staggered configurations with one, two, and three pairs are shown in Fig. 5. For one pair, the VGs are placed on the right side of the first-row tube and on the left side of the second. The VGs are placed on the right side of the first and third row tubes and on the left side of the second and fourth tubes for two pairs. For the three pairs, the VGs are placed on the right side of the first, third and fifth rows of the tubes and on the left side of the second, fourth and sixth tubes.

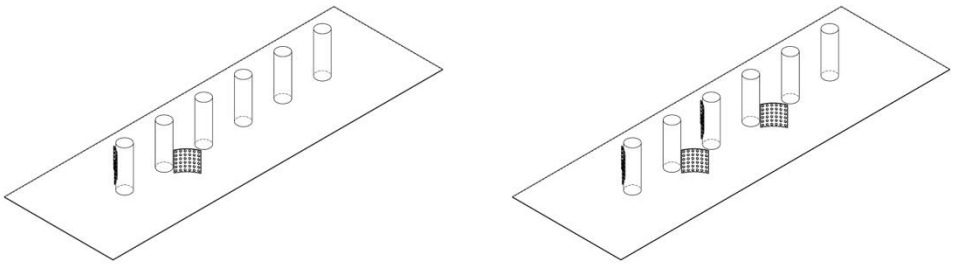

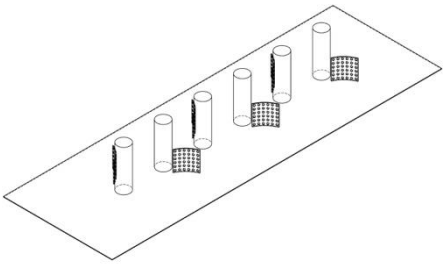

Three pairs PCRW staggered

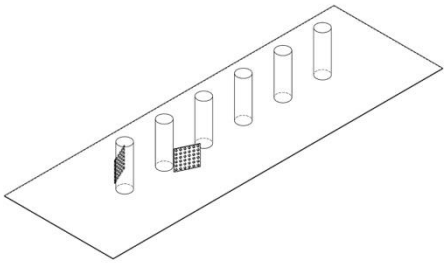

One pair PRW staggered

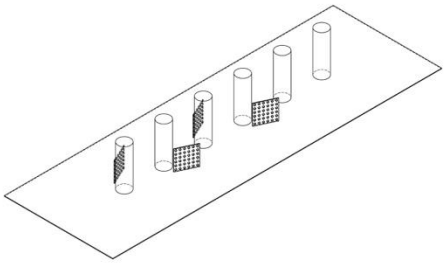

Two pairs PRW staggered

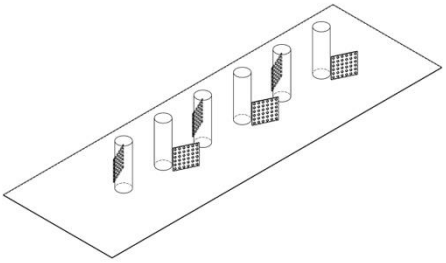

Three pairs PRW staggered

Fig. 5. VGs pairs staggered configurations

2.2 Parameter definitions

The parameters in this study were derived from the equation used by Oneissi et al. to obtain the thermal enhancement factor (*TEF*) [22]

$$TEF = \frac{\frac{Nu}{Nu_0}}{\left(\frac{f}{f_0}\right)^{\frac{1}{3}}} \quad (1)$$

The Nusselt number dan friction factor for the baseline conditions are symbolised as (Nu_o) and (f_0), and (Nu) and (f) based on the research of Zeeshan et al[23]

$$Nu = \frac{q\, D_h}{A_{tube}\, \Delta T_{LMTD}\, k} \quad (2)$$

$$h = \frac{q}{A_{tube}\,\Delta T_{LMTD}} \quad (3)$$

$$q = \dot{m}\, c_p\, (T_{out} - T_{in}) \quad (4)$$

where D_h, A_{tube}, ΔT_{LMTD}, $\dot{m}$, c_p, T_{out} and T_{in}, are hydraulic diameter, tube surface area, log mean temperature difference, mass flow rate, specific heat, outlet temperature, and inlet temperature, respectively

$$D_h = \frac{4A_c}{p} = \frac{4ab}{2(a+b)} = \frac{2ab}{a+b} \quad (5)$$

$$\Delta T_{LMTD} = \frac{(\bar{T}_{tube} - \bar{T}_{out}) - (\bar{T}_{tube} - \bar{T}_{in})}{\ln[(\bar{T}_{tube} - \bar{T}_{out}) - (\bar{T}_{tube} - \bar{T}_{in})]} \quad (6)$$

where A_c dan T_{tube} are channel surface area and tube temperature, respectively.

The result of D_h is used to calculate *Re* with the formula

$$Re = \frac{\rho u_{in} D_h}{\mu} \quad (7)$$

and friction factor (*f*) was determined to evalute the performance of hydro dynamic using

$$f = \frac{2\,\Delta P\, D_h}{\rho\, V^2 (L+6D)} \quad (8)$$

where $\rho, V,$ and L are the air density, inlet airflow velocity and length of the test specimen, respectively.

The equation required to determine the cost-benefit ratio (*CBR*), defined as the ratio of pressure drop per variation in *Nu* number, as formulated by Tian et al. [25], is as follows:

$$CBR = \frac{\%\Delta P}{\%Nu} \quad (9)$$

This concept investigates whether the method used to enhance the heat-transfer rate is economically efficient. In the hydrodynamic test, the pressure drop (ΔP) is measured by the pressure difference on the sides of P_{inlet} and P_{outlet} of the test specimen in the tested part using equation (10):

$$\Delta P = P_{inlet} - P_{outlet} \quad (10)$$

2.3 Validation

The current study is a follow-up investigation to the work of Yafid et al.[24], and the experimental setup was similar to that of Yafid et al. The difference between the current study and the experiment of Yafid et al. is a test object in which the current study uses concave rectangular winglet (CRW) VGs; in Yafid et al.'s experiment concave delta winglet (CDW) VGs are used. Whitaker et al. [25] studied the heat transfer characteristics of airflow through a single cylinder in a rectangular duct. The results of Yafid et al. were valid, and the same experimental set-up was determined. The *Nu* value from the experiment of Yafid et al. were comparable with the *Nu* values from the experiments of Whitaker et al. in the Reynolds number (*Re*) range of 2,143 to 11,763.

3. Results and Discussion

3.1 Flow visualisation

A flow visualisation test was performed to observe the longitudinal vortices (LV) formed after the flow passed through the VGs in the rectangular channel. This test was conducted under low-light conditions to clarify the LV. The laser beam was refracted by a cylindrical glass (diameter 5 mm), which produced a cross-sectional area perpendicular to the direction of the flow. Smoke formed from the evaporation of the liquid was used to visualise the LV in the flow. The VGs used in this visualisation test were PRWP and PCRWP with an in-line arrangement, as shown in Fig. 6.

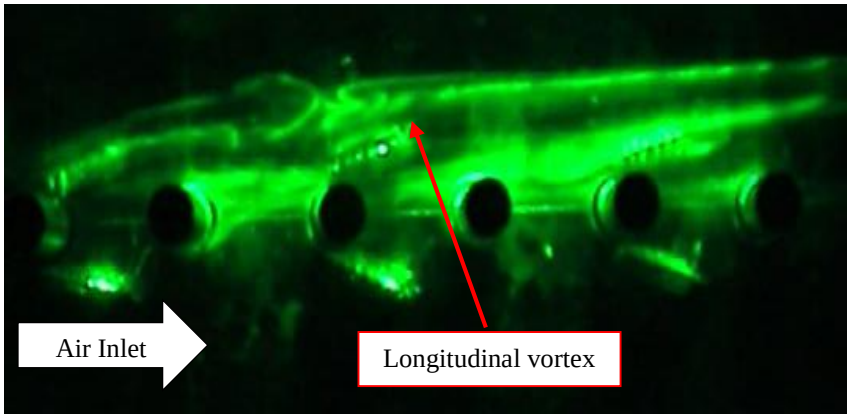

(a)

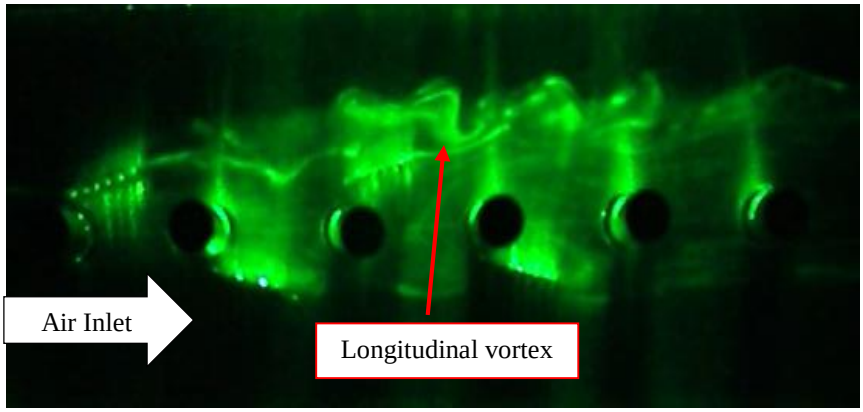

(b)

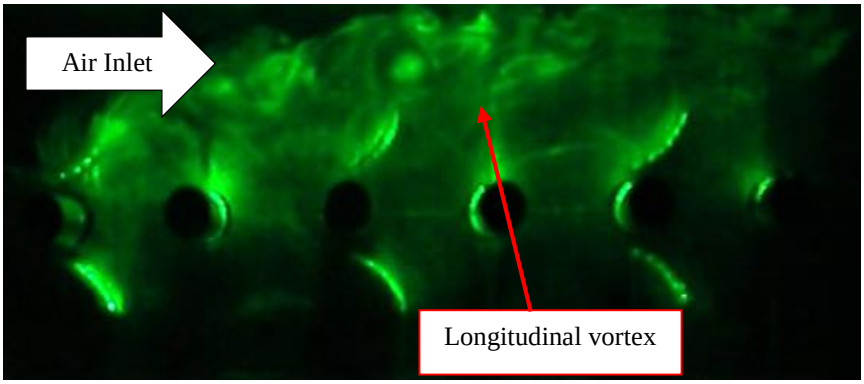

(c)

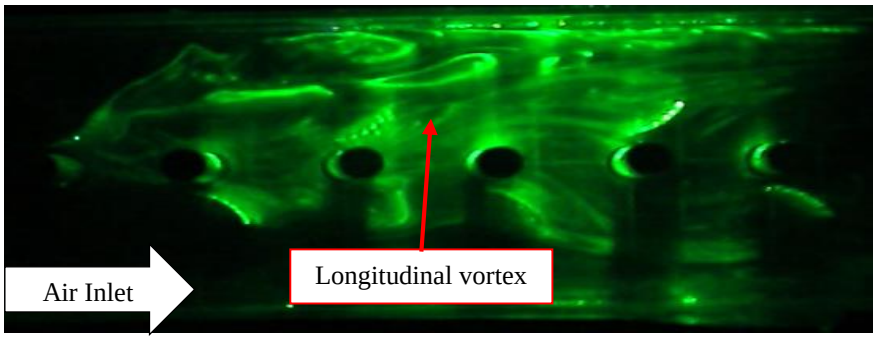

(d)

Fig. 6. Visualisation of LV generated by (a) in-line PRWP, (b) staggered PRWP, (c) in-line PCRWP and (d) staggered PCRWP

In Fig. 6 (c) and (d), the PCRWP VGs appear to produce longitudinal vortices (LV) in a wide flow area compared with the PRWP VGs in Fig 6 (a) and (b) downstream. The back region of the PCRWP VGs had a wider frontal surface area than the PRWP VGs. Consequently, mixing the near-fluid the channel walls with the fluid in the mainstream is better, meaning that the heat transfer rate is increased [26]. Downstream, the LV compression in the wake area increases the fluid flow velocity passing through the cylindrical structure, thereby increasing the heat transfer rate from the channel surface to the fluid flow in the wake region [27]. The increase in heat transfer produced when using PCRWP VGs was better than that with PRWP VGs.

3.2 Perforated vortex generators effect on heat transfer

The increase in the convection heat transfer was due to the mixing of fluids caused by the strong longitudinal vortices (LVs)[28]. The strength of the LVs is caused by the amount of VGs sets; increasing the amount of VGs pairs in the test specimen can increase the coefficient of the convection heat transfer [29], as shown in Fig. 7.

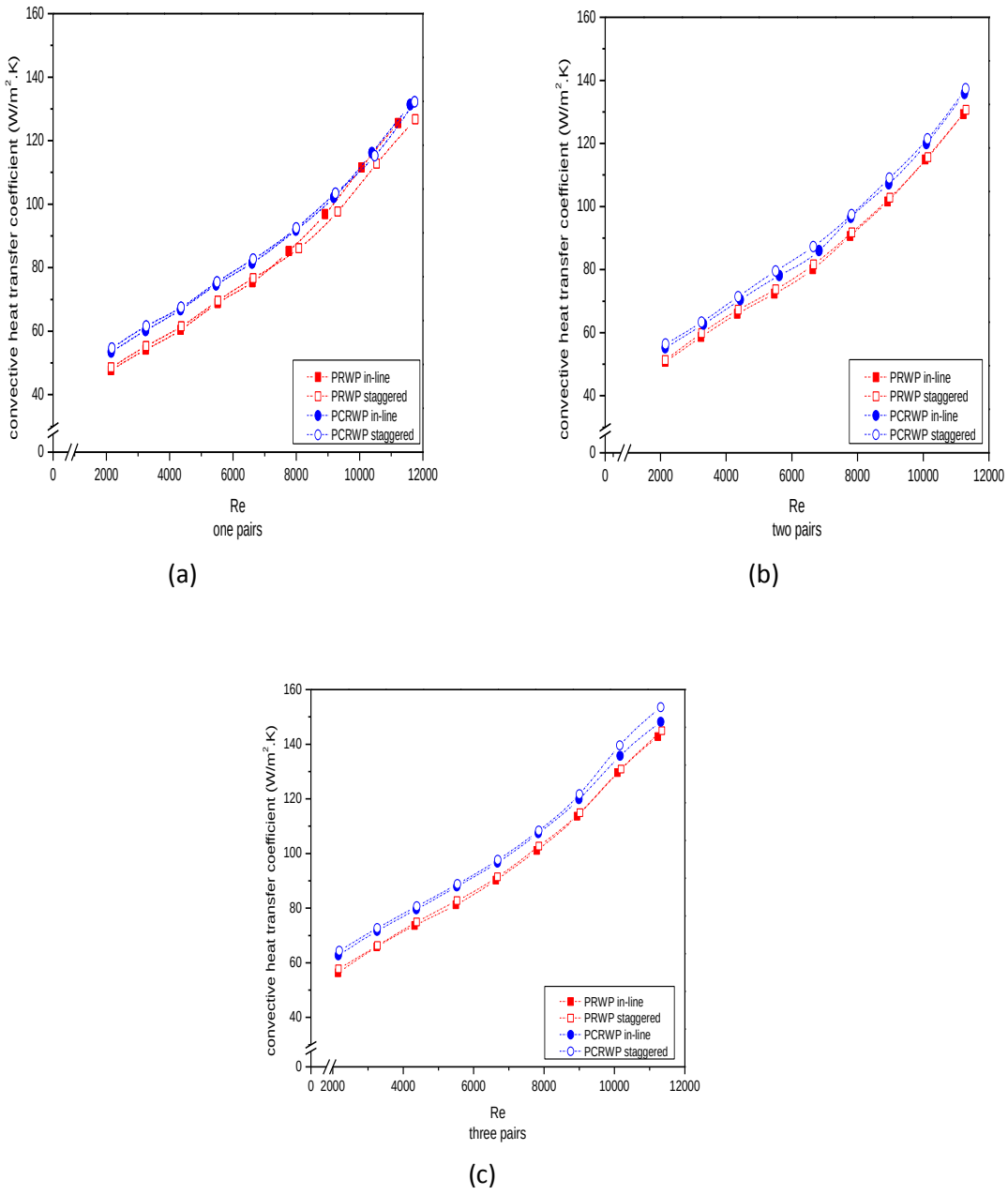

Fig. 7 Graphs of convective heat-transfer coefficient against Reynolds number: (a) one, (b) two and (c) three pairs.

In Fig 7, we can see the convective heat transfer coefficient with respect to the Reynolds number (*Re*), analysed after installing the PCRWP and PRWP with pairs ranging from one, two and three, arranged in-line or staggered. Based on Fig. 7, the convective heat transfer coefficient increased with a rise in *Re* due to an increase in flow vortices and high turbulence intensity in the channel[30], alongside a reduction in the wage region and stagnation area for each increase in flow velocity[31]. The improve in heat transfer for the staggered was better than that for the PCRW VGs with any number of pairs at the

highest *R*e (11,000). The results in Fig. 7 show that the PCRWP VGs worked better than the PRWP VGs, and the staggered arrangement of the former, with three pairs, gave the highest yield (153.5 W/m^2·K), as shown in Fig. 7(c). Two PCRW pairs (137.33 W/m^2·K, Fig. 7(b)) were better than one (132.25 W/m^2·K) (Fig. 7(a)) because the VGs with a concave surface destabilise the force of centrifugal of the fluid flow, strengthening the flow vortices and making the mixing of the hot fluid near the wall with the cold fluid of the main flow more robust[32]. In Fig. 7(a), the convection heat-transfer coefficient for the case of the in-line PRW VGs has the same value as that of the in-line or staggered PCRW VGs in a pair of VGs. In one pair of VGs, a longitudinal vortex is generated after the flow hits and weakens the VGs[29]. This result contrasts with the cases with two and three pairs of VGs, where the longitudinal vortex produced after striking the first VGs is amplified again when the flow strikes the second VGs and so on. Therefore, the value of the heat transfer coefficient in the case of a pair of PRW VGs is the same value as that of PCRW VGs at Reynolds numbers above 8,000.

3.3 Effect of perforated vortex generators on pressure drop

Using VGs can affect the increase in heat transfer, but there is often an accompanying increase in pressure drop, as shown in Fig. 8, where an increase in pressure drop can be seen along with the increases in *Re* and pair numbers for both the VG types PCRW and PRW. In general, the highest pressure drop was observed using the PCRWP VGs with a staggered configuration for all *Re*, except for one pair of VGs. The highest pressure drop was found in the PRWP VGs with an in-line configuration at *Re* greater than 8,000. The pressure drop on the staggered VGs was found to be higher than that on the in-line configuration because of the shorter distance between the VGs of the staggered configuration than that of the in-line[29], caused by the resistance of fluid flow against the walls of the VGs and the expansion of the frontal zone of the VGs in the next-pair arrangement [33]. The pressure drop in the staggered arrangement was lower than that in the in-line arrangement, whereas the PRW VGs type created a lower pressure drop than the PCRW VGs because the latter reduced the frontal area hit by the airflow, resulting in a decrease in drag [34]. In addition, the jet flow from the VG hole can reduce the stagnation flow, which can reduce the pressure drop [35]. A significant decrease in the pressure drop was due to the VG perforation[36]. The best pressure drop value for one pair with a staggered arrangement was 4.58 Pa (see Figure 8(a)), whereas two pairs (5 Pa, Figure 8(b)) were better than three (5.4 Pa, Figure 8(c)).

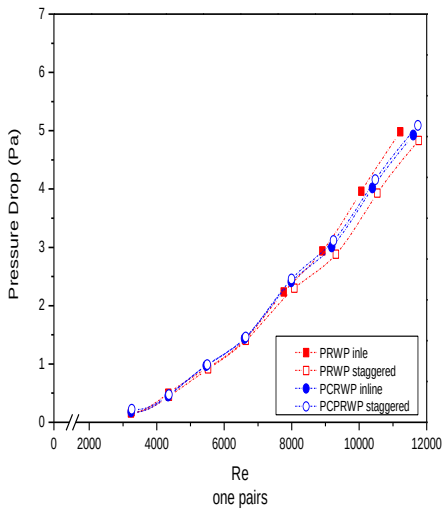

(a)

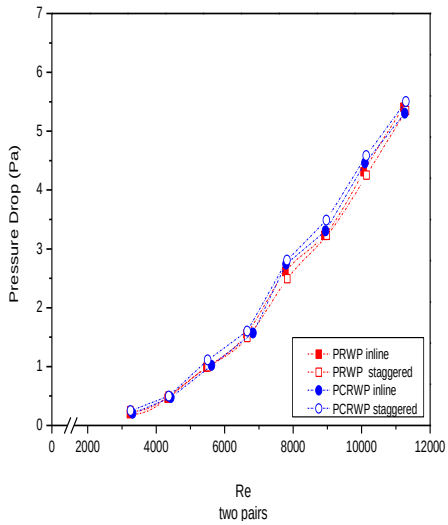

(b)

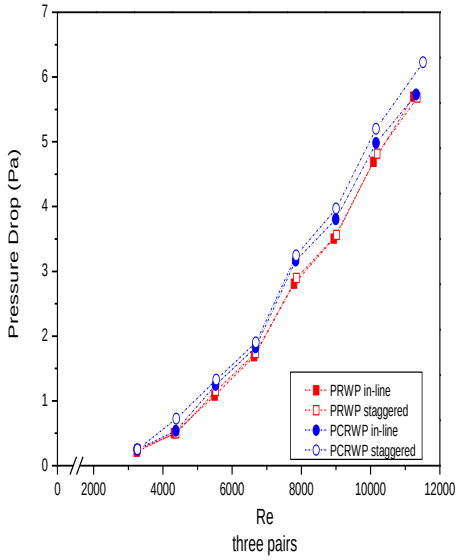

(c)

Fig. 8 Graph of pressure drop against Reynolds number: (a) one, (b) two and (c) three pairs

3.4 Effect of perforated VGs on thermal enhancement factor

TEF exhibited the hydraulic thermal performance while using VGs, which played a role in restructuring the incoming fluid flow pattern. The increase in the *TEF* was due to the influence of complex overlapping structures, which meant that the flow developed into a turbulent structure, significantly affecting the heat transfer increase [37]. The experimental *TEF* values are shown in Fig. 9.

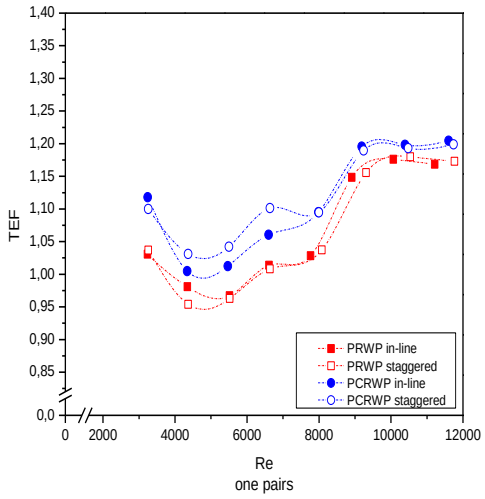

(a)

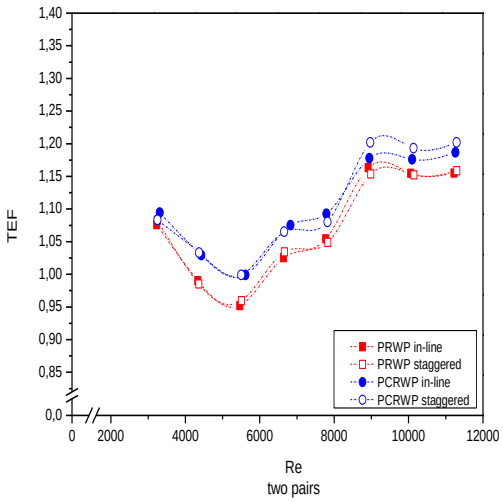

(b)

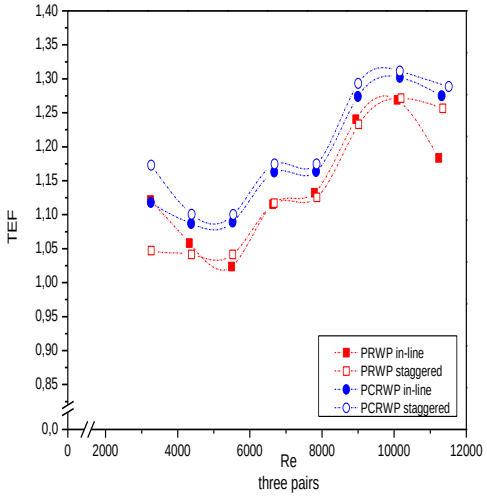

(c)

Fig. 9 Graph of thermal enhancement factor against Reynolds number: (a) one, (b) two and (c) three pairs

The *TEF* is the thermal-hydraulic performance which is the ratio of the increase in heat transfer to the pressure drop ratio. In general, the highest *TEF* was observed when the PCRWP VGs were used with a staggered configuration, as depicted in Fig 9. The PCRW creates wider flow vortices that can reduce the wake area behind the cylinder. Reducing the wake area can reduce the recirculation zone, affecting the heat transfer from the back of the cylinder to the stream [26]. A large-radius, high-intensity anterior-posterior vortex can reduce the wake area. A lessening within the wake zone increased the flow velocity behind the tube and reduced the recirculation area, resulting in increased heat transfer in this area [27, 38]. As shown in Fig 9, there was an increase in the *TEF* with greater pairs of VGs used for both the PCRW and PRW VG because the PCRW produced wider flow vortices, which reduced the wake region behind the cylinder, thereby reducing the recirculation zone and impacting the heat transfer increment from the rear cylinder surface to the stream[39]. In this process, a large number of longitudinal vortices with high intensities can reduce the wake area, which increases the flow velocity downstream of the tube and reduces the recirculation region, leading to an increased heat-ransfer rate in the region [40, 41]. Based on Figure 9, the best *TEF* increase occurred at Re between 8,000–9,000. The best *TEF* values, with one, two and three pairs occurred in the staggered arrangement with PCRW VGs, at 1.18, 1.20 and 1.29, respectively (see Fig. 9).

3.5 Effects of perforated VGs on the cost-benefit ratio

Economic evaluation cannot be conducted based only on the *TEF* and the net profit from the heat load of the transferred unit[26]. Instead, it must be determined by evaluating the economic value of the heat-transfer improvement by calculating the cost benefit ratio (*CBR*), as shown in Fig. 10.

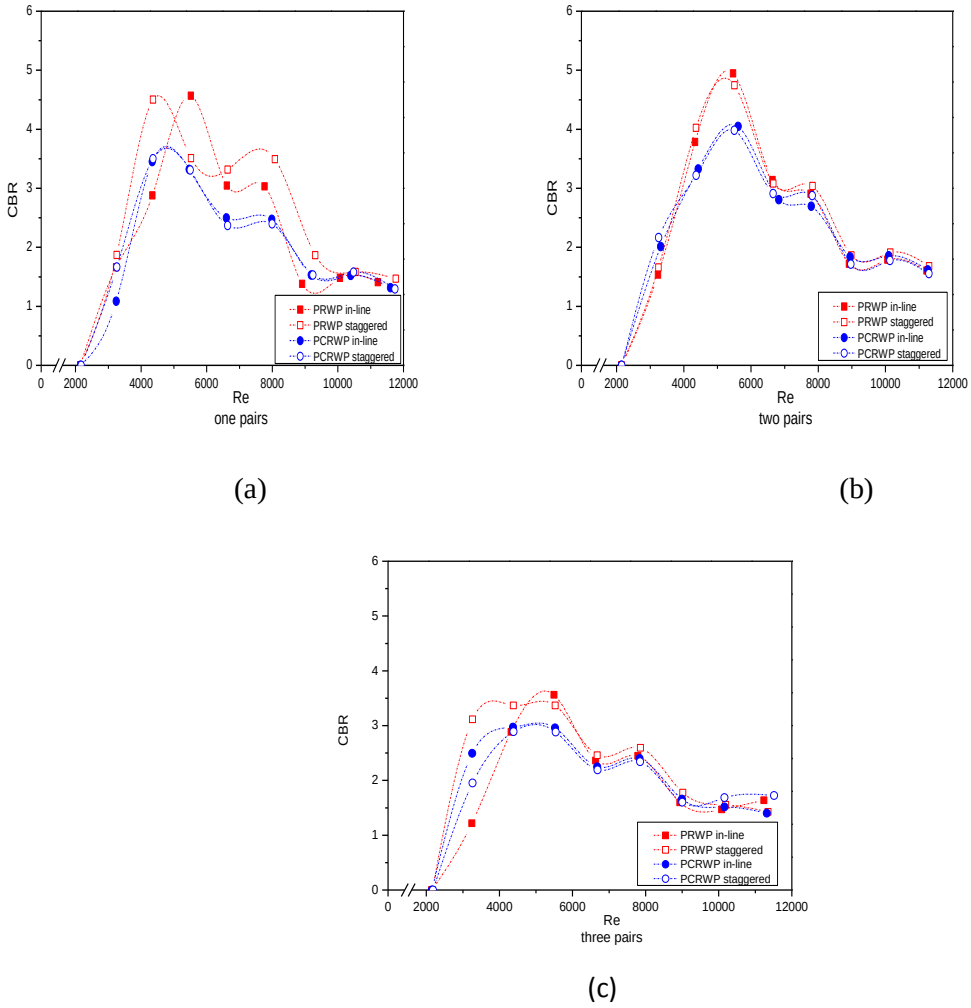

Fig. 10 Graph of cost-benefit ratio against Reynolds number: (a) one, (b) two and (c) three pairs

Fig. 10 show the result of the *CBR* calculation to compare the percentage increase in the pressure drop with the percentage increase in the Nusselt number when using VGs. These results indicate that a lower *CBR* improves thermal performance, which is greater than the drag force [25]. The greatest increase in *CBR* occured with the PRW VGs, with an in-line arrangement, totalling 4.57, 4.95 and 3.56 for one, two and three pairs, respectively. The lowest *CBR* was measured when three sets of PCRW vortex generators with a staggered arrangement were used. The lowest *CBR* were obtained with the three pairs of staggered-type VGs PCRW. The three VG pairs showed a lower *CBR* than the one and two pairs because they resulted in the greatest increase in the Nusselt number, accompanied by a lower pressure drop increase, which lowered the *CBR*. These results show that a lower *CBR* improves thermal performance relative to resistivity [26]. A low value *CBR* inicates a more economical value using VGs. In general, using PCRWP VGs with a staggered configuration is the best.

3.6 Heat Loss Analysis

Heat loss analysis was performed by considering the convection heat transfer from the six tubes to the surrounding fluid flow. The heat transfer rate was calculated for laminar and turbulent flows.

The heat loss in this experiment was calculated by calculating the difference between the induced electric power and total heat through convection from the surface of the tubes to the fluid. In this experiment, six tubes in a wind tunnel were heated using a heater at a power of 40 W; the velocity of the inlet fluid is varied from 0.4 to 2 m/s at intervals of 0.2 m/s or in the Reynolds number range from 2,143 to 11,763. Based on the Reynolds number range, two types of flows were determined; laminar and turbulent. Therefore, the heat loss was determined from the correlation between laminar at 0.4 m/s and turbulent for other velocities. The experimental data for the hydraulic diameter D_h, tube surface area A_{tube}, channel surface area A_c and air specific heat c_p are 0.09223 m, 0.02338908 m^2, 0.01056 m^2 and 1.007 J/kgK, respectively. Table 1 is a baseline for calculating heat loss

Table 1 Heat Loss Baseline

	v (m/s)	*Re*	Mass flow rate (kg/s)	**Density (kg/m^3)**	Dynamics viscous (kg/ms)	*k*	*Pr*	*T* inlet (C)	*T* outlet (C)	*T* tube (C)	**Δ***T* LMTD	**Δ***T* (*T* tube - *T* inlet)	*Nu*	*h* (W/mK)	*q* conv (W)	*q* input (W)	*q* loss (W)
baseline	0.4	2165	0.004757	1.13	1.9.E-05	0.03	0.73	29	33	50	19	21	155	45	19.48	40	20.52
	0.6	3291	0.00719	1.13	1.9.E-05	0.03	0.73	28	31	46	16	18	174	50	18.98	40	21.02
	0.8	4413	0.009618	1.14	1.9.E-05	0.03	0.03	28	30	44	15	16	192	50	19.19	40	20.81
	1	5545	0.012056	1.14	1.9.E-05	0.03	0.73	28	30	43	14	15	214	55	19.84	40	20.16
	1.2	6661	0.014477	1.14	1.9.E-05	0.03	0.73	28	29	43	14	15	228	61	21.15	40	18.85
	1.4	7826	0.016958	1.15	1.9.E-05	0.03	0.73	28	29	41	12	13	247	70	20.30	40	19.70
	1.6	8965	0.019407	1.15	1.9.E-05	0.03	0.73	27	29	40	12	13	263	75	21.03	40	18.97
	1.8	10110	0.021863	1.15	1.9.E-05	0.03	0.73	27	28	39	12	12	296	84	22.54	40	17.46
	2	11272	0.024341	1.15	1.9.E-05	0.03	0.73	27	28	38	11	11	342	97	24.17	40	15.83

From Table 1, the greater the velocity with an increase in the *Re*, the lower the heat loss. It can be observed that the heat flow from the heater not only spreads into the tube, but convection also occurs outside the tube. The heat output increased with *Re*, i.e, the higher the flow velocity, the greater the turbulence through the cylinder and the higher the turbulence intensity. An increase in the turbulence intensity between a cold airflow and hot cylinder with a constant surface temperature is caused by the airflow velocity[26]. In row-tube arrays, this recirculation area increased for the second and subsequent columns. A lower air velocity in the circulation region indicated less airflow in the region participating in the local heating process[37]. The heat loss under all conditions in this experiment is listed in table 2.

Table 2 Calculation of heat loss for the whole case

type VGs	*q* conv (W)	*q* input (W)	*q* loss (W)
Baseline	20.74	40	19.26
PCRWPI1	25.15	40	14.85
PCRWPI2	27.55	40	12.45

PCRWPI3	27.61	40	12.39
PCRWPS1	26.43	40	13.57
PCRWPS2	26.43	40	13.57
PCRWPS3	27.94	40	12.06
PRWPI1	24.09	40	15.91
PRWPI2	27.25	40	12.75
PRWPI3	28.82	40	11.18
PRWPS1	23.94	40	16.06
PRWPS2	26.37	40	13.63
PRWPS3	28.12	40	11.88

Table 2 shows that the lowest heat loss occurs when three sets of PCRWPs are staggered. The placement of the VGs can increase heat transfer in square ducts as the VGs create longitudinal vortices, which in turn increase vortex strength in the wake region downstream of the tube. Longitudinal vortices make the overall temperature field more uniform, improve heat mixing and boundary layer modification, and improve heat transfer performance. A higher number of vortex generators creates more longitudinal vortices and significantly increases heat transfer [29, 26].

3.7 Uncertainty Analysis

In this section, uncertainty analysis calculation data will be shown for the temperature at base-line conditions with a velocity of 0.4 m/s as shown in Table 3.

Table 3 Base-line test temperature data at a speed of 0.4 m/s

$T\ (Tube_1)$	$T\ (Tube_2)$	$T\ (Tube_3)$	$T\ (Tube_4)$	$T\ (Tube_5)$	$T\ (Tube_6)$
49.19093	51.21368	48.32313	49.76915	47.80219	51.27142
49.1834	51.17728	48.3156	49.79053	47.7657	51.2639
49.14545	51.16826	48.30655	49.7526	47.7856	51.25489
49.12105	51.17277	48.28214	49.72821	47.76118	51.2594
49.15297	51.20465	48.28515	49.73122	47.73524	51.2624
49.09966	51.15141	48.28967	49.73573	47.76871	51.26691
49.09815	51.14991	48.23029	49.73423	47.73826	51.29428
49.08912	51.14089	48.25019	49.66739	47.72922	51.22751

From these data, it is found that $\overline{\boldsymbol{T}}_{\boldsymbol{Tube}}$ can be calculated by the equation as

$$\overline{\boldsymbol{T}}_{\boldsymbol{Tube}} = \frac{\overline{\boldsymbol{T}}_{\boldsymbol{Tube1}}+\overline{\boldsymbol{T}}_{\boldsymbol{Tube2}}+\overline{\boldsymbol{T}}_{\boldsymbol{Tube3}}+\overline{\boldsymbol{T}}_{\boldsymbol{Tube4}}+\overline{\boldsymbol{T}}_{\boldsymbol{Tube5}}+\overline{\boldsymbol{T}}_{\boldsymbol{Tube6}}}{\boldsymbol{6}} = \boldsymbol{49.56}℃ \quad (11)$$

Then, the average standard deviation is obtained by the following formula.

$$s_{tube} = \sqrt{\frac{\sum_{i=1}^{N}(T_{tubei} - \bar{T}_{tube})^2}{N(N-1)}} = 0.029 \quad (12)$$

Therefore, the average T_{tube} can be written as 49.5 ± 0.029℃. $\bar{T}_{out}$ calculation results obtained 32.95℃. The average standard deviation was calculated using the following equation:

$$s_{Tout} = \sqrt{\frac{\sum_{i=1}^{N}(T_{outi} - \bar{T}_{out})^2}{N(N-1)}} = 0,051 \quad (13)$$

Furthermore, the average value of T_{out} can be written as 32.95 ± 0.051℃. Using the same equation, the standard deviation of T_{in} was found to be 0.033. Thus, the average T_{in} value was 29.75 ± 0.016℃.

The value of q at a speed of 0.4 m/s was found to be 19.48 W. To determine of the standard deviation of q, the following equation was used:

$$RSS_q = \sqrt{\left(s(\Delta T_{out})\frac{\partial q}{\partial T_{out}}\right)^2 + \left(s(\Delta T_{in})\frac{\partial q}{\partial T_{in}}\right)^2} \quad (14)$$

$$\frac{\partial q}{\partial T_{out}} = \frac{\partial(m \cdot c_p \cdot T_{out} - m \cdot c_p \cdot T_{in})}{\partial T_{out}} = m \cdot c \cdot p$$

$$\frac{\partial q}{\partial T_{in}} = \frac{\partial(m \cdot c_p \cdot T_{out} - m \cdot c_p \cdot T_{in})}{\partial T_{in}} = -(m \cdot c \cdot p)$$

where $s(\Delta T_{out}) = 0.051$℃ and $s(\Delta T_{in}) = 0.033$℃, ensuring, that RSS_q= ± 0.290 W. Therefore, the heat transfer rate q becomes 19.48 ± 0.290 W. The value of ΔT_{lmtd} at a speed of 0.4 m/s was found to be 18.56℃. To determine the value of the standard deviation of ΔT_{lmtd} we used the following equation:

$$RSS_{\Delta T_{lmtd}} = \sqrt{\left(s(\Delta T_{tube})\frac{\partial(\Delta T_{lmtd})}{\partial T_{tube}}\right)^2 + \left(s(\Delta T_{out})\frac{\partial(\Delta T_{lmtd})}{\partial T_{out}}\right)^2 + \left(s(\Delta T_{in})\frac{\partial(\Delta T_{lmtd})}{\partial T_{in}}\right)^2} \quad (15)$$

$$\frac{\partial(\Delta T_{lmtd})}{\partial T_{tube}} = \frac{\partial\left(\frac{(T_{tube} - T_{out}) - (T_{tube} - T_{in})}{\ln\frac{T_{tube} - T_{out}}{T_{tube} - T_{in}}}\right)}{\partial T_{tube}}$$

$$\frac{\partial(\Delta T_{lmtd})}{\partial T_{out}} = \frac{\partial\left(\frac{(T_{tube} - T_{out}) - (T_{tube} - T_{in})}{\ln\frac{T_{tube} - T_{out}}{T_{tube} - T_{in}}}\right)}{\partial T_{out}}$$

$$\frac{\partial(\Delta T_{lmtd})}{\partial T_{in}} = \frac{\partial\left(\frac{(T_{tube} - T_{out}) - (T_{tube} - T_{in})}{\ln\frac{T_{tube} - T_{out}}{T_{tube} - T_{in}}}\right)}{\partial T_{in}}$$

where $s(\Delta T_{tube}) = 0{,}029$℃, $s(\Delta T_{out}) = 0{,}051$℃ and $s(\Delta T_{in}) = 0{,}033$℃; we get $RSS_{\Delta T_{lmtd}}$ of ± 0.043, ensuring, that the obtained ΔT_{lmtd} is 8.56 ± 0.043.

The value of Nu at a speed of 0.4 m/s was found to be 155.31. The standard deviation of *Nu* was obtained using following equation

$$RSS_{Nu} = \sqrt{\left(s(q)\frac{\partial Nu}{\partial Q}\right)^2 + s(\Delta T_{lmtd})\frac{\partial Nu}{\partial \Delta T_{lmtd}}} \quad (16)$$

$$\frac{\partial Nu}{\partial q} = \frac{\partial\left(q \cdot D_h . At^{-1} \cdot {\Delta T_{lmtd}}^{-1} \cdot k^{-1}\right)}{\partial q} = \frac{D_h}{(At)(\Delta T_{lmtd})(k)}$$

$$\frac{\partial Nu}{\partial \Delta T_{lmtd}} = \frac{\partial\left(q \cdot D_h \cdot At^{-1} \cdot {\Delta T_{lmtd}}^{-1} . k^{-1}\right)}{\partial \Delta T_{lmtd}} = \frac{q . D_h}{(At)(\Delta T_{lmtd})^2(k)}$$

With the values of $s(q) = 0.290\ W$ and $s(\Delta T_{lmtd}) = 0.043$, the obtained RSS_{Nu} was ± 2.889 W/(m²℃). Therefore, the value of RSS_{Nu} is 155.31 ± 2.889 W/m²℃.

The value of h at a speed of 0.4 m/s was found to be 44.86. To determine the standard deviation of *Nu* the following equation is used

$$RSS_h = \sqrt{\left(s(Nu)\frac{\partial h}{Nu}\right)^2} \quad (17)$$

$$\frac{\partial h}{\partial Nu} = \frac{\partial(h . D_h . k^{-1})}{\partial h} = \frac{k}{D_h}$$

Furthermore, the value of_D_h is 0.092 m and *k* at T_f= 40.24 is 0.026. So the value of h at a speed of 0.4 m/s is:

$$RSS_h = \sqrt{\left(s(Nu)\frac{\partial h}{Nu}\right)^2} = 0{,}83$$

Thus, the number *h* at a speed of 0.4 m/s is 44.86 ± 0.83. So, the error h for the baseline at a speed of 0.4 m/s is

$$Error = \frac{RSS_h}{h} \times 100 \quad (18)$$

$$Error = \frac{0.83}{44.86} \times 100 = 1.51\%$$

From the test in the baseline case with a speed of 2.0 m/s, the results of the pressure drop are listed in Table 4, which show that the average *P* can be calculated as follows:

$$\overline{\Delta P} = \frac{\Delta P_1 + \Delta P_2 + \Delta P_3 + \cdots + \Delta P_{30}}{30} = 3.51 \text{ Pa} \quad (19)$$

The average standard deviation of the pressure drop can then be calculated using the equation

$$s = \sqrt{\frac{\sum_{i=1}^{N}(\Delta P_i - \overline{\Delta P})^2}{N(N-1)}} = 8.9 \times 10^{-5} \quad (20)$$

Baseline case for the pressure drop value at a speed of 2.0 m/s is $3.51 \pm 8.9 \times 10^{-5}$Pa. Then, the error in the form of percentage can be calculated using the following equation:

$$\frac{8.9 \times 10^{-5}}{3.51} \times 100 = 0.71$$

Table 4 Baseline pressure drop data at a speed of 2.0 m/s

ΔP (Pa)			
Data to	2.0 m/s	Data to	2.0 m/s
1	0.013	16	0.012
2	0.013	17	0.013
3	0.013	18	0.012
4	0.013	19	0.012
5	0.012	20	0.013
6	0.013	21	0.013
7	0.013	22	0.012
8	0.012	23	0.013
9	0.013	24	0.012
10	0.013	25	0.013
11	0.013	26	0.013
12	0.013	27	0.013
13	0.012	28	0.013
14	0.012	29	0.012
15	0.013	30	0.012

The equal calculation approach changed into used for all data. Therefore, the overall error outputs for the pressure-drop vortex generator with placement variations (in-line and staggered), *Re* and amount of VG sets (one, two and three) are listed in Table 5.

Table 5. Overall Pressure Drop (ΔP)

Vortex Generator Variations	*Overall Error P (perforated)*
1 PRWP *in-line*	2.94%
2 PRWP *in-line*	2.87%
3 PRWP *in-line*	1.98%
1 PRWP *staggered*	2.88%
2 PRWP *staggered*	2.34%
3 PRWP *staggered*	1.36%
1 PCRWP *in-line*	2.72%
2 PCRWP *in-line*	1.80%
3 PCRWP *in-line*	1.80%
1 PCRWP *staggered*	2.43%
2 PCRWP *staggered*	1.91%

3 PCRWP *staggered*	0.97%

The average TEF results from the experimental results can be calculated as follows.

$$\overline{TEF} = \frac{TEF_1+TEF_2+TEF_3+\cdots+TEF_{12}}{12} = 1.12 \quad (21)$$

Then, the average standard deviation of the TEF can be calculated with the equation

$$s = \sqrt{\frac{\sum_{i=1}^{N}(TEF_i-\overline{TEF})^2}{N(N-1)}} = 1.07 \quad (22)$$

Therefore, the TEF value was 1.12 ± 1.07. Then, the error in the form of percentage can be calculated using the following equation:

$$\frac{1.07}{1.12} \times 100 = 0.94\%$$

The overall error results for the TEF vortex generator with placement variations (in-line and staggered), *Re* and amount of VG sets (one, two and three) are are listed inTable 6.

Table 6. Overall error *TEF*

Variasi Vortex Generator	*Overall Error TEF* (Berlubang)
1 RWP *in-line*	0.47 %
2 RWP *in-line*	0.47%
3 RWP *in-line*	0.43%
1 RWP *staggered*	0.47%
2 RWP *staggered*	0.47%
3 RWP *staggered*	0.43%
1 CRWP *in-line*	0.45%
2 CRWP *in-line*	0.45%
3 CRWP *in-line*	0.42%
1 CRWP *staggered*	0.45%
2 CRWP *staggered*	0.45%
3 CRWP *staggered*	0.41%

First, find the average *CBR* of the experimental results with the following formula.

$$\overline{CBR} = \frac{CBR_1+CBR_2+CBR_3+\cdots+CBR_{12}}{12} = 2.14 \quad (23)$$

The average standard deviation of the pressure drop *CBR* can then be calculated using the following equation:

$$s = \sqrt{\frac{\sum_{i=1}^{N}(CBR_i-\overline{CBR})^2}{N(N-1)}} = 1.60 \quad (24)$$

The *CBR* value is 2.14 ± 1.60. Then the error in the form of percentage can be calculated using thefollowing equation:

$$\frac{1.60}{2.14} \times 100 = 0.63\%$$

The overall error results for the *CBR* vortex generator with placement variations (in-line and staggered), *Re* and amount of VG sets (one, two and three) are listed in Table 7

Table 7. Overall *error CBR*

Variasi Vortex Generator	*Overall Error CBR* (Berlubang)
1 RWP *in-line*	0.32%
2 RWP *in-line*	0.29%
3 RWP *in-line*	0.45%
1 RWP *staggered*	0.32%
2 RWP *staggered*	0.31%
3 RWP *staggered*	0.45%
1 CRWP *in-line*	0.4%
2 CRWP *in-line*	0.42%
3 CRWP *in-line*	0.56%
1 CRWP *staggered*	0.43%
2 CRWP *staggered*	0.42%
3 CRWP *staggered*	0.66%

Conclusion

Based on the experimental results for perforated concave rectangular winglet pair vortex generators (PCRWP VGs) used to increase the heat transfer of airflow through heated tubes arranged in-line in the duct, we conclude that using PCRWP VGs affects the convection heat transfer coefficient, pressure drop in achieving hydraulic thermal performance and cost-benefit ratio. In our investigation, the best heat-transfer convection coefficient was 153.5 W/m^2·K for the three pairs of PCRW VGs, in a staggered manner. The greatest improvement in the pressure drop value (4.58 Pa), occurred for one pair of PCRW VGs arranged in a staggered manner, whereas the hydraulic thermal performance was the best (1.29) in this experiment with the three pairs of PCRW VGs arranged in a staggered manner. Finally, the best *CBR* (3.56) was recorded for the three pairs of PCRW VGs composed in a staggered manner.

Acknowledgements

The authors would like to thank LEMLITBANG UHAMKA which has funded this research through internal grants from UHAMKA and UPPI UHAMKA what have contributed in facilitating translation and proof reading. The authors also thank the UNDIP thermofluidics laboratory, where the authors carried out this experiment.

Bibliography

[1] R. Sebayang, "AC Akan Jadi Pengkonsumsi Listrik Utama di Dunia," *CNBC Indonesia*. 2018.

[2] Z. Qian, Q. Wang, and J. Cheng, “Analysis of heat and resistance performance of plate fin-and-tube heat exchanger with rectangle-winglet vortex generator,” *Int J Heat Mass Transf*, vol. 124, pp. 1198–1211, 2018, doi: 10.1016/j.ijheatmasstransfer.2018.04.037.

[3] D. Mugisidi, O. Heriyani, P. H. Gunawan, and D. Apriani, “Performance improvement of a forced draught cooling tower using a vortex generator,” *CFD Letters*, vol. 13, no. 1, pp. 45–57, 2021, doi: 10.37934/cfdl.13.1.4557.

[4] A. J. Modi, N. A. Kalel, and M. K. Rathod, “Thermal performance augmentation of fin-and-tube heat exchanger using rectangular winglet vortex generators having circular punched holes,” *Int J Heat Mass Transf*, vol. 158, pp. 1–16, 2020, doi: 10.1016/j.ijheatmasstransfer.2020.119724.

[5] K. W. Song and T. Tagawa, “The optimal arrangement of vortex generators for best heat transfer enhancement in flat-tube-fin heat exchanger,” *International Journal of Thermal Sciences*, 2018, doi: 10.1016/j.ijthermalsci.2018.06.011.

[6] C. Yu, H. Zhang, M. Zeng, R. Wang, and B. Gao, “Numerical study on turbulent heat transfer performance of a new compound parallel flow shell and tube heat exchanger with longitudinal vortex generator,” *Appl Therm Eng*, vol. 164, no. May 2019, p. 114449, 2020, doi: 10.1016/j.applthermaleng.2019.114449.

[7] M. Samadifar and D. Toghraie, “Numerical simulation of heat transfer enhancement in a plate-fin heat exchanger using a new type of vortex generators,” *Appl Therm Eng*, vol. 133, no. September 2017, pp. 671–681, 2018, doi: 10.1016/j.applthermaleng.2018.01.062.

[8] U. Kashyap, K. Das, and B. K. Debnath, “Effect of surface modification of a rectangular vortex generator on heat transfer rate from a surface to fluid,” *International Journal of Thermal Sciences*, vol. 127, no. August 2017, pp. 61–78, 2018, doi: 10.1016/j.ijthermalsci.2018.01.004.

[9] U. Kashyap, K. Das, and B. K. Debnath, “Effect of surface modification of a rectangular vortex generator on heat transfer rate from a surface to fluid: An extended study,” *International Journal of Thermal Sciences*, vol. 134, no. August, pp. 269–281, 2018, doi: 10.1016/j.ijthermalsci.2018.08.020.

[10] A. Q. Ibrahim and R. S. Alturaihi, “Experimental Work for Single-Phase and Two-Phase Flow in Duct Banks with Vortex Generators,” *Results in Engineering*, p. 100497, Sep. 2022, doi: 10.1016/J.RINENG.2022.100497.

[11] K. W. Song, T. Tagawa, Z. H. Chen, and Q. Zhang, “Heat transfer characteristics of concave and convex curved vortex generators in the channel of plate heat exchanger under laminar flow,” *International Journal of Thermal Sciences*, vol. 137, no. November 2018, pp. 215–228, 2019, doi: 10.1016/j.ijthermalsci.2018.11.002.

[12] K. A. Hammoodi, H. A. Hasan, M. H. Abed, A. Basem, and A. M. Al-Tajer, “Control of heat transfer in circular channels using oblique triangular ribs,” *Results in Engineering*, vol. 15, p. 100471, Sep. 2022, doi: 10.1016/J.RINENG.2022.100471.

[13] M. Zeeshan, S. Nath, D. Bhanja, and A. Das, “Numerical investigation for the optimal placements of rectangular vortex generators for improved thermal performance of fin-and-tube heat exchangers,” *Appl Therm Eng*, 2018, doi: 10.1016/j.applthermaleng.2018.03.006.

[14] H. Linardos, G. Mavrogenis, and D. Margaris, “Novel designs of LVGs conformations and introduction of Batch Heated and Channeled Pipe for increasing heat transfer efficiency in pipes,” *Results in Engineering*, vol. 13, p. 100357, Mar. 2022, doi: 10.1016/J.RINENG.2022.100357.

[15] O. Heriyani, M. Djaeni, and . Syaiful, “Thermal-Hydraulic Performance Analysis by Means of Rectangular Winglet Vortex Generators in a Channel: An Experimental Study,” *European Journal of Engineering and Technology Research*, vol. 6, no. 3, pp. 150–153, 2021, doi: 10.24018/ejers.2021.6.3.2424.

[16] C. Wang, Z. Wang, L. Wang, L. Luo, and B. Sundén, “Experimental study of fluid flow and heat transfer of jet impingement in cross-flow with a vortex generator pair,” *Int J Heat Mass Transf*, vol. 135, pp. 935–949, 2019, doi: 10.1016/j.ijheatmasstransfer.2019.02.024.

[17] Z. Sun, K. Zhang, W. Li, Q. Chen, and N. Zheng, “Investigations of the turbulent thermal-hydraulic performance in circular heat exchanger tubes with multiple rectangular winglet vortex generators,” *Appl Therm Eng*, vol. 168, p. 114838, Mar. 2020, doi: 10.1016/J.APPLTHERMALENG.2019.114838.

[18] P. Promvonge and S. Skullong, “Thermo-hydraulic performance in heat exchanger tube with V-shaped winglet vortex generator,” *Appl Therm Eng*, 2020, doi: 10.1016/j.applthermaleng.2019.114424.

[19] S. Skullong, P. Promthaisong, P. Promvonge, C. Thianpong, and M. Pimsarn, “Thermal performance in solar air heater with perforated-winglet-type vortex generator,” *Solar Energy*, vol. 170, no. June, pp. 1101–1117, 2018, doi: 10.1016/j.solener.2018.05.093.

[20] Z. Han, Z. Xu, and J. Wang, “Numerical simulation on heat transfer characteristics of rectangular vortex generators with a hole,” *Int J Heat Mass Transf*, vol. 126, pp. 993–1001, 2018, doi: 10.1016/j.ijheatmasstransfer.2018.06.081.

[21] C. Luo, S. Wu, K. Song, L. Hua, and L. Wang, “Thermo-hydraulic performance optimization of wavy fin heat exchanger by combining delta winglet vortex generators,” *Appl Therm Eng*, 2019, doi: 10.1016/j.applthermaleng.2019.114343.

[22] H. Naik and S. Tiwari, “Effect of winglet location on performance of fin-tube heat exchangers with inline tube arrangement,” *Int J Heat Mass Transf*, vol. 125, pp. 248–261, 2018, doi: 10.1016/j.ijheatmasstransfer.2018.04.071.

[23] M. Zeeshan, S. Nath, D. Bhanja, and A. Das, “Numerical investigation for the optimal placements of rectangular vortex generators for improved thermal performance of fin-and-tube heat exchangers,” *Appl Therm Eng*, vol. 136, pp. 589–601, May 2018, doi: 10.1016/J.APPLTHERMALENG.2018.03.006.

[24] Y. Effendi, A. Prayogo, Syaiful, M. Djaeni, and E. Yohana, “Effect of perforated concave delta winglet vortex generators on heat transfer and flow resistance through the heated tubes in the channel,” *Experimental Heat Transfer*, vol. 35, no. 5, pp. 553–576, 2022, doi: 10.1080/08916152.2021.1919245.

[25] S. Whitaker, “Forced Convection Heat Transfer Correlations for Flow In Pipes, Past Flat Plates, Single e Cylinders, Single Spheres, and for Flow In Packed Beds and Tube Bundles,” *Reprillted from AIChE JOURNAL*, 1972.

[26] M. Awais and A. A. Bhuiyan, “Enhancement of thermal and hydraulic performance of compact finned-tube heat exchanger using vortex generators (VGs): A parametric study,” *International Journal of Thermal Sciences*, vol. 140, pp. 154–166, Jun. 2019, doi: 10.1016/J.IJTHERMALSCI.2019.02.041.

[27] A. Gupta, A. Roy, S. Gupta, and M. Gupta, “Numerical investigation towards implementation of punched winglet as vortex generator for performance improvement of a fin-and-tube heat exchanger,” *Int J Heat Mass Transf*, vol. 149, p. 119171, Mar. 2020, doi: 10.1016/J.IJHEATMASSTRANSFER.2019.119171.

[28] M. W. Tian, S. Khorasani, H. Moria, S. Pourhedayat, and H. S. Dizaji, “Profit and efficiency boost of triangular vortex-generators by novel techniques,” *Int J Heat Mass Transf*, vol. 156, p. 119842, 2020, doi: 10.1016/j.ijheatmasstransfer.2020.119842.

[29] Y. L. He, P. Chu, W. Q. Tao, Y. W. Zhang, and T. Xie, “Analysis of heat transfer and pressure drop for fin-and-tube heat exchangers with rectangular winglet-type vortex generators,” *Appl Therm Eng*, vol. 61, no. 2, pp. 770–783, Nov. 2013, doi: 10.1016/J.APPLTHERMALENG.2012.02.040.

[30] M. Pranita Hendraswari, M. S. Tony, and M. F. Soetanto, “Heat Transfer Enhancement inside Rectangular Channel by Means of Vortex Generated by Perforated Concave Rectangular Winglets,” 2021, doi: 10.3390/fluids6010043.

[31] Syaiful, A. R. Siwi, T. S. Utomo, Yurianto, and R. Wulandari, “Numerical analysis of heat and fluid flow characteristics of airflow inside rectangular channel with presence of perforated concave delta winglet vortex generators,” *International Journal of Heat and Technology*, vol. 37, no. 4, pp. 1059–1070, 2019, doi: 10.18280/IJHT.370415.

[32] A. Sinha, H. Chattopadhyay, A. K. Iyengar, and G. Biswas, “Enhancement of heat transfer in a fin-tube heat exchanger using rectangular winglet type vortex generators,” *Int J Heat Mass Transf*, vol. 101, pp. 667–681, Oct. 2016, doi: 10.1016/J.IJHEATMASSTRANSFER.2016.05.032.

[33] H. Ke *et al.*, “Thermal-hydraulic performance and optimization of attack angle of delta winglets in plain and wavy finned-tube heat exchangers,” *Appl Therm Eng*, vol. 150, pp. 1054–1065, Mar. 2019, doi: 10.1016/j.applthermaleng.2019.01.083.

[34] A. Arora, P. M. V. Subbarao, and R. S. Agarwal, “Development of parametric space for the vortex generator location for improving thermal compactness of an existing inline fin and tube heat exchanger,” *Appl Therm Eng*, vol. 98, pp. 727–742, Apr. 2016, doi: 10.1016/J.APPLTHERMALENG.2015.12.117.

[35] S. Gururatana and S. Skullong, “Heat transfer augmentation in a pipe with 3D printed wavy insert,” *Case Studies in Thermal Engineering*, vol. 21, p. 100698, Oct. 2020, doi: 10.1016/J.CSITE.2020.100698.

[36] A. Sinha, H. Chattopadhyay, A. K. Iyengar, and G. Biswas, “Enhancement of heat transfer in a fin-tube heat exchanger using rectangular winglet type vortex generators,” *Int J Heat Mass Transf*, vol. 101, pp. 667–681, Oct. 2016, doi: 10.1016/J.IJHEATMASSTRANSFER.2016.05.032.

[37] A. J. Modi and M. K. Rathod, “Experimental investigation of heat transfer enhancement and pressure drop of fin-and-circular tube heat exchangers with modified rectangular winglet vortex generator,” *Int J Heat Mass Transf*, vol. 189, p. 122742, Jun. 2022, doi: 10.1016/J.IJHEATMASSTRANSFER.2022.122742.

[38] Y. Li, Z. Qian, and Q. Wang, “Numerical investigation of thermohydraulic performance on wake region in finned tube heat exchanger with section-streamlined tube,” *Case Studies in Thermal Engineering*, vol. 33, p. 101898, May 2022, doi: 10.1016/J.CSITE.2022.101898.

[39] K. Boukhadia, H. Ameur, D. Sahel, and M. Bozit, “Effect of the perforation design on the fluid flow and heat transfer characteristics of a plate fin heat exchanger,” *International Journal of Thermal Sciences*, vol. 126, no. December 2017, pp. 172–180, Apr. 2018, doi: 10.1016/j.ijthermalsci.2017.12.025.

[40] C.-H. Huang and L.-W. Liu, “Optimal position and perforated radius of punched vortex generators for heat sink,” *Case Studies in Thermal Engineering*, vol. 32, p. 101916, Apr. 2022, doi: 10.1016/J.CSITE.2022.101916.

[41] Y. Menni *et al.*, “Effects of two-equation turbulence models on the convective instability in finned channel heat exchangers,” *Case Studies in Thermal Engineering*, vol. 31, p. 101824, Mar. 2022, doi: 10.1016/J.CSITE.2022.101824.

Perforated concave rectangular winglet pair vortex generators enhance the heat transfer of air flowing through heated tubes inside a channel

Oktarina Heriyani[*12], Mohammad Djaeni[1], Syaiful[*1], Aldila Kurnia Putri[1]
[1]Mechanical Engineering Department, Engineering Faculty, University of Diponegoro, Semarang, Indonesia
[2]Mechanical Engineering Program, Engineering Faculty, University of Muhammadiyah Prof. DR. HAMKA, Jakarta, Indonesia

Abstract

A significant increase in the rate heat transfer in a heat exchanger system is made possible by increasing the convection heat-transfer coefficient using a passive method. The addition of vortex generators (VGs) to the fins and tubes of a heat exchanger is currently the most effective passive method. However, the increase in heat was accompanied by an increase in pressure drop. Therefore, in this study, we installed perforated concave rectangular winglet pair vortex generators (PCRWP VGs) on plates in rectangular ducts to increase the heat transfer through the six heated tubes to the air stream by lowering the enhancement in the pressure drop. We attempted to determine the best cost-benefit ratio (*CBR*) with a fluid flow velocity difference of 0.4 –2 m/s at intervals of 0.2 m/s (Reynolds number (*Re*) of 2,143 to 11,763) in the channel. The PCRWP VGs were composed of in-line and staggered configurations. The results showed a lower *CBR* (3.56) for the in-line configuration than for the staggered configuration. Moreover, the lowest *CBR* was accompanied by an increase in thermal performance (*TEF*) of 1.29.

Keywords: Perforated; Rectangular winglet; Concave; Pressure drop; Vortex generator; Heat transfer; Thermal performance

1. Introduction

The global energy demand is expected to triple over the next few years. According to a statement by the International Energy Agency (IEA), the main driver is the increasing use of air conditioning (AC) machines [1]. Thus, promoting energy efficiency in air conditioners is important and requires maximising their thermal performance, which involves increasing the rate of heat transfer in its main component, i.e., the condenser. A condenser, commonly used in air conditioners, comprises a fin and a tube and functions as a refrigerant cooling medium. However, the high thermal resistance (75%) of the fin air side of the condenser lowers the heat-transfer rate in the heat exchanger[2]. Thus, the thermal resistance must be lowered to enhance the heat transfer rate.

A commonly used active methods to increase the rate of heat transfer involves adding vortex generators (VGs), which, according to the research results obtained by Mugisidi et al., increases the performance of a condenser[3]. The added VGs cause longitudinal vortices (LVs), damage the primary flow, make the second flow as large as the first and increase air mixing in the area[4][5]. The size of the LVs, shape of the flow, and mixing are influenced by the shape, geometry and position of the VGs added to the fins and tubes of the heat exchanger[6].

Samidifat et al. showed that simple rectangular vortex generators (RVGs) can increase the heat transfer rate by 7%; however, this causes a pressure drop in the heat exchanger system[7]. Meanwhile, modified RVGs with a concave shape on the front and rear surfaces decreased the heat transfer performance of the heat exchanger tube. A better option is to use RVGs with a double convex front surface and a single concave back surface, which can strengthen the primary vortex, increasing the rate of heat transfer from the plate to the fluid, as demonstrated in a study by Kashyap et al.[8]. Further research conducted by Kashyap et al. in the same year concluded that modifying the surface shape of rectangular winglet vortex generators (RWVGs) can create longitudinal eddies that interact with the boundary layer, thereby increasing the rate of convection heat transfer[9]. Based on their research, the

increase in the optimal heat transfer rate was 14.4. The optimal heat transfer performance was also obtained from the results of experiments conducted by Adnan et al. on rectangular ducts by adding delta and rectangular winglet VGs[10]. Concave curved delta winglet VGs were compared with convex curved delta winglet VGs by Song et al. to observe changes in the heat transfer rate[11].The results showed that the concave VGs improved the heat transfer better than the convex VGs. The differences in the shape of the VGs affects the change in the heat transfer rate and the change in the geometry of the VG, such as a new rib geometry in the cylinder channel[12].

Zeeshan et al. showed that increasing the angle of attack increased the rate of heat transfer (to 37.01–64.54%) if a pair of RWVGs were placed at the back of the tube even though this did not reduce the pressure drop[13]. A decrease in the value of the pressure drop also did not occur significantly, even though there was an increase in heat of 260% in heat, as per the results of the research conducted by Linardo et al. using the batched heat and channelled pipe (BHCP) approach[14]. The increase in heat transfer performance is influenced by the number of RWVG pairs based on the research results of Heriyani et al., where there is an increase in the hydraulic thermal performance evaluation criteria by 15.17% for three pairs of RWVG compared with the baseline [15]. Wang et al. found that the more pairs of VGs placed in the crossflow, the higher the increase in the heat transfer coefficient[16]. Sun et al. further discovered that increasing the number of RWVGs in the heat exchanger tube increased the heat transfer, with a maximum thermal enhancement factor (*TEF*) of 1.27 [17]. The *TEF* value of a V-delta winglet VG reached 1.82–3% higher than that of a V-rectangular winglet VG, as revealed by Promvonge et al.[18]. These results were obtained with an optimal blockage ratio (*BR*) of 0.15 and pitch ratio (*PR*) 1.0. Skullong et al. modified the shapes of RWVGs with optimal BRs and PRs to achieve an optimum heat transfer performance and reduced pressure drop; their shape modification involved perforating RWVGs [19].

The positions of the holes in the RWVGs did not significantly affect the increase in heat transfer; however, they significantly affected the flow resistance of the VGs. The heat-transfer rate increased as the height (vertical position) of the hole increased. Widthwise, although there is an initial increase, the heat transfer rate decreased with increasing lateral distance[20]. An increase in the number of holes in the RWVGs indicates an increase in fluid flow, which forces the fluid to flow behind the RWVGs, thereby increasing heat transfer[4]. The heat transfer rate increased during laminar flow when the Reynolds number (Re) increased and then decreased with an increase in Re during turbulent flow [20]. Positioning the tube in-line with a pair of RWVGs in a common flow-down configuration provides better performance than the common flow-up configuration. However, a staggered tube position is superior, resulting in a 25.85% higher heat-transfer performance than when a pair of RWVGs is not used[21].

In the existing studies, no detailed analyses of heat transfer were conducted on from the surfaces of several cylinders heated and arranged in-line when using a perforated vortex generator. Therefore, the focus herein is on investigating the advantages of using perforated concave rectangular winglet pair vortex generators (PCRWP VGs) to increase the heat transfer of the airflow through heated tubes arranged in-line in the ducts.

2. Experimental Approach

2.1 Experimental setup

This research was conducted experimentally with a test equipment scheme comprising a rectangular channel sized 370 x 18 x 8 cm. The duct was made of 1 cm thick glass, as shown in Fig. 1.

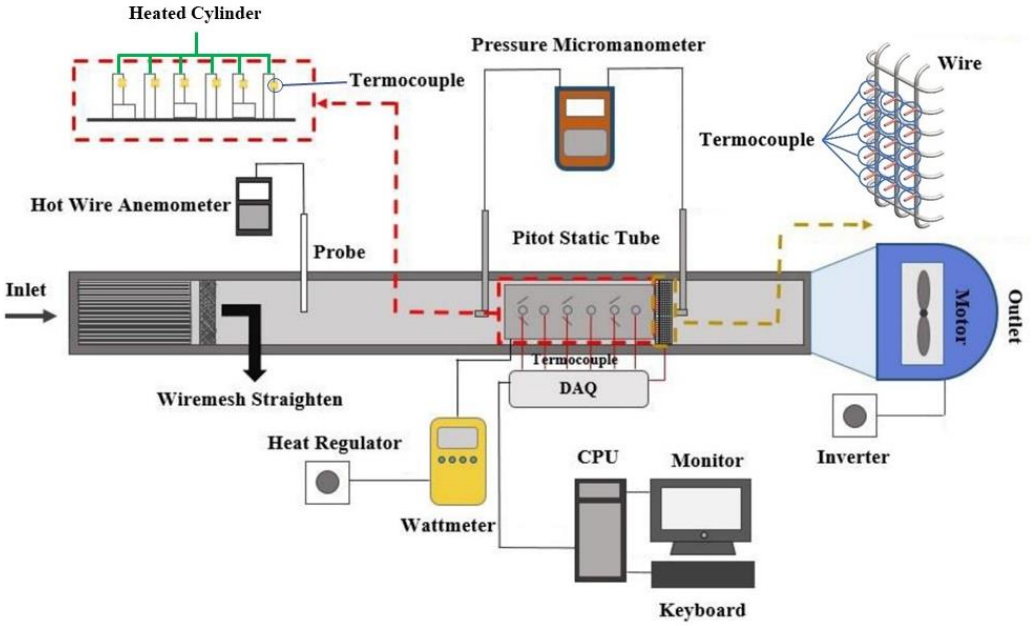

Fig. 1. Experimental tool schematic

Based on Fig. 1, the rectangular channel is equipped with a blower (50 Hz, Wipro with a rated voltage of 220V), an inverter (Mitsubishi Electric type FR-D700 with an accuracy of 0.01), straightener, hot wire anemometer (Lutron type AM-4204 with an accuracy of 0.1), wattmeter (Lutron DW-6060 with an accuracy ± 1.0), central processing unit (CPU), micromanometer, thermocouple (K type with a temperature interval of -200 –1250℃ and an accuracy ± 0.5) where one thermocouple was placed in the air inlet area, six thermocouples on the back surface of the tubes and 15 on the outlet side of the wire, data acquisition (Advantech USB-4718 type with an accuracy of 0.001) and heater regulator. The heater was connected to six tubes with a diameter of 19.05 mm and height of 65.8 mm, with each tube having the same power. Total heating power of 40 W was applied to the six tubes using a regulator. The heating air flowing through the tubes occurs via convection. Thus, the air at the outlet side becomes hotter than that at the inlet side.

A pressure micromanometer (Fluke type 922, with an accuracy of ± 0.05) was used to monitor the flow pressure drop. Two pitot tubes, each set 26 cm ahead of the inlet of the test specimen and 2.5 cm behind it, were connected to a micromanometer to measure the pressure drop. The pressure drop measurements were recorded 30 times for 5 sekon at each speed variation. Furthermore, flow visualisation was performed by directing the smoke from vaporised fluid in the fluid vaporator into the mainflow.

The VGs used as test specimens were perforated rectangular winglet pair (PRWP) and perforated concave rectangular winglet pair (PCRWP) vortex generators (VGs). Perforated is a term for holes in the VGs, as shown in Fig. 2. The VGs have dimensions of the same length and width of 30 mm, with

36 holes. The bore diameter on the VGs was 2.5 mm. The distance between the holes was 5 mm from the center.

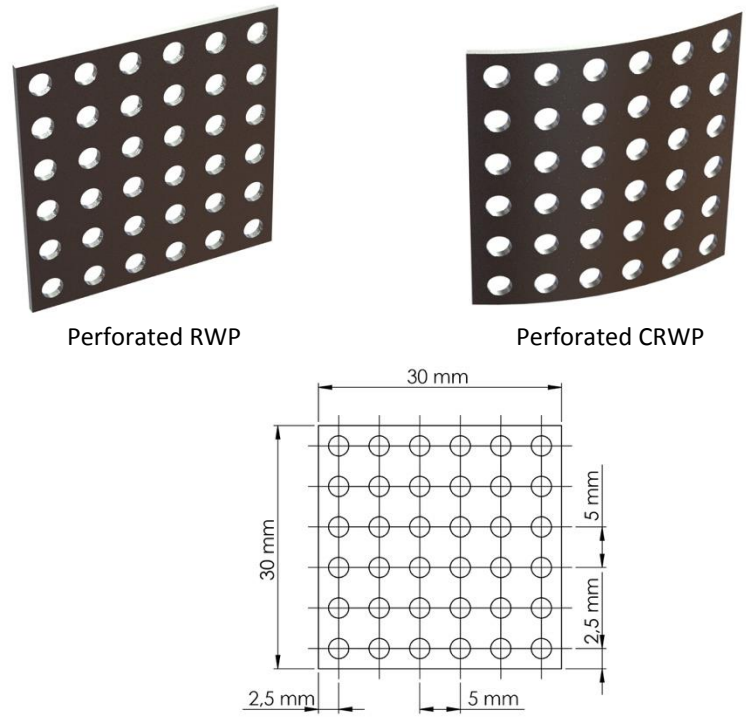

Fig. 2. Geometry of the VGs

The VGs are placed on an aluminium plate measuring 500 x 165 x 1 mm. The geometry and the pitch between VGs for both in-line and staggered configurations are shown in Fig 3, with an angle of attack (α) of 150[2]. The distance between the cylinders is 120 mm, with a cylinder diameter of 19.05 mm.

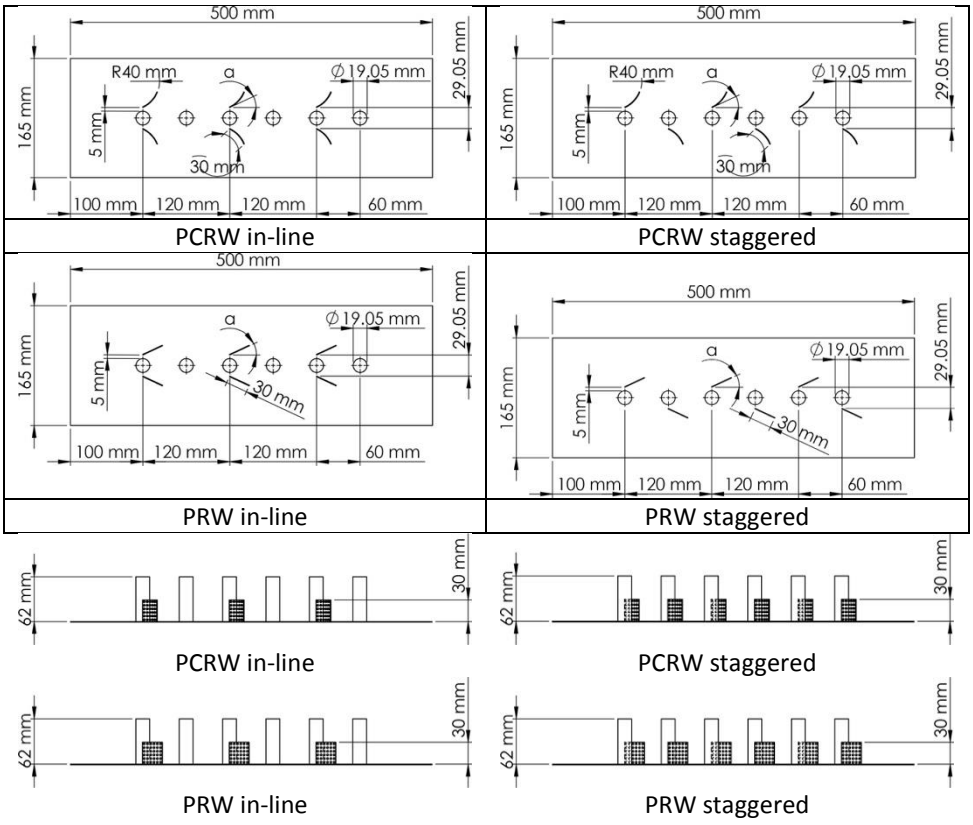

Fig. 3. Geometry and pitch of the VGs

The VGs configurations were arranged in-line and staggered on the plate. The perforated rectangular winglet (PRW) and perforated concave rectangular winglet (PCRW) VGs in-line configurations with one, two and three pairs are shown in Fig. 4. For each pair, the VGs were placed on the left and right sides of the first row of tubes. VGs were placed in the first- and third- row tubes for two pairs. For the three pairs, VGs were placed on the first-, third-, and fifth-row tubes.

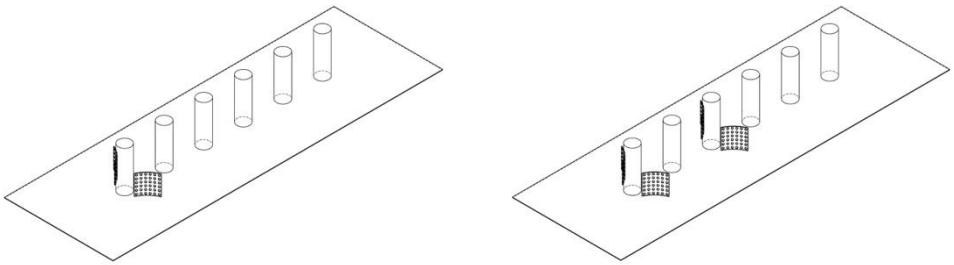

One pair PCRW in-line

Two pairs PCRW in-line

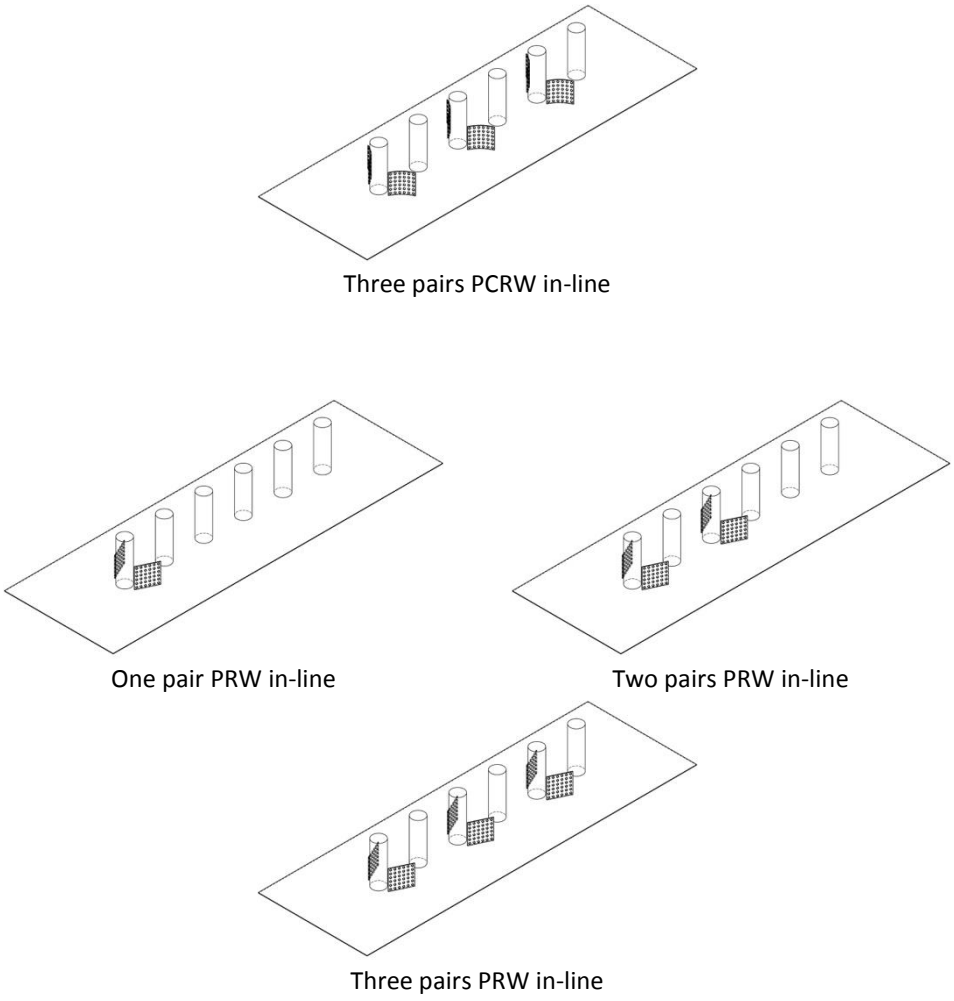

Fig. 4. VGs pairs in-line configurations

The PRW and PCRW VGs staggered configurations with one, two, and three pairs are shown in Fig. 5. For one pair, the VGs are placed on the right side of the first-row tube and on the left side of the second. The VGs are placed on the right side of the first and third row tubes and on the left side of the second and fourth tubes for two pairs. For the three pairs, the VGs are placed on the right side of the first, third and fifth rows of the tubes and on the left side of the second, fourth and sixth tubes.

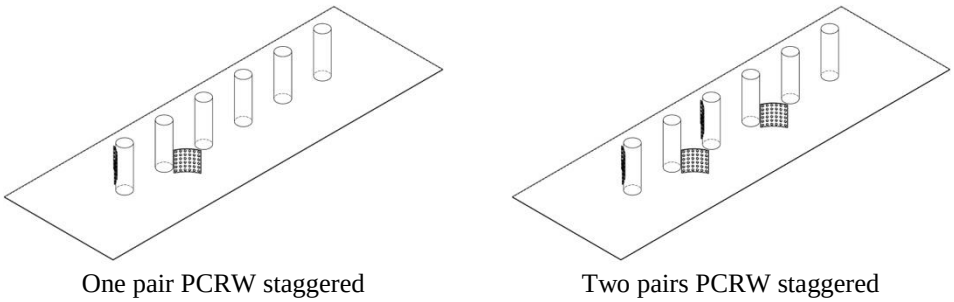

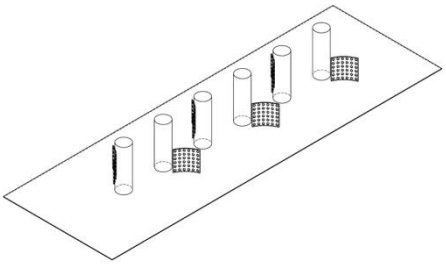

Three pairs PCRW staggered

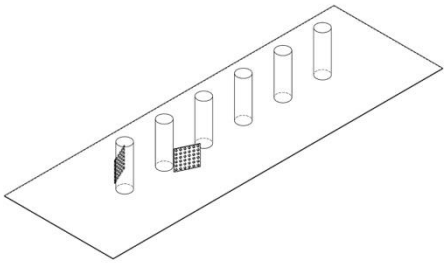

One pair PRW staggered

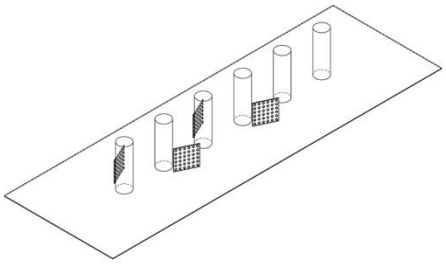

Two pairs PRW staggered

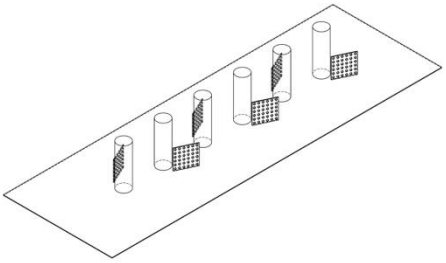

Three pairs PRW staggered

Fig. 5. VGs pairs staggered configurations

2.2 Parameter definitions

The parameters in this study were derived from the equation used by Oneissi et al. to obtain the thermal enhancement factor (*TEF*) [22]

$$TEF = \frac{\frac{Nu}{Nu_0}}{\left(\frac{f}{f_0}\right)^{\frac{1}{3}}} \qquad (1)$$

The Nusselt number dan friction factor for the baseline conditions are symbolised as (Nu_o) and (f_0), and (Nu) and (f) based on the research of Zeeshan et al[23]

$$Nu = \frac{q\, D_h}{A_{tube}\, \Delta T_{LMTD}\, k} \qquad (2)$$

$$h = \frac{q}{A_{tube}\,\Delta T_{LMTD}} \quad (3)$$

$$q = \dot{m}\, c_p\, (T_{out} - T_{in}) \quad (4)$$

where D_h, A_{tube}, ΔT_{LMTD}, $\dot{m}$, c_p, T_{out} and T_{in}, are hydraulic diameter, tube surface area, log mean temperature difference, mass flow rate, specific heat, outlet temperature, and inlet temperature, respectively

$$D_h = \frac{4A_c}{p} = \frac{4ab}{2(a+b)} = \frac{2ab}{a+b} \quad (5)$$

$$\Delta T_{LMTD} = \frac{(\bar{T}_{tube} - \bar{T}_{out}) - (\bar{T}_{tube} - \bar{T}_{in})}{\ln[(\bar{T}_{tube} - \bar{T}_{out}) - (\bar{T}_{tube} - \bar{T}_{in})]} \quad (6)$$

where A_c dan T_{tube} are channel surface area and tube temperature, respectively.

The result of D_h is used to calculate *Re* with the formula

$$Re = \frac{\rho u_{in} D_h}{\mu} \quad (7)$$

and friction factor (*f*) was determined to evalute the performance of hydro dynamic using

$$f = \frac{2\,\Delta P\, D_h}{\rho\, V^2 (L+6D)} \quad (8)$$

where $\rho, V,$ and L are the air density, inlet airflow velocity and length of the test specimen, respectively.

The equation required to determine the cost-benefit ratio (*CBR*), defined as the ratio of pressure drop per variation in *Nu* number, as formulated by Tian et al. [25], is as follows:

$$CBR = \frac{\%\Delta P}{\%Nu} \quad (9)$$

This concept investigates whether the method used to enhance the heat-transfer rate is economically efficient. In the hydrodynamic test, the pressure drop (ΔP) is measured by the pressure difference on the sides of P_{inlet} and P_{outlet} of the test specimen in the tested part using equation (10):

$$\Delta P = P_{inlet} - P_{outlet} \quad (10)$$

2.3 Validation

The current study is a follow-up investigation to the work of Yafid et al.[24], and the experimental setup was similar to that of Yafid et al. The difference between the current study and the experiment of Yafid et al. is a test object in which the current study uses concave rectangular winglet (CRW) VGs; in Yafid et al.'s experiment concave delta winglet (CDW) VGs are used. Whitaker et al. [25] studied the heat transfer characteristics of airflow through a single cylinder in a rectangular duct. The results of Yafid et al. were valid, and the same experimental set-up was determined. The *Nu* value from the experiment of Yafid et al. were comparable with the *Nu* values from the experiments of Whitaker et al. in the Reynolds number (*Re*) range of 2,143 to 11,763.

3. Results and Discussion

3.1 Flow visualisation

A flow visualisation test was performed to observe the longitudinal vortices (LV) formed after the flow passed through the VGs in the rectangular channel. This test was conducted under low-light conditions to clarify the LV. The laser beam was refracted by a cylindrical glass (diameter 5 mm), which produced a cross-sectional area perpendicular to the direction of the flow. Smoke formed from the evaporation of the liquid was used to visualise the LV in the flow. The VGs used in this visualisation test were PRWP and PCRWP with an in-line arrangement, as shown in Fig. 6.

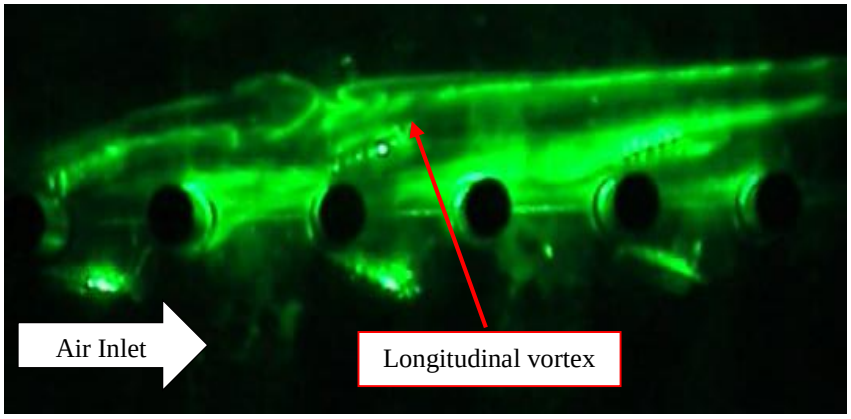

(a)

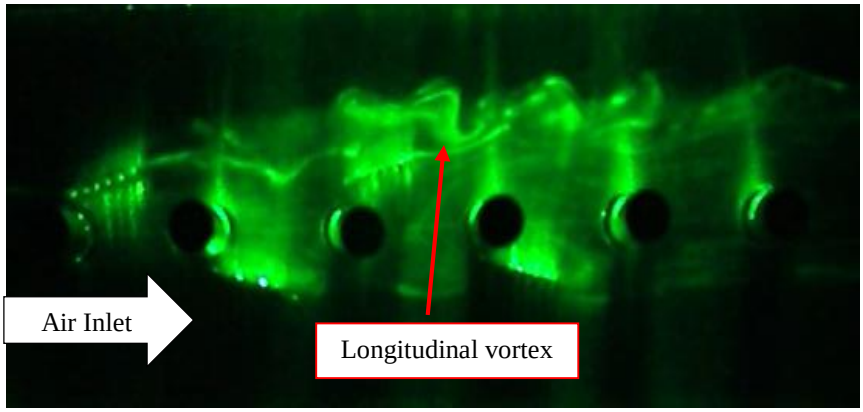

(b)

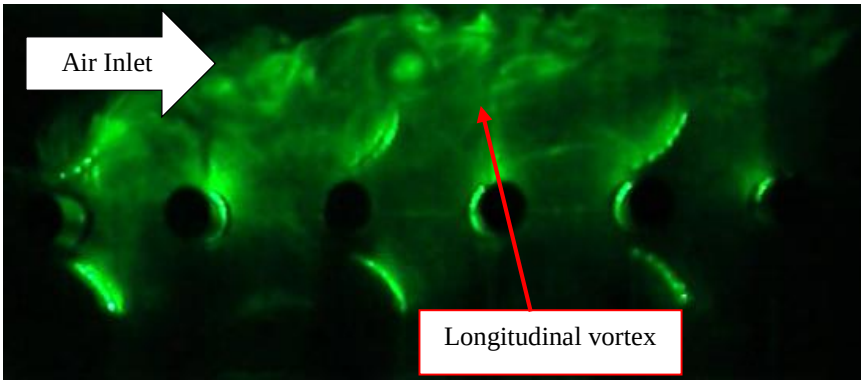

(c)

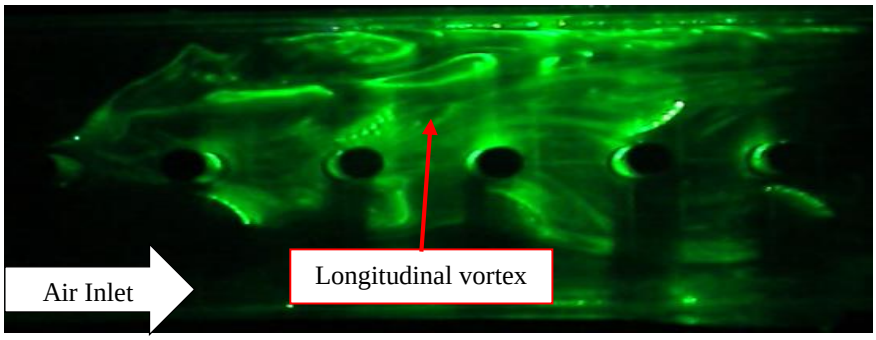

(d)

Fig. 6. Visualisation of LV generated by (a) in-line PRWP, (b) staggered PRWP, (c) in-line PCRWP and (d) staggered PCRWP

In Fig. 6 (c) and (d), the PCRWP VGs appear to produce longitudinal vortices (LV) in a wide flow area compared with the PRWP VGs in Fig 6 (a) and (b) downstream. The back region of the PCRWP VGs had a wider frontal surface area than the PRWP VGs. Consequently, mixing the near-fluid the channel walls with the fluid in the mainstream is better, meaning that the heat transfer rate is increased [26]. Downstream, the LV compression in the wake area increases the fluid flow velocity passing through the cylindrical structure, thereby increasing the heat transfer rate from the channel surface to the fluid flow in the wake region [27]. The increase in heat transfer produced when using PCRWP VGs was better than that with PRWP VGs.

3.2 Perforated vortex generators effect on heat transfer

The increase in the convection heat transfer was due to the mixing of fluids caused by the strong longitudinal vortices (LVs)[28]. The strength of the LVs is caused by the amount of VGs sets; increasing the amount of VGs pairs in the test specimen can increase the coefficient of the convection heat transfer [29], as shown in Fig. 7.

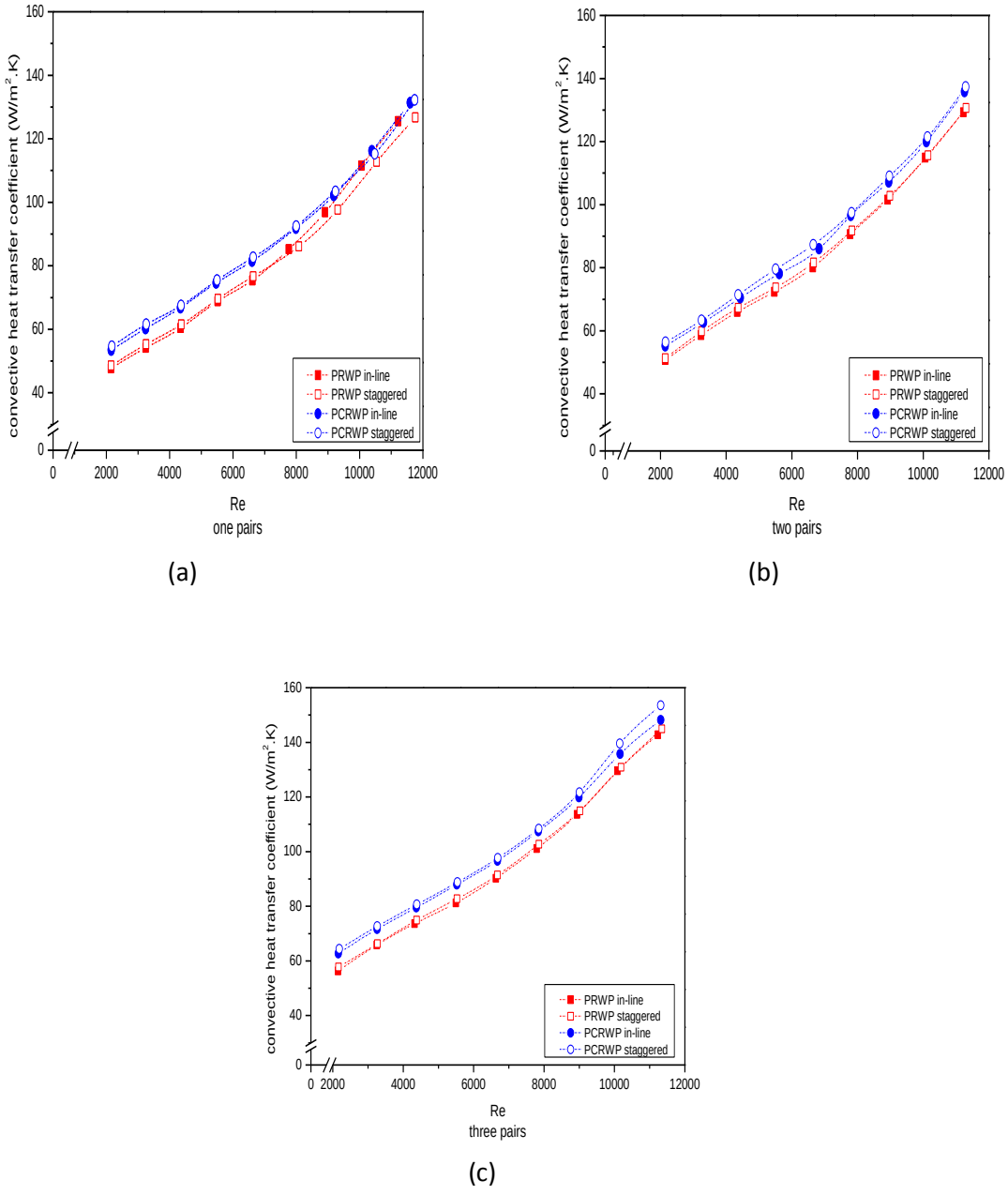

Fig. 7 Graphs of convective heat-transfer coefficient against Reynolds number: (a) one, (b) two and (c) three pairs.

In Fig 7, we can see the convective heat transfer coefficient with respect to the Reynolds number (*Re*), analysed after installing the PCRWP and PRWP with pairs ranging from one, two and three, arranged in-line or staggered. Based on Fig. 7, the convective heat transfer coefficient increased with a rise in *Re* due to an increase in flow vortices and high turbulence intensity in the channel[30], alongside a reduction in the wage region and stagnation area for each increase in flow velocity[31]. The improve in heat transfer for the staggered was better than that for the PCRW VGs with any number of pairs at the

highest *Re* (11,000). The results in Fig. 7 show that the PCRWP VGs worked better than the PRWP VGs, and the staggered arrangement of the former, with three pairs, gave the highest yield (153.5 W/m^2·K), as shown in Fig. 7(c). Two PCRW pairs (137.33 W/m^2·K, Fig. 7(b)) were better than one (132.25 W/m^2·K) (Fig. 7(a)) because the VGs with a concave surface destabilise the force of centrifugal of the fluid flow, strengthening the flow vortices and making the mixing of the hot fluid near the wall with the cold fluid of the main flow more robust[32]. In Fig. 7(a), the convection heat-transfer coefficient for the case of the in-line PRW VGs has the same value as that of the in-line or staggered PCRW VGs in a pair of VGs. In one pair of VGs, a longitudinal vortex is generated after the flow hits and weakens the VGs[29]. This result contrasts with the cases with two and three pairs of VGs, where the longitudinal vortex produced after striking the first VGs is amplified again when the flow strikes the second VGs and so on. Therefore, the value of the heat transfer coefficient in the case of a pair of PRW VGs is the same value as that of PCRW VGs at Reynolds numbers above 8,000.

3.3 Effect of perforated vortex generators on pressure drop

Using VGs can affect the increase in heat transfer, but there is often an accompanying increase in pressure drop, as shown in Fig. 8, where an increase in pressure drop can be seen along with the increases in *Re* and pair numbers for both the VG types PCRW and PRW. In general, the highest pressure drop was observed using the PCRWP VGs with a staggered configuration for all *Re*, except for one pair of VGs. The highest pressure drop was found in the PRWP VGs with an in-line configuration at *Re* greater than 8,000. The pressure drop on the staggered VGs was found to be higher than that on the in-line configuration because of the shorter distance between the VGs of the staggered configuration than that of the in-line[29], caused by the resistance of fluid flow against the walls of the VGs and the expansion of the frontal zone of the VGs in the next-pair arrangement [33]. The pressure drop in the staggered arrangement was lower than that in the in-line arrangement, whereas the PRW VGs type created a lower pressure drop than the PCRW VGs because the latter reduced the frontal area hit by the airflow, resulting in a decrease in drag [34]. In addition, the jet flow from the VG hole can reduce the stagnation flow, which can reduce the pressure drop [35]. A significant decrease in the pressure drop was due to the VG perforation[36]. The best pressure drop value for one pair with a staggered arrangement was 4.58 Pa (see Figure 8(a)), whereas two pairs (5 Pa, Figure 8(b)) were better than three (5.4 Pa, Figure 8(c)).

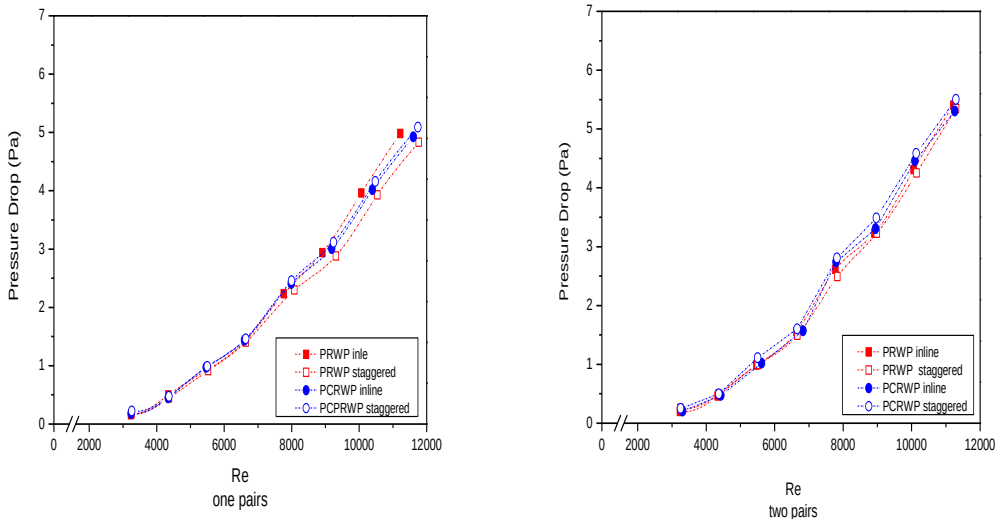

(a) (b)

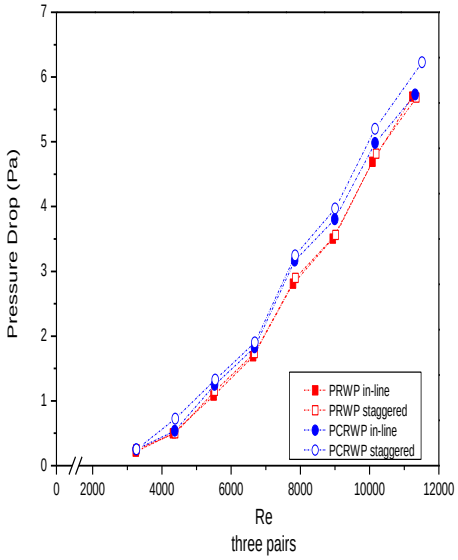

(c)

Fig. 8 Graph of pressure drop against Reynolds number: (a) one, (b) two and (c) three pairs

3.4 Effect of perforated VGs on thermal enhancement factor

TEF exhibited the hydraulic thermal performance while using VGs, which played a role in restructuring the incoming fluid flow pattern. The increase in the *TEF* was due to the influence of complex overlapping structures, which meant that the flow developed into a turbulent structure, significantly affecting the heat transfer increase [37]. The experimental *TEF* values are shown in Fig. 9.

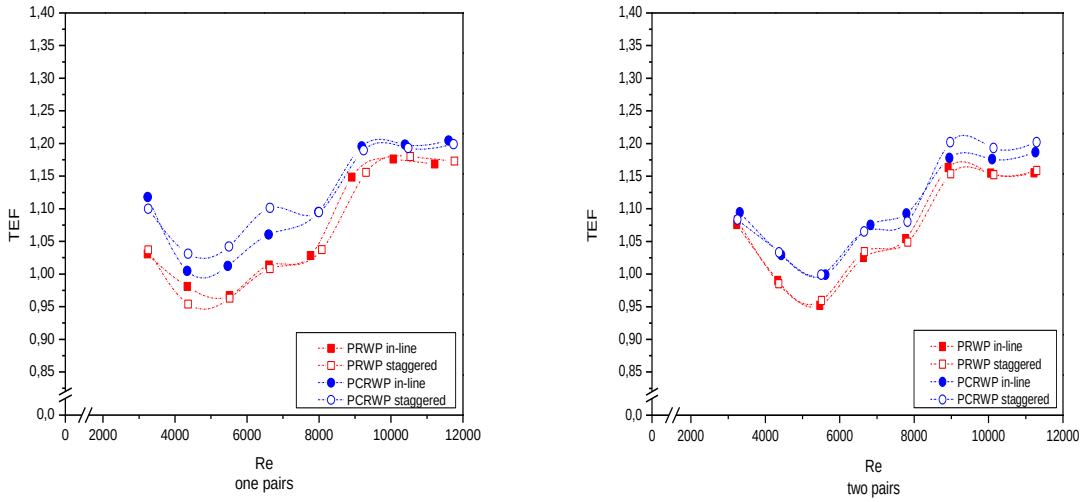

(a) (b)

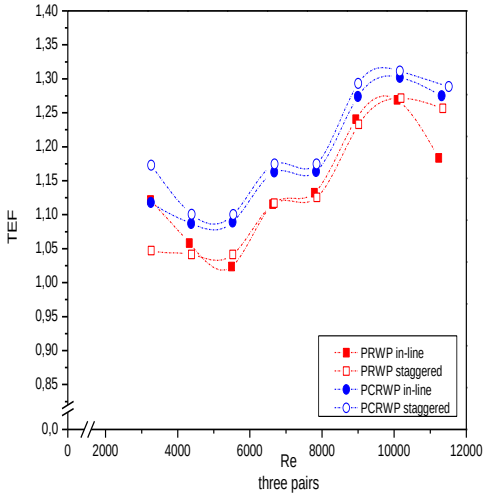

(c)

Fig. 9 Graph of thermal enhancement factor against Reynolds number: (a) one, (b) two and (c) three pairs

The *TEF* is the thermal-hydraulic performance which is the ratio of the increase in heat transfer to the pressure drop ratio. In general, the highest *TEF* was observed when the PCRWP VGs were used with a staggered configuration, as depicted in Fig 9. The PCRW creates wider flow vortices that can reduce the wake area behind the cylinder. Reducing the wake area can reduce the recirculation zone, affecting the heat transfer from the back of the cylinder to the stream [26]. A large-radius, high-intensity anterior-posterior vortex can reduce the wake area. A lessening within the wake zone increased the flow velocity behind the tube and reduced the recirculation area, resulting in increased heat transfer in this area [27, 38]. As shown in Fig 9, there was an increase in the *TEF* with greater pairs of VGs used for both the PCRW and PRW VG because the PCRW produced wider flow vortices, which reduced the wake region behind the cylinder, thereby reducing the recirculation zone and impacting the heat transfer increment from the rear cylinder surface to the stream[39]. In this process, a large number of longitudinal vortices with high intensities can reduce the wake area, which increases the flow velocity downstream of the tube and reduces the recirculation region, leading to an increased heat-ransfer rate in the region [40, 41]. Based on Figure 9, the best *TEF* increase occurred at Re between 8,000–9,000. The best *TEF* values, with one, two and three pairs occurred in the staggered arrangement with PCRW VGs, at 1.18, 1.20 and 1.29, respectively (see Fig. 9).

3.5 Effects of perforated VGs on the cost-benefit ratio

Economic evaluation cannot be conducted based only on the *TEF* and the net profit from the heat load of the transferred unit[26]. Instead, it must be determined by evaluating the economic value of the heat-transfer improvement by calculating the cost benefit ratio (*CBR*), as shown in Fig. 10.

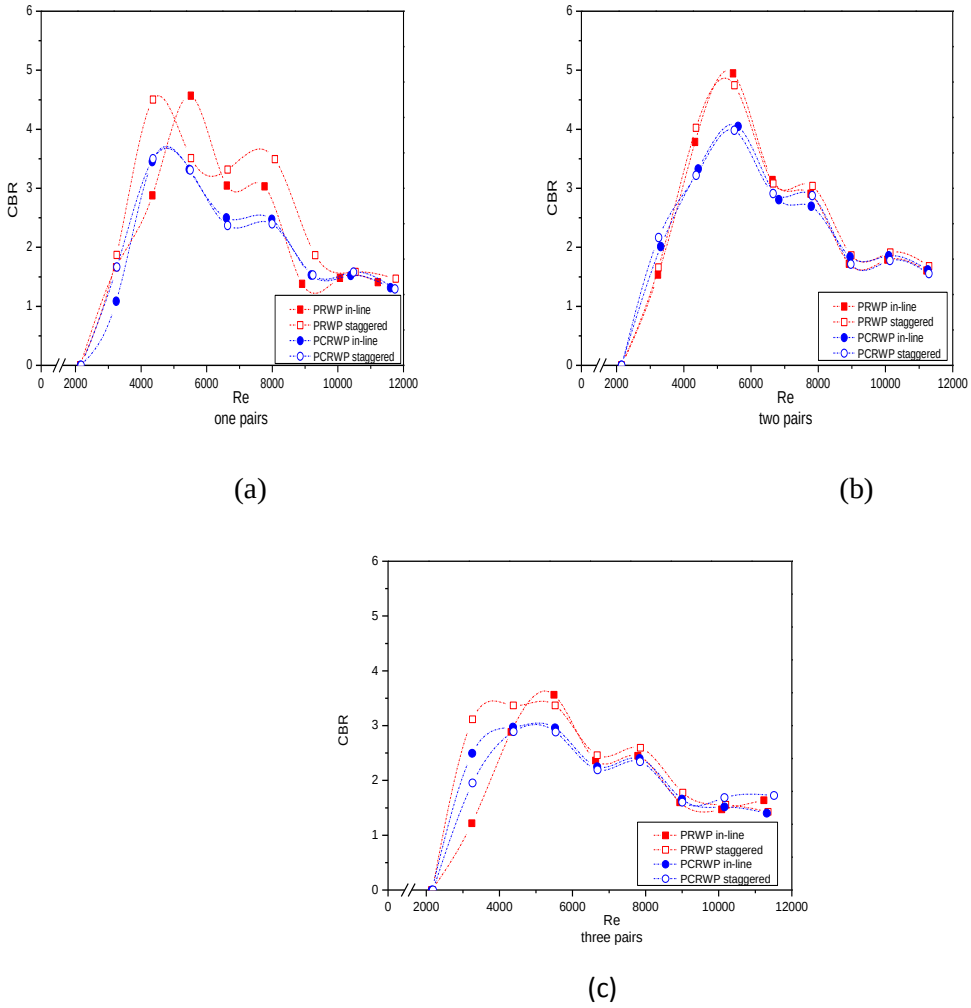

Fig. 10 Graph of cost-benefit ratio against Reynolds number: (a) one, (b) two and (c) three pairs

Fig. 10 show the result of the *CBR* calculation to compare the percentage increase in the pressure drop with the percentage increase in the Nusselt number when using VGs. These results indicate that a lower *CBR* improves thermal performance, which is greater than the drag force [25]. The greatest increase in *CBR* occured with the PRW VGs, with an in-line arrangement, totalling 4.57, 4.95 and 3.56 for one, two and three pairs, respectively. The lowest *CBR* was measured when three sets of PCRW vortex generators with a staggered arrangement were used. The lowest *CBR* were obtained with the three pairs of staggered-type VGs PCRW. The three VG pairs showed a lower *CBR* than the one and two pairs because they resulted in the greatest increase in the Nusselt number, accompanied by a lower pressure drop increase, which lowered the *CBR*. These results show that a lower *CBR* improves thermal performance relative to resistivity [26]. A low value *CBR* inicates a more economical value using VGs. In general, using PCRWP VGs with a staggered configuration is the best.

3.6 Heat Loss Analysis

Heat loss analysis was performed by considering the convection heat transfer from the six tubes to the surrounding fluid flow. The heat transfer rate was calculated for laminar and turbulent flows.

The heat loss in this experiment was calculated by calculating the difference between the induced electric power and total heat through convection from the surface of the tubes to the fluid. In this experiment, six tubes in a wind tunnel were heated using a heater at a power of 40 W; the velocity of the inlet fluid is varied from 0.4 to 2 m/s at intervals of 0.2 m/s or in the Reynolds number range from 2,143 to 11,763. Based on the Reynolds number range, two types of flows were determined; laminar and turbulent. Therefore, the heat loss was determined from the correlation between laminar at 0.4 m/s and turbulent for other velocities. The experimental data for the hydraulic diameter D_h, tube surface area A_{tube}, channel surface area A_c and air specific heat c_p are 0.09223 m, 0.02338908 m^2, 0.01056 m^2 and 1.007 J/kgK, respectively. Table 1 is a baseline for calculating heat loss

Table 1 Heat Loss Baseline

	v (m/s)	*Re*	Mass flow rate (kg/s)	**Density (kg/m^3)**	Dynamics viscous (kg/ms)	*k*	*Pr*	*T* inlet (C)	*T* outlet (C)	*T* tube (C)	**Δ***T* LMTD	**Δ***T* (*T* tube - *T* inlet)	*Nu*	*h* (W/mK)	*q* conv (W)	*q* input (W)	*q* loss (W)
baseline	0.4	2165	0.004757	1.13	1.9.E-05	0.03	0.73	29	33	50	19	21	155	45	19.48	40	20.52
	0.6	3291	0.00719	1.13	1.9.E-05	0.03	0.73	28	31	46	16	18	174	50	18.98	40	21.02
	0.8	4413	0.009618	1.14	1.9.E-05	0.03	0.03	28	30	44	15	16	192	50	19.19	40	20.81
	1	5545	0.012056	1.14	1.9.E-05	0.03	0.73	28	30	43	14	15	214	55	19.84	40	20.16
	1.2	6661	0.014477	1.14	1.9.E-05	0.03	0.73	28	29	43	14	15	228	61	21.15	40	18.85
	1.4	7826	0.016958	1.15	1.9.E-05	0.03	0.73	28	29	41	12	13	247	70	20.30	40	19.70
	1.6	8965	0.019407	1.15	1.9.E-05	0.03	0.73	27	29	40	12	13	263	75	21.03	40	18.97
	1.8	10110	0.021863	1.15	1.9.E-05	0.03	0.73	27	28	39	12	12	296	84	22.54	40	17.46
	2	11272	0.024341	1.15	1.9.E-05	0.03	0.73	27	28	38	11	11	342	97	24.17	40	15.83

From Table 1, the greater the velocity with an increase in the *Re*, the lower the heat loss. It can be observed that the heat flow from the heater not only spreads into the tube, but convection also occurs outside the tube. The heat output increased with *Re*, i.e, the higher the flow velocity, the greater the turbulence through the cylinder and the higher the turbulence intensity. An increase in the turbulence intensity between a cold airflow and hot cylinder with a constant surface temperature is caused by the airflow velocity[26]. In row-tube arrays, this recirculation area increased for the second and subsequent columns. A lower air velocity in the circulation region indicated less airflow in the region participating in the local heating process[37]. The heat loss under all conditions in this experiment is listed in table 2.

Table 2 Calculation of heat loss for the whole case

type VGs	*q* conv (W)	*q* input (W)	*q* loss (W)
Baseline	20.74	40	19.26
PCRWPI1	25.15	40	14.85
PCRWPI2	27.55	40	12.45

PCRWPI3	27.61	40	12.39
PCRWPS1	26.43	40	13.57
PCRWPS2	26.43	40	13.57
PCRWPS3	27.94	40	12.06
PRWPI1	24.09	40	15.91
PRWPI2	27.25	40	12.75
PRWPI3	28.82	40	11.18
PRWPS1	23.94	40	16.06
PRWPS2	26.37	40	13.63
PRWPS3	28.12	40	11.88

Table 2 shows that the lowest heat loss occurs when three sets of PCRWPs are staggered. The placement of the VGs can increase heat transfer in square ducts as the VGs create longitudinal vortices, which in turn increase vortex strength in the wake region downstream of the tube. Longitudinal vortices make the overall temperature field more uniform, improve heat mixing and boundary layer modification, and improve heat transfer performance. A higher number of vortex generators creates more longitudinal vortices and significantly increases heat transfer [29, 26].

3.7 Uncertainty Analysis

In this section, uncertainty analysis calculation data will be shown for the temperature at base-line conditions with a velocity of 0.4 m/s as shown in Table 3.

Table 3 Base-line test temperature data at a speed of 0.4 m/s

$T\ (Tube_1)$	$T\ (Tube_2)$	$T\ (Tube_3)$	$T\ (Tube_4)$	$T\ (Tube_5)$	$T\ (Tube_6)$
49.19093	51.21368	48.32313	49.76915	47.80219	51.27142
49.1834	51.17728	48.3156	49.79053	47.7657	51.2639
49.14545	51.16826	48.30655	49.7526	47.7856	51.25489
49.12105	51.17277	48.28214	49.72821	47.76118	51.2594
49.15297	51.20465	48.28515	49.73122	47.73524	51.2624
49.09966	51.15141	48.28967	49.73573	47.76871	51.26691
49.09815	51.14991	48.23029	49.73423	47.73826	51.29428
49.08912	51.14089	48.25019	49.66739	47.72922	51.22751

From these data, it is found that $\overline{\boldsymbol{T}}_{\boldsymbol{Tube}}$ can be calculated by the equation as

$$\overline{\boldsymbol{T}}_{\boldsymbol{Tube}} = \frac{\overline{\boldsymbol{T}}_{\boldsymbol{Tube1}}+\overline{\boldsymbol{T}}_{\boldsymbol{Tube2}}+\overline{\boldsymbol{T}}_{\boldsymbol{Tube3}}+\overline{\boldsymbol{T}}_{\boldsymbol{Tube4}}+\overline{\boldsymbol{T}}_{\boldsymbol{Tube5}}+\overline{\boldsymbol{T}}_{\boldsymbol{Tube6}}}{\boldsymbol{6}} = \boldsymbol{49.56}℃ \quad (11)$$

Then, the average standard deviation is obtained by the following formula.

$$s_{tube} = \sqrt{\frac{\sum_{i=1}^{N}(T_{tubei} - \bar{T}_{tube})^2}{N(N-1)}} = 0.029 \quad (12)$$

Therefore, the average T_{tube} can be written as 49.5 ± 0.029℃. $\bar{T}_{out}$ calculation results obtained 32.95℃. The average standard deviation was calculated using the following equation:

$$s_{Tout} = \sqrt{\frac{\sum_{i=1}^{N}(T_{outi} - \bar{T}_{out})^2}{N(N-1)}} = 0,051 \quad (13)$$

Furthermore, the average value of T_{out} can be written as 32.95 ± 0.051℃. Using the same equation, the standard deviation of T_{in} was found to be 0.033. Thus, the average T_{in} value was 29.75 ± 0.016℃.

The value of q at a speed of 0.4 m/s was found to be 19.48 W. To determine of the standard deviation of q, the following equation was used:

$$RSS_q = \sqrt{\left(s(\Delta T_{out})\frac{\partial q}{\partial T_{out}}\right)^2 + \left(s(\Delta T_{in})\frac{\partial q}{\partial T_{in}}\right)^2} \quad (14)$$

$$\frac{\partial q}{\partial T_{out}} = \frac{\partial(m \cdot c_p \cdot T_{out} - m \cdot c_p \cdot T_{in})}{\partial T_{out}} = m \cdot c \cdot p$$

$$\frac{\partial q}{\partial T_{in}} = \frac{\partial(m \cdot c_p \cdot T_{out} - m \cdot c_p \cdot T_{in})}{\partial T_{in}} = -(m \cdot c \cdot p)$$

where $s(\Delta T_{out}) = 0.051$℃ and $s(\Delta T_{in}) = 0.033$℃, ensuring, that RSS_q= ± 0.290 W. Therefore, the heat transfer rate q becomes 19.48 ± 0.290 W. The value of ΔT_{lmtd} at a speed of 0.4 m/s was found to be 18.56℃. To determine the value of the standard deviation of ΔT_{lmtd} we used the following equation:

$$RSS_{\Delta T_{lmtd}} = \sqrt{\left(s(\Delta T_{tube})\frac{\partial(\Delta T_{lmtd})}{\partial T_{tube}}\right)^2 + \left(s(\Delta T_{out})\frac{\partial(\Delta T_{lmtd})}{\partial T_{out}}\right)^2 + \left(s(\Delta T_{in})\frac{\partial(\Delta T_{lmtd})}{\partial T_{in}}\right)^2} \quad (15)$$

$$\frac{\partial(\Delta T_{lmtd})}{\partial T_{tube}} = \frac{\partial\left(\frac{(T_{tube} - T_{out}) - (T_{tube} - T_{in})}{\ln\frac{T_{tube} - T_{out}}{T_{tube} - T_{in}}}\right)}{\partial T_{tube}}$$

$$\frac{\partial(\Delta T_{lmtd})}{\partial T_{out}} = \frac{\partial\left(\frac{(T_{tube} - T_{out}) - (T_{tube} - T_{in})}{\ln\frac{T_{tube} - T_{out}}{T_{tube} - T_{in}}}\right)}{\partial T_{out}}$$

$$\frac{\partial(\Delta T_{lmtd})}{\partial T_{in}} = \frac{\partial\left(\frac{(T_{tube} - T_{out}) - (T_{tube} - T_{in})}{\ln\frac{T_{tube} - T_{out}}{T_{tube} - T_{in}}}\right)}{\partial T_{in}}$$

where $s(\Delta T_{tube}) = 0{,}029$℃, $s(\Delta T_{out}) = 0{,}051$℃ and $s(\Delta T_{in}) = 0{,}033$℃; we get $RSS_{\Delta T_{lmtd}}$ of ± 0.043, ensuring, that the obtained ΔT_{lmtd} is 8.56 ± 0.043.

The value of Nu at a speed of 0.4 m/s was found to be 155.31. The standard deviation of *Nu* was obtained using following equation

$$RSS_{Nu} = \sqrt{\left(s(q)\frac{\partial Nu}{\partial Q}\right)^2 + s(\Delta T_{lmtd})\frac{\partial Nu}{\partial \Delta T_{lmtd}}} \quad (16)$$

$$\frac{\partial Nu}{\partial q} = \frac{\partial\left(q \cdot D_h . At^{-1} \cdot {\Delta T_{lmtd}}^{-1} \cdot k^{-1}\right)}{\partial q} = \frac{D_h}{(At)(\Delta T_{lmtd})(k)}$$

$$\frac{\partial Nu}{\partial \Delta T_{lmtd}} = \frac{\partial\left(q \cdot D_h \cdot At^{-1} \cdot {\Delta T_{lmtd}}^{-1} . k^{-1}\right)}{\partial \Delta T_{lmtd}} = \frac{q . D_h}{(At)(\Delta T_{lmtd})^2(k)}$$

With the values of $s(q) = 0.290\ W$ and $s(\Delta T_{lmtd}) = 0.043$, the obtained RSS_{Nu} was ± 2.889 W/(m²℃). Therefore, the value of RSS_{Nu} is 155.31 ± 2.889 W/m²℃.

The value of h at a speed of 0.4 m/s was found to be 44.86. To determine the standard deviation of *Nu* the following equation is used

$$RSS_h = \sqrt{\left(s(Nu)\frac{\partial h}{Nu}\right)^2} \quad (17)$$

$$\frac{\partial h}{\partial Nu} = \frac{\partial(h . D_h . k^{-1})}{\partial h} = \frac{k}{D_h}$$

Furthermore, the value of_D_h is 0.092 m and *k* at T_f= 40.24 is 0.026. So the value of h at a speed of 0.4 m/s is:

$$RSS_h = \sqrt{\left(s(Nu)\frac{\partial h}{Nu}\right)^2} = 0{,}83$$

Thus, the number *h* at a speed of 0.4 m/s is 44.86 ± 0.83. So, the error h for the baseline at a speed of 0.4 m/s is

$$Error = \frac{RSS_h}{h} \times 100 \quad (18)$$

$$Error = \frac{0.83}{44.86} \times 100 = 1.51\%$$

From the test in the baseline case with a speed of 2.0 m/s, the results of the pressure drop are listed in Table 4, which show that the average *P* can be calculated as follows:

$$\overline{\Delta P} = \frac{\Delta P_1 + \Delta P_2 + \Delta P_3 + \cdots + \Delta P_{30}}{30} = 3.51 \text{ Pa} \quad (19)$$

The average standard deviation of the pressure drop can then be calculated using the equation

$$s = \sqrt{\frac{\sum_{i=1}^{N}(\Delta P_i - \overline{\Delta P})^2}{N(N-1)}} = 8.9 \times 10^{-5} \quad (20)$$

Baseline case for the pressure drop value at a speed of 2.0 m/s is $3.51 \pm 8.9 \times 10^{-5}$Pa. Then, the error in the form of percentage can be calculated using the following equation:

$$\frac{8.9 \times 10^{-5}}{3.51} \times 100 = 0.71$$

Table 4 Baseline pressure drop data at a speed of 2.0 m/s

ΔP (Pa)			
Data to	2.0 m/s	Data to	2.0 m/s
1	0.013	16	0.012
2	0.013	17	0.013
3	0.013	18	0.012
4	0.013	19	0.012
5	0.012	20	0.013
6	0.013	21	0.013
7	0.013	22	0.012
8	0.012	23	0.013
9	0.013	24	0.012
10	0.013	25	0.013
11	0.013	26	0.013
12	0.013	27	0.013
13	0.012	28	0.013
14	0.012	29	0.012
15	0.013	30	0.012

The equal calculation approach changed into used for all data. Therefore, the overall error outputs for the pressure-drop vortex generator with placement variations (in-line and staggered), *Re* and amount of VG sets (one, two and three) are listed in Table 5.

Table 5. Overall Pressure Drop (ΔP)

Vortex Generator Variations	*Overall Error P (perforated)*
1 PRWP *in-line*	2.94%
2 PRWP *in-line*	2.87%
3 PRWP *in-line*	1.98%
1 PRWP *staggered*	2.88%
2 PRWP *staggered*	2.34%
3 PRWP *staggered*	1.36%
1 PCRWP *in-line*	2.72%
2 PCRWP *in-line*	1.80%
3 PCRWP *in-line*	1.80%
1 PCRWP *staggered*	2.43%
2 PCRWP *staggered*	1.91%

3 PCRWP *staggered*	0.97%

The average TEF results from the experimental results can be calculated as follows.

$$\overline{TEF} = \frac{TEF_1+TEF_2+TEF_3+\cdots+TEF_{12}}{12} = 1.12 \quad (21)$$

Then, the average standard deviation of the TEF can be calculated with the equation

$$s = \sqrt{\frac{\sum_{i=1}^{N}(TEF_i-\overline{TEF})^2}{N(N-1)}} = 1.07 \quad (22)$$

Therefore, the TEF value was 1.12 ± 1.07. Then, the error in the form of percentage can be calculated using the following equation:

$$\frac{1.07}{1.12} \times 100 = 0.94\%$$

The overall error results for the TEF vortex generator with placement variations (in-line and staggered), *Re* and amount of VG sets (one, two and three) are are listed inTable 6.

Table 6. Overall error *TEF*

Variasi Vortex Generator	*Overall Error TEF* (Berlubang)
1 RWP *in-line*	0.47 %
2 RWP *in-line*	0.47%
3 RWP *in-line*	0.43%
1 RWP *staggered*	0.47%
2 RWP *staggered*	0.47%
3 RWP *staggered*	0.43%
1 CRWP *in-line*	0.45%
2 CRWP *in-line*	0.45%
3 CRWP *in-line*	0.42%
1 CRWP *staggered*	0.45%
2 CRWP *staggered*	0.45%
3 CRWP *staggered*	0.41%

First, find the average *CBR* of the experimental results with the following formula.

$$\overline{CBR} = \frac{CBR_1+CBR_2+CBR_3+\cdots+CBR_{12}}{12} = 2.14 \quad (23)$$

The average standard deviation of the pressure drop *CBR* can then be calculated using the following equation:

$$s = \sqrt{\frac{\sum_{i=1}^{N}(CBR_i-\overline{CBR})^2}{N(N-1)}} = 1.60 \quad (24)$$

The *CBR* value is 2.14 ± 1.60. Then the error in the form of percentage can be calculated using thefollowing equation:

$$\frac{1.60}{2.14} \times 100 = 0.63\%$$

The overall error results for the *CBR* vortex generator with placement variations (in-line and staggered), *Re* and amount of VG sets (one, two and three) are listed in Table 7

Table 7. Overall *error CBR*

Variasi Vortex Generator	*Overall Error CBR* (Berlubang)
1 RWP *in-line*	0.32%
2 RWP *in-line*	0.29%
3 RWP *in-line*	0.45%
1 RWP *staggered*	0.32%
2 RWP *staggered*	0.31%
3 RWP *staggered*	0.45%
1 CRWP *in-line*	0.4%
2 CRWP *in-line*	0.42%
3 CRWP *in-line*	0.56%
1 CRWP *staggered*	0.43%
2 CRWP *staggered*	0.42%
3 CRWP *staggered*	0.66%

Conclusion

Based on the experimental results for perforated concave rectangular winglet pair vortex generators (PCRWP VGs) used to increase the heat transfer of airflow through heated tubes arranged in-line in the duct, we conclude that using PCRWP VGs affects the convection heat transfer coefficient, pressure drop in achieving hydraulic thermal performance and cost-benefit ratio. In our investigation, the best heat-transfer convection coefficient was 153.5 W/m^2·K for the three pairs of PCRW VGs, in a staggered manner. The greatest improvement in the pressure drop value (4.58 Pa), occurred for one pair of PCRW VGs arranged in a staggered manner, whereas the hydraulic thermal performance was the best (1.29) in this experiment with the three pairs of PCRW VGs arranged in a staggered manner. Finally, the best *CBR* (3.56) was recorded for the three pairs of PCRW VGs composed in a staggered manner.

Acknowledgements

The authors would like to thank LEMLITBANG UHAMKA which has funded this research through internal grants from UHAMKA and UPPI UHAMKA what have contributed in facilitating translation and proof reading. The authors also thank the UNDIP thermofluidics laboratory, where the authors carried out this experiment.

Bibliography

[1] R. Sebayang, "AC Akan Jadi Pengkonsumsi Listrik Utama di Dunia," *CNBC Indonesia*. 2018.

[2] Z. Qian, Q. Wang, and J. Cheng, “Analysis of heat and resistance performance of plate fin-and-tube heat exchanger with rectangle-winglet vortex generator,” *Int J Heat Mass Transf*, vol. 124, pp. 1198–1211, 2018, doi: 10.1016/j.ijheatmasstransfer.2018.04.037.

[3] D. Mugisidi, O. Heriyani, P. H. Gunawan, and D. Apriani, “Performance improvement of a forced draught cooling tower using a vortex generator,” *CFD Letters*, vol. 13, no. 1, pp. 45–57, 2021, doi: 10.37934/cfdl.13.1.4557.

[4] A. J. Modi, N. A. Kalel, and M. K. Rathod, “Thermal performance augmentation of fin-and-tube heat exchanger using rectangular winglet vortex generators having circular punched holes,” *Int J Heat Mass Transf*, vol. 158, pp. 1–16, 2020, doi: 10.1016/j.ijheatmasstransfer.2020.119724.

[5] K. W. Song and T. Tagawa, “The optimal arrangement of vortex generators for best heat transfer enhancement in flat-tube-fin heat exchanger,” *International Journal of Thermal Sciences*, 2018, doi: 10.1016/j.ijthermalsci.2018.06.011.

[6] C. Yu, H. Zhang, M. Zeng, R. Wang, and B. Gao, “Numerical study on turbulent heat transfer performance of a new compound parallel flow shell and tube heat exchanger with longitudinal vortex generator,” *Appl Therm Eng*, vol. 164, no. May 2019, p. 114449, 2020, doi: 10.1016/j.applthermaleng.2019.114449.

[7] M. Samadifar and D. Toghraie, “Numerical simulation of heat transfer enhancement in a plate-fin heat exchanger using a new type of vortex generators,” *Appl Therm Eng*, vol. 133, no. September 2017, pp. 671–681, 2018, doi: 10.1016/j.applthermaleng.2018.01.062.

[8] U. Kashyap, K. Das, and B. K. Debnath, “Effect of surface modification of a rectangular vortex generator on heat transfer rate from a surface to fluid,” *International Journal of Thermal Sciences*, vol. 127, no. August 2017, pp. 61–78, 2018, doi: 10.1016/j.ijthermalsci.2018.01.004.

[9] U. Kashyap, K. Das, and B. K. Debnath, “Effect of surface modification of a rectangular vortex generator on heat transfer rate from a surface to fluid: An extended study,” *International Journal of Thermal Sciences*, vol. 134, no. August, pp. 269–281, 2018, doi: 10.1016/j.ijthermalsci.2018.08.020.

[10] A. Q. Ibrahim and R. S. Alturaihi, “Experimental Work for Single-Phase and Two-Phase Flow in Duct Banks with Vortex Generators,” *Results in Engineering*, p. 100497, Sep. 2022, doi: 10.1016/J.RINENG.2022.100497.

[11] K. W. Song, T. Tagawa, Z. H. Chen, and Q. Zhang, “Heat transfer characteristics of concave and convex curved vortex generators in the channel of plate heat exchanger under laminar flow,” *International Journal of Thermal Sciences*, vol. 137, no. November 2018, pp. 215–228, 2019, doi: 10.1016/j.ijthermalsci.2018.11.002.

[12] K. A. Hammoodi, H. A. Hasan, M. H. Abed, A. Basem, and A. M. Al-Tajer, “Control of heat transfer in circular channels using oblique triangular ribs,” *Results in Engineering*, vol. 15, p. 100471, Sep. 2022, doi: 10.1016/J.RINENG.2022.100471.

[13] M. Zeeshan, S. Nath, D. Bhanja, and A. Das, “Numerical investigation for the optimal placements of rectangular vortex generators for improved thermal performance of fin-and-tube heat exchangers,” *Appl Therm Eng*, 2018, doi: 10.1016/j.applthermaleng.2018.03.006.

[14] H. Linardos, G. Mavrogenis, and D. Margaris, “Novel designs of LVGs conformations and introduction of Batch Heated and Channeled Pipe for increasing heat transfer efficiency in pipes,” *Results in Engineering*, vol. 13, p. 100357, Mar. 2022, doi: 10.1016/J.RINENG.2022.100357.

[15] O. Heriyani, M. Djaeni, and . Syaiful, “Thermal-Hydraulic Performance Analysis by Means of Rectangular Winglet Vortex Generators in a Channel: An Experimental Study,” *European Journal of Engineering and Technology Research*, vol. 6, no. 3, pp. 150–153, 2021, doi: 10.24018/ejers.2021.6.3.2424.

[16] C. Wang, Z. Wang, L. Wang, L. Luo, and B. Sundén, “Experimental study of fluid flow and heat transfer of jet impingement in cross-flow with a vortex generator pair,” *Int J Heat Mass Transf*, vol. 135, pp. 935–949, 2019, doi: 10.1016/j.ijheatmasstransfer.2019.02.024.

[17] Z. Sun, K. Zhang, W. Li, Q. Chen, and N. Zheng, “Investigations of the turbulent thermal-hydraulic performance in circular heat exchanger tubes with multiple rectangular winglet vortex generators,” *Appl Therm Eng*, vol. 168, p. 114838, Mar. 2020, doi: 10.1016/J.APPLTHERMALENG.2019.114838.

[18] P. Promvonge and S. Skullong, “Thermo-hydraulic performance in heat exchanger tube with V-shaped winglet vortex generator,” *Appl Therm Eng*, 2020, doi: 10.1016/j.applthermaleng.2019.114424.

[19] S. Skullong, P. Promthaisong, P. Promvonge, C. Thianpong, and M. Pimsarn, “Thermal performance in solar air heater with perforated-winglet-type vortex generator,” *Solar Energy*, vol. 170, no. June, pp. 1101–1117, 2018, doi: 10.1016/j.solener.2018.05.093.

[20] Z. Han, Z. Xu, and J. Wang, “Numerical simulation on heat transfer characteristics of rectangular vortex generators with a hole,” *Int J Heat Mass Transf*, vol. 126, pp. 993–1001, 2018, doi: 10.1016/j.ijheatmasstransfer.2018.06.081.

[21] C. Luo, S. Wu, K. Song, L. Hua, and L. Wang, “Thermo-hydraulic performance optimization of wavy fin heat exchanger by combining delta winglet vortex generators,” *Appl Therm Eng*, 2019, doi: 10.1016/j.applthermaleng.2019.114343.

[22] H. Naik and S. Tiwari, “Effect of winglet location on performance of fin-tube heat exchangers with inline tube arrangement,” *Int J Heat Mass Transf*, vol. 125, pp. 248–261, 2018, doi: 10.1016/j.ijheatmasstransfer.2018.04.071.

[23] M. Zeeshan, S. Nath, D. Bhanja, and A. Das, “Numerical investigation for the optimal placements of rectangular vortex generators for improved thermal performance of fin-and-tube heat exchangers,” *Appl Therm Eng*, vol. 136, pp. 589–601, May 2018, doi: 10.1016/J.APPLTHERMALENG.2018.03.006.

[24] Y. Effendi, A. Prayogo, Syaiful, M. Djaeni, and E. Yohana, “Effect of perforated concave delta winglet vortex generators on heat transfer and flow resistance through the heated tubes in the channel,” *Experimental Heat Transfer*, vol. 35, no. 5, pp. 553–576, 2022, doi: 10.1080/08916152.2021.1919245.

[25] S. Whitaker, “Forced Convection Heat Transfer Correlations for Flow In Pipes, Past Flat Plates, Single e Cylinders, Single Spheres, and for Flow In Packed Beds and Tube Bundles,” *Reprillted from AIChE JOURNAL*, 1972.

[26] M. Awais and A. A. Bhuiyan, “Enhancement of thermal and hydraulic performance of compact finned-tube heat exchanger using vortex generators (VGs): A parametric study,” *International Journal of Thermal Sciences*, vol. 140, pp. 154–166, Jun. 2019, doi: 10.1016/J.IJTHERMALSCI.2019.02.041.

[27] A. Gupta, A. Roy, S. Gupta, and M. Gupta, “Numerical investigation towards implementation of punched winglet as vortex generator for performance improvement of a fin-and-tube heat exchanger,” *Int J Heat Mass Transf*, vol. 149, p. 119171, Mar. 2020, doi: 10.1016/J.IJHEATMASSTRANSFER.2019.119171.

[28] M. W. Tian, S. Khorasani, H. Moria, S. Pourhedayat, and H. S. Dizaji, “Profit and efficiency boost of triangular vortex-generators by novel techniques,” *Int J Heat Mass Transf*, vol. 156, p. 119842, 2020, doi: 10.1016/j.ijheatmasstransfer.2020.119842.

[29] Y. L. He, P. Chu, W. Q. Tao, Y. W. Zhang, and T. Xie, “Analysis of heat transfer and pressure drop for fin-and-tube heat exchangers with rectangular winglet-type vortex generators,” *Appl Therm Eng*, vol. 61, no. 2, pp. 770–783, Nov. 2013, doi: 10.1016/J.APPLTHERMALENG.2012.02.040.

[30] M. Pranita Hendraswari, M. S. Tony, and M. F. Soetanto, “Heat Transfer Enhancement inside Rectangular Channel by Means of Vortex Generated by Perforated Concave Rectangular Winglets,” 2021, doi: 10.3390/fluids6010043.

[31] Syaiful, A. R. Siwi, T. S. Utomo, Yurianto, and R. Wulandari, “Numerical analysis of heat and fluid flow characteristics of airflow inside rectangular channel with presence of perforated concave delta winglet vortex generators,” *International Journal of Heat and Technology*, vol. 37, no. 4, pp. 1059–1070, 2019, doi: 10.18280/IJHT.370415.

[32] A. Sinha, H. Chattopadhyay, A. K. Iyengar, and G. Biswas, “Enhancement of heat transfer in a fin-tube heat exchanger using rectangular winglet type vortex generators,” *Int J Heat Mass Transf*, vol. 101, pp. 667–681, Oct. 2016, doi: 10.1016/J.IJHEATMASSTRANSFER.2016.05.032.

[33] H. Ke *et al.*, “Thermal-hydraulic performance and optimization of attack angle of delta winglets in plain and wavy finned-tube heat exchangers,” *Appl Therm Eng*, vol. 150, pp. 1054–1065, Mar. 2019, doi: 10.1016/j.applthermaleng.2019.01.083.

[34] A. Arora, P. M. V. Subbarao, and R. S. Agarwal, “Development of parametric space for the vortex generator location for improving thermal compactness of an existing inline fin and tube heat exchanger,” *Appl Therm Eng*, vol. 98, pp. 727–742, Apr. 2016, doi: 10.1016/J.APPLTHERMALENG.2015.12.117.

[35] S. Gururatana and S. Skullong, “Heat transfer augmentation in a pipe with 3D printed wavy insert,” *Case Studies in Thermal Engineering*, vol. 21, p. 100698, Oct. 2020, doi: 10.1016/J.CSITE.2020.100698.

[36] A. Sinha, H. Chattopadhyay, A. K. Iyengar, and G. Biswas, “Enhancement of heat transfer in a fin-tube heat exchanger using rectangular winglet type vortex generators,” *Int J Heat Mass Transf*, vol. 101, pp. 667–681, Oct. 2016, doi: 10.1016/J.IJHEATMASSTRANSFER.2016.05.032.

[37] A. J. Modi and M. K. Rathod, “Experimental investigation of heat transfer enhancement and pressure drop of fin-and-circular tube heat exchangers with modified rectangular winglet vortex generator,” *Int J Heat Mass Transf*, vol. 189, p. 122742, Jun. 2022, doi: 10.1016/J.IJHEATMASSTRANSFER.2022.122742.

[38] Y. Li, Z. Qian, and Q. Wang, “Numerical investigation of thermohydraulic performance on wake region in finned tube heat exchanger with section-streamlined tube,” *Case Studies in Thermal Engineering*, vol. 33, p. 101898, May 2022, doi: 10.1016/J.CSITE.2022.101898.

[39] K. Boukhadia, H. Ameur, D. Sahel, and M. Bozit, “Effect of the perforation design on the fluid flow and heat transfer characteristics of a plate fin heat exchanger,” *International Journal of Thermal Sciences*, vol. 126, no. December 2017, pp. 172–180, Apr. 2018, doi: 10.1016/j.ijthermalsci.2017.12.025.

[40] C.-H. Huang and L.-W. Liu, “Optimal position and perforated radius of punched vortex generators for heat sink,” *Case Studies in Thermal Engineering*, vol. 32, p. 101916, Apr. 2022, doi: 10.1016/J.CSITE.2022.101916.

[41] Y. Menni *et al.*, “Effects of two-equation turbulence models on the convective instability in finned channel heat exchangers,” *Case Studies in Thermal Engineering*, vol. 31, p. 101824, Mar. 2022, doi: 10.1016/J.CSITE.2022.101824.

Dear Editors and Reviewer

Thank you for your letter and for the reviewers' comments concerning our manuscript entitled "Perforated concave rectangular winglet pair vortex generators enhance the heat transfer of air flowing through heated tubes inside a channel" (Manuscript Number: Rineng-D-22-00804R1). The comments are all valuable and very helpful to revise and improve our paper, as well as significant guidelines for our research. We have learned comments carefully and have made the correction that we hope you meet with your approval. We have included the parts requested to be revised in the manuscript. Revised portions are marked in red in the revised paper. The main correction in papers and responses to reviewing comments is flowing.

Reviewer 1: Following are the few observations:

1. Author should add figure of location of thermocouple.

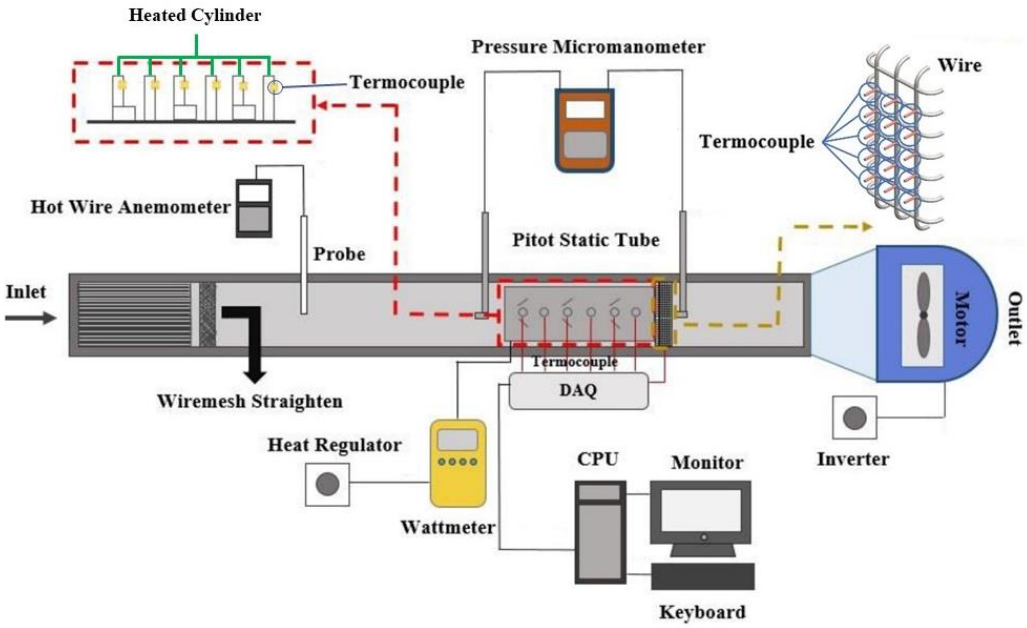

Thank you very much for the proposal. I've revised Figure 1 because I made a mistake in captioning the figure. One thermocouple is placed in the air inlet area, six thermocouples on the back surface of the tubes, and 15 on the outlet side of the wire, as observed in Figure 1.

2. Heaters are placed after test section? How the heating of air takes place?

   Thanks for the question. The heater is connected to six tubes with each tube getting the same power. The total heating power of 40 W is induced in the six tubes by a regulator. Heating air flowing through the tubes occurs by convection. So that the air at the outlet side becomes hotter than that from the inlet side.

3. Details of perforations on rectangular and concave winglet is missing. pl add.

Thank you for the correction. I have added in the paper the detailed geometry of the perforated rectangular winglet (PRW) and perforated concave rectangular winglet (PCRW) vortex generators (VGs), as shown in Figure 2.

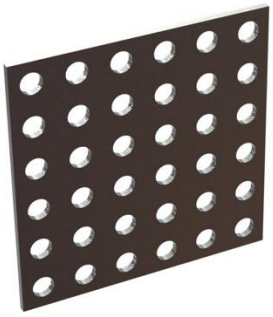

Perforated RWP

Perforated CRWP

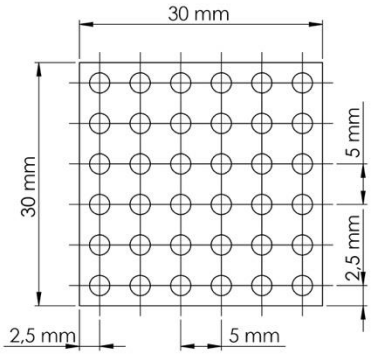

VGs have dimensions of the same length and width of 30 mm and have 36 holes. The bore diameter on the VGs is 2.5 mm. The distance between the holes is 5 mm from the center of the holes.

4. Provide details of validation of set up and heat loss analysis.
   a. Set up validation

   Thank you for your suggestion. The current study is a follow-up investigation of the work of Yafid et al [1]. The experimental set-up of this study is similar to that of Yafid et al. experiment. The difference between the current study and the experiment of Yafid et al. is a test object where the current study uses concave rectangular winglet (CRW) VGs, while the work of Yafid et al. uses concave delta winglet (CDW) VGs. Whitaker et al. [2] studied the heat transfer characteristics of airflow through a single cylinder in a rectangular duct. To confirm the results of the experiment Yafid et al. are

valid, the same experimental set-up is determined. The Nu value from the experiment of Yafid et al. compared with Nu values from the experiments of Whitaker et al. in the Reynolds number range of 2,143 to 11,763, as shown in the figure below.

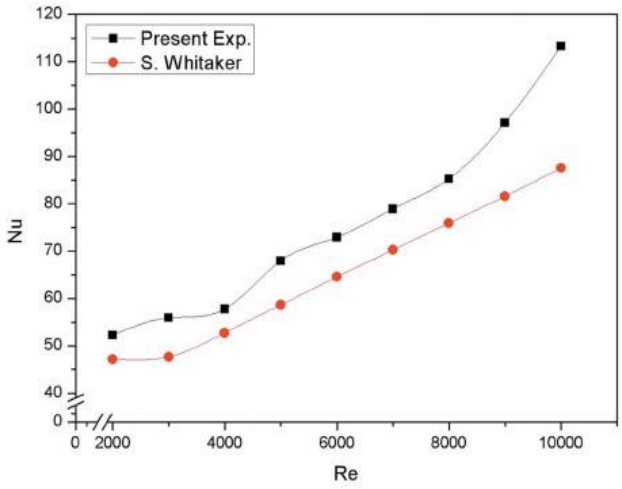

From the figure, it can be observed that Nu from the experimental results of Yafid et al. have the same trend as the experiments of Whitaker et al.

b. Heat Loss analysis

Heat loss analysis is carried out by taking into account the convection heat transfer from the six tubes to the surrounding fluid flow. Calculation of the heat transfer rate is carried out for two types of flow, namely laminar flow and turbulent flow.

The calculation of heat loss in this experiment is determined by calculating the difference between the induced electric power and the total heat through convection from the surface of the tubes to the fluid. In this experiment, six tubes in a wind tunnel are heated by a heater with a power of 40 W. In this work, the velocity of the inlet fluid is varied from 0.4 to 2 m/s at intervals of 0.2 m/s or in the Reynolds number range from 2,143 to 11,763. Based on the Reynolds number range, two types of flow are determined, namely laminar and turbulent. Therefore, the heat loss was determined from the correlation between laminar at 0.4 m/s and turbulent for other velocities.

The described formulas *Nu*, *h,* and *q* were used to determine the heat loss in the conduit of the six tubes.

$$Nu = \frac{q\, D_h}{A_{tube}\, \Delta T_{LMTD}\, k} \qquad (2)$$

$$h = \frac{q}{A_{tube}\, \Delta T_{LMTD}} \qquad (3)$$

$$q = \dot{m}\, c_p\, (T_{out} - T_{in}) \qquad (4)$$

Where D_h, A_{tube}, ΔT_{LMTD}, $\dot{m}$, c_p, T_{out}, T_{in}, are hydraulic diameter, tube surface area, log mean temperature difference, mass flow rate, specific heat, outlet temperature, and inlet temperature.

$$D_h = \frac{4A_c}{P} \quad (5)$$

$$\Delta T_{LMTD} = \frac{(\bar{T}_{tube} - \bar{T}_{out}) - (\bar{T}_{tube} - \bar{T}_{in})}{\ln[(\bar{T}_{tube} - \bar{T}_{out}) - (\bar{T}_{tube} - \bar{T}_{in})]} \quad (6)$$

Where A_c dan T_{tube} are channel surface area and tube temperature, respectively. The experimental data for hydraulic diameter D_h,, tube surface area A_{tube}, channel surface area A_c, and air specific heat c_p are 0.09223 m, 0.02338908 m^2, 0.01056 m^2, and 1.007 J/kgK, respectively. The following is a table for calculating the heat loss baseline.

Table 1 Heat Loss Baseline

	v (m/s)	*Re*	Mass flow rate (kg/s)	**Density (kg/m³)**	Dynamics viscous (kg/ms)	*k*	*Pr*	*T* inlet (C)	*T* outlet (C)	*T* tube (C)	**Δ***T* LMTD	**Δ***T* (*T* tube - *T* inlet)	*Nu*	*h* (W/mK)	*q* conv (W)	*q* input (W)	*q* loss (W)
baseline	0.4	2165	0.004757	1.13	1.9.E-05	0.03	0.73	29	33	50	19	21	155	45	19.48	40	20.52
	0.6	3291	0.00719	1.13	1.9.E-05	0.03	0.73	28	31	46	16	18	174	50	18.98	40	21.02
	0.8	4413	0.009618	1.14	1.9.E-05	0.03	0.03	28	30	44	15	16	192	50	19.19	40	20.81
	1	5545	0.012056	1.14	1.9.E-05	0.03	0.73	28	30	43	14	15	214	55	19.84	40	20.16
	1.2	6661	0.014477	1.14	1.9.E-05	0.03	0.73	28	29	43	14	15	228	61	21.15	40	18.85
	1.4	7826	0.016958	1.15	1.9.E-05	0.03	0.73	28	29	41	12	13	247	70	20.30	40	19.70
	1.6	8965	0.019407	1.15	1.9.E-05	0.03	0.73	27	29	40	12	13	263	75	21.03	40	18.97
	1.8	10110	0.021863	1.15	1.9.E-05	0.03	0.73	27	28	39	12	12	296	84	22.54	40	17.46
	2	11272	0.024341	1.15	1.9.E-05	0.03	0.73	27	28	38	11	11	342	97	24.17	40	15.83

In the table 1, it can be seen that the greater the velocity with the increase in Re number, the lower the heat loss. It can be seen that the heat flow from the heater does not only spread into the tube, but convection occurs to the outside of the tube. Heat output increases with increasing Re. That is, the higher the flow velocity, the greater the turbulence through the silinder and the higher the turbulence intensity. An increase in turbulence intensity between a cold airflow and a hot cylinder with constant surface temperature is caused by the airflow velocity [3]. In row-tube arrays, this recirculation area increases for the second and subsequent columns. A lower air velocity in the circulation region indicates less airflow in that region participating in

the local heating process [4]. The heat loss of all conditions in this experiment is shown in table 2 below.

Table 2 Calculation of heat loss for the whole case

type VGs	*q* conv (W)	*q* input (W)	*q* loss (W)
Baseline	20.74	40	19.26
PCRWPI1	25.15	40	14.85
PCRWPI2	27.55	40	12.45
PCRWPI3	27.61	40	12.39
PCRWPS1	26.43	40	13.57
PCRWPS2	26.43	40	13.57
PCRWPS3	27.94	40	12.06
PRWPI1	24.09	40	15.91
PRWPI2	27.25	40	12.75
PRWPI3	28.82	40	11.18
PRWPS1	23.94	40	16.06
PRWPS2	26.37	40	13.63
PRWPS3	28.12	40	11.88

Table 2 shows that the lowest heat loss occurs when three sets of PCRWPs are staggered. The placement of the VGs can increase heat transfer in square ducts as the VGs create longitudinal vortices that increase vortex strength in the wake region downstream of the tube. Longitudinal vortices make the overall temperature field more uniform, improve heat mixing and boundary layer modification, and improve heat transfer performance. A higher number of vortex generators creates more longitudinal vortices and greatly increases heat transfer [5], [3].

5. Mention pitch kept between two pins/winglet.
   Thank you for the question. I've added Figure 3 (in the paper) showing the pitch between VGs for both inline and staggered configurations.

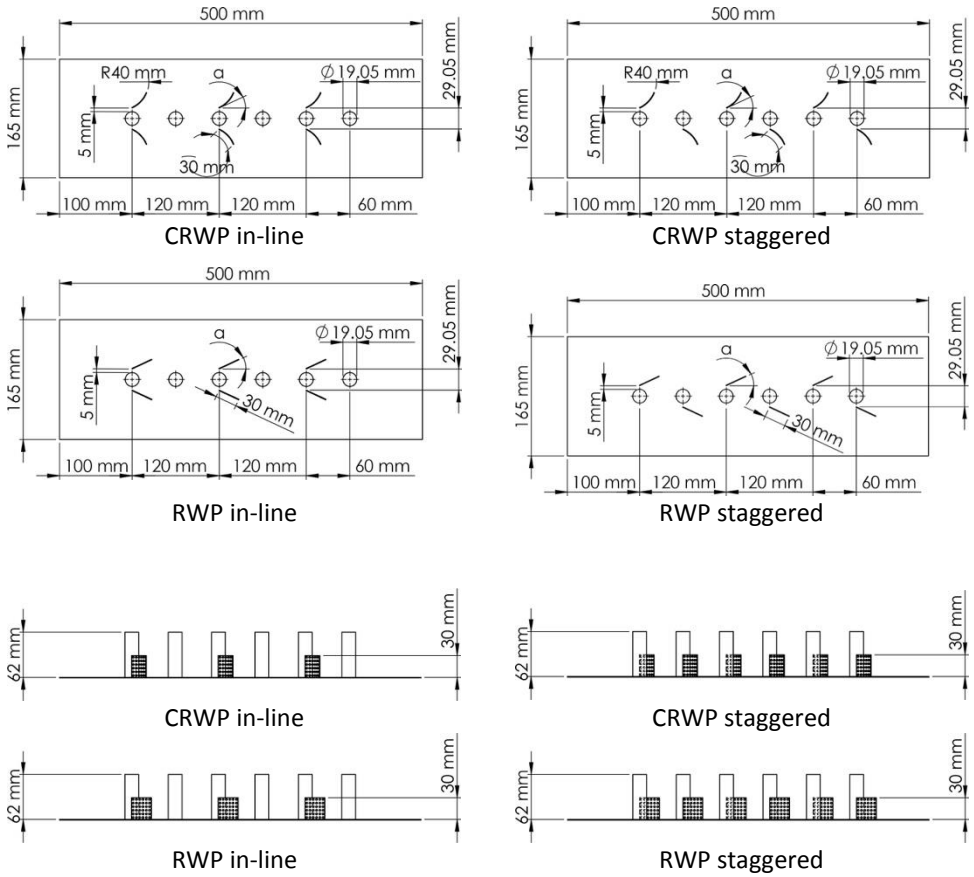

6. At lower Re both inline and staggered arrangement gives the same result, while deviation is observed after Re 8000. The author has to justify.

   Thank you for your suggestion. In Figure 7(a) (in the paper), the convection heat transfer coefficient for the case of PRW VGs in-line has the same value as that of PCRW VGs in-line or staggered in a pair of VGs. In one pair of VGs, the longitudinal vortex is generated after the flow hits the VGs and weakens (He et al., 2013). This is in contrast to two and three pairs of VGs where the longitudinal vortex produced after striking the first VGs has amplified again when the flow strikes the second VGs and so on. Therefore, the value of the heat transfer coefficient in the case of a pair of PRW VGs has the same value as that of PCRW VGs at Reynolds numbers above 8,000.

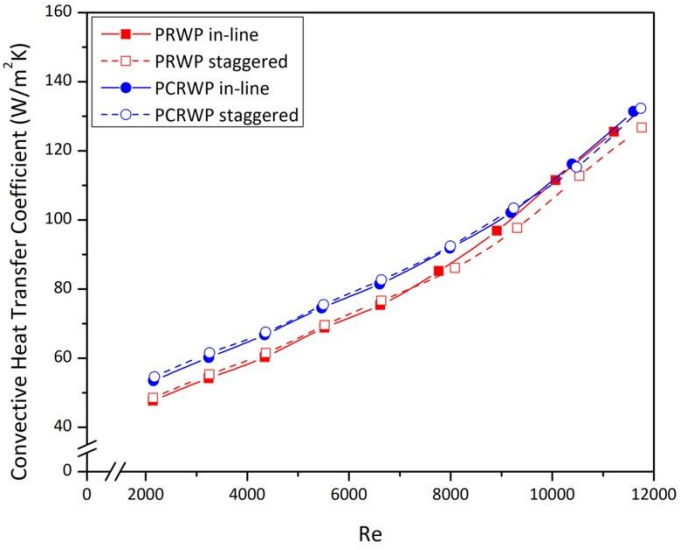

7. Provide more clarification about 1,2 & 3 pairs.

   Thank you for your suggestion. This study describes the cases of PCRW and PRW VGs for one, two, and three pairs. I have added explanations for cases one, two, and three pairs of perforated VGs to the paper.

   For PRW and PCRW VGs in-line configurations with one, two, and three pairs are shown in Figures 4. For one pair, the VGs are placed on the left and right sides of the first row of tubes. VGs are placed on the first and third row tubes for two pairs. As for the three pairs, VGs are placed on the first, third, and fifth row tubes.

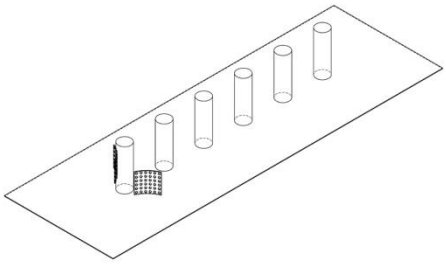

one pair PCRW inlline

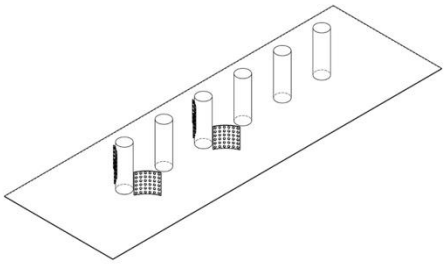

two pairs PCRW inline

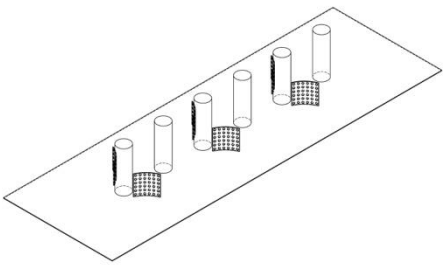

three pairs PCRW inline

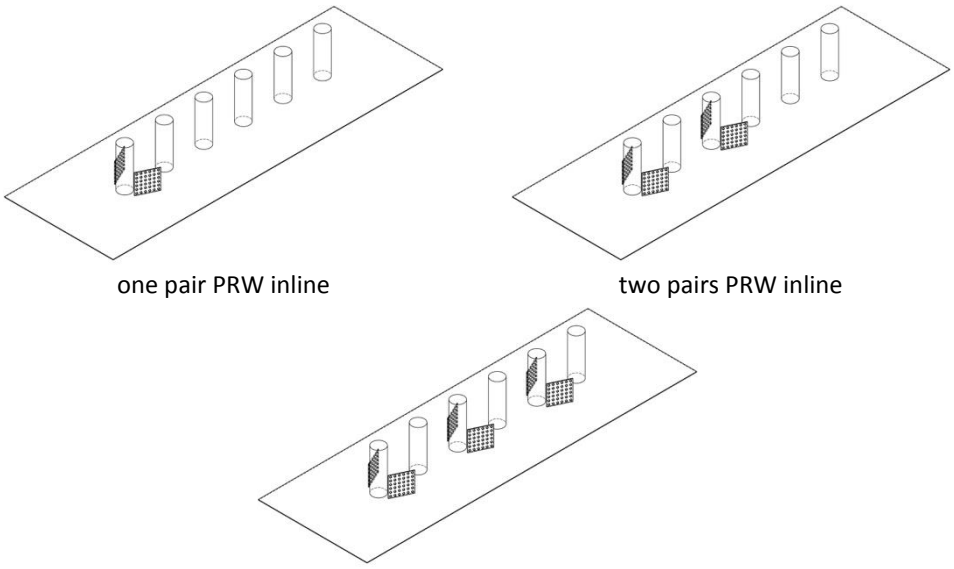

Figure 4. VGs pairs in-line configurations

For PRW and PCRW VGs staggered configurations with one, two, and three pairs are shown in Figures 5. For one pair, the VGs are placed on the right side of the first row tube and the left side of the second row tube. VGs are placed on the right side of the first, third row tubes and on the left side of the second and fourth tubes for two pairs. As for the three pairs, the VGs are placed on the right side of the first, third, fifth row of tubes and on the left side of the second, fourth and sixth tubes.

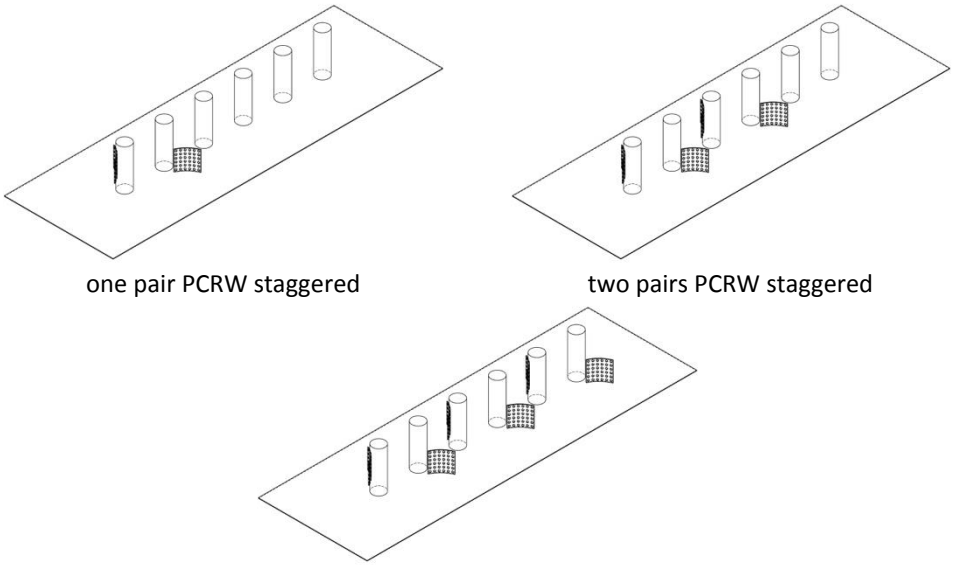

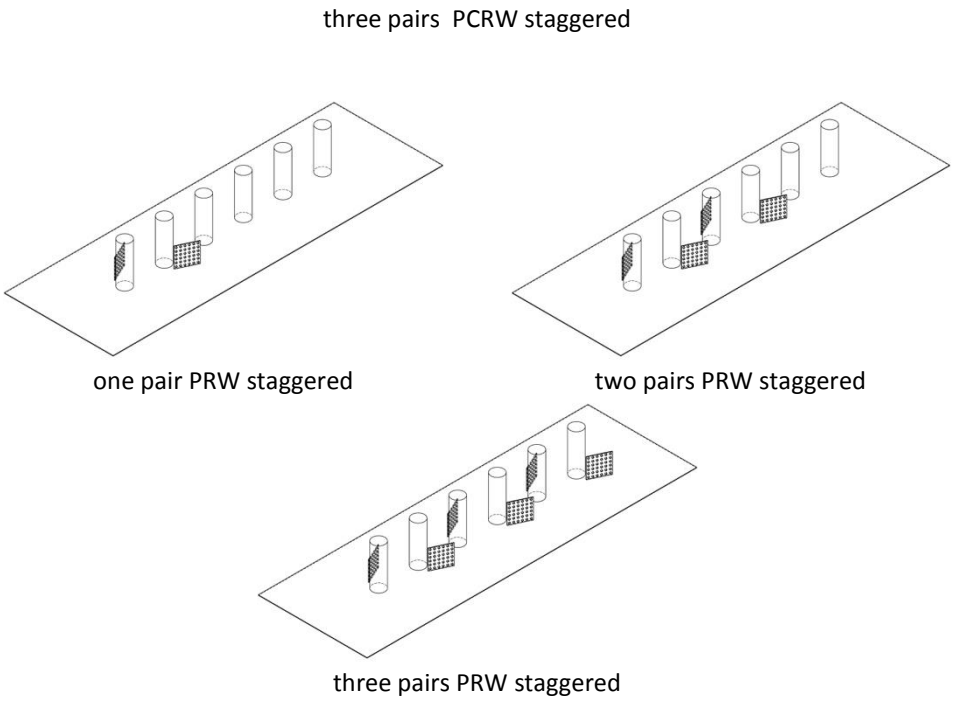

Figure 5. VGs pairs staggered configurations

8. Compare the PRWP and PCRWP with without perforation.
   Thank you for your request. In this study, an experiment was conducted to compare PRW VGs and PCRW VGs in improving heat transfer in a rectangular channel, as shown in Figures 7 to 9.

   a. Comparison of convection heat transfer coefficient values.
   Figure 7 provides a comparison of the convection heat transfer coefficients for PRW and PCRW. It can be seen that there was an increase in the convection heat transfer coeeficient with a rise in *Re* due to an increase in flow vortices and high turbulence intensity in the channel [6], alongside a reduction in the wage region and stagnation area for each increase in flow velocity [7]. The increase in heat transfer for staggered VGs was better than in-line for PCRW VGs with any number of pairs at the highest *R*e (11,000). The results in Figure 7 show that the PCRWP VGs worked better than the PRWP VGs, and the staggered arrangement of the former with three pairs gave the highest yield, of 153.5 $W/m^2.K$, as shown in Figure 7(c). Meanwhile, two PCRW pairs (137.33 $W/m^2.K$, Figure 7(b)) were better than one (132.25 $W/m^2.K$, Figure 7(a)) because VGs with a concave surface destabilise the centrifugal force of the fluid flow, which strengthens the flow vortices. This makes the mixing of the hot fluid near the wall with the cold fluid of the main flow more robust [8].

   b. Pressure drop comparison

In general, the highest pressure drop was observed using PCRWP VGs with staggered configuration for all Reynolds numbers except for one pair of VGs, as shown in Figure 8. The highest pressure drop was found in PRWP VGs with in-line configuration at Reynolds numbers greater than 8,000. The pressure drop on the staggered VGs was found to be higher than that of the in-line due to the shorter distance between the VGs of the staggered configuration than that of the in-line [5].

c. TEF comparison

TEF is the thermal-hydraulic performance which is the ratio of the increase in heat transfer to the pressure drop ratio. In general, the highest TEF was observed in the use of PCRWP VGs with staggered configuration, as depicted in Figure 9. PCRW creates wider flow vortices that can reduce the wake area behind the cylinder. Reducing the wake area can reduce the recirculation zone. This affects the increased heat transfer from the back of the cylinder to the stream [3]. A large radius, high intensity antrior-posterior vortex can reduce the wake area. A reduction in the wake area increases the flow velocity behind the tube and reduces the recirculation area, resulting in an increased heat transfer in this area [9], [10].

d. CBR comparison

A low value of CBR means a more economical value from the use of VGs. In general, CBR on the use of PCRWP VGs with staggered configuration is the best, as informed in Figure 10. The lowest CBR value results were obtained with three pairs of staggered type VGs PCRW. Three pairs of VGs lower CBR than one and two VG pairs. This is because the installation of three pairs VGs results in a higher Nusselt number increase than one and two pairs VGs, resulting in a lower pressure drop increase and therefore a lower CBR. These results show that lower CBR improves thermal performance relative to resistivity [11].

9. Discuss how number of pairs contribute in improving TEF

Thank you for your question. Figure 9 shows the effect of the number of pairs and configuration of VGs on TEF, this is also found in Ref. (He et al., 2013), (Sun et al., 2020), and (Ranjan et al., 2022).

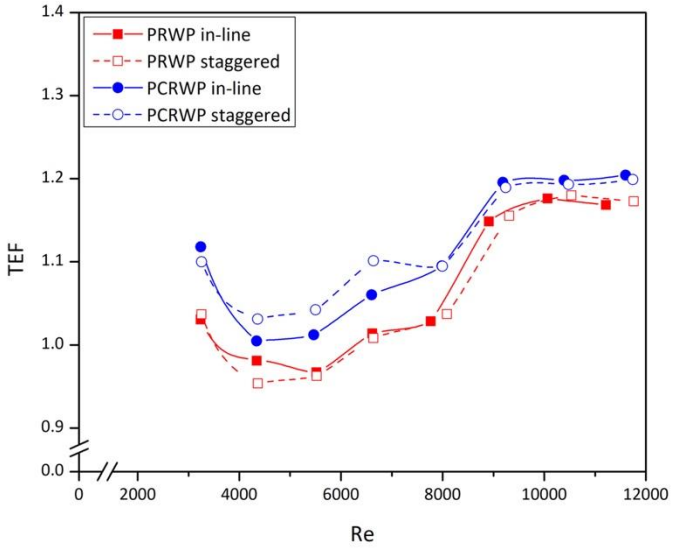

a. One pair

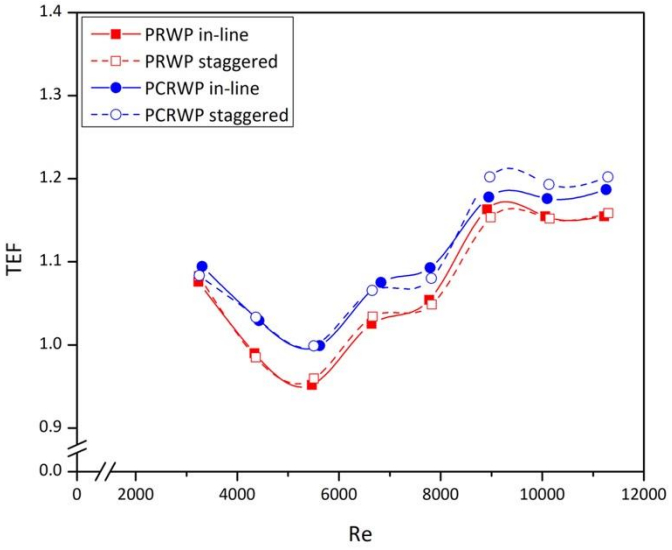

b. Two pairs

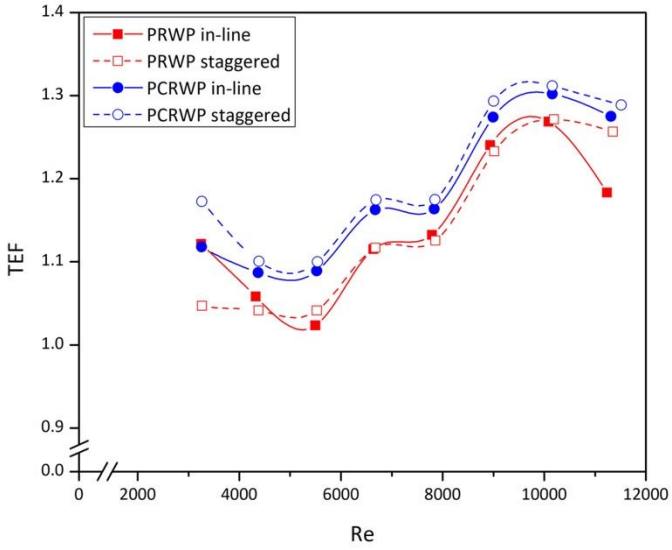

c. Three pairs

From the experimental results, as shown in Figure 9, the TEF with three pairs of VGs for both inline and staggered was the highest. The TEF for the case of 3 pairs of PCRWs was 5.02% greater than that of one and two pairs of PRWP VGs. The main reason is because the concave surface of the PCR causes the flow to be thrown away due to the centrifugal force which results in a stronger flow vorticity [12]. Larger and stronger flow vortices can reduce the recirculation zone which has an impact on increasing heat transfer from the rear surface of the tube to the flow [10]. The presence of flow that is formed in each gap between the VGA and the tube causes the TEF in the staggered configuration to be greater than that of the in-line [13]. The increase in TEF for the three-pair case with the staggered configuration was 1.50% and 4.91% greater than that of the inline PCRWP and PRWP, respectively.

Reference

[1] Y. Effendi, A. Prayogo, Syaiful, M. Djaeni, and E. Yohana, "Effect of perforated concave delta winglet vortex generators on heat transfer and flow resistance through the heated tubes in the channel," *Experimental Heat Transfer*, vol. 35, no. 5, pp. 553–576, 2022, doi: 10.1080/08916152.2021.1919245.

[2] S. Whitaker, "Forced Convection Heat Transfer Correlations for Flow In Pipes, Past Flat Plates, Single e Cylinders, Single Spheres, and for Flow In Packed Beds and Tube Bundles," *Reprillted from AIChE JOURNAL*, 1972.

[3] M. Awais and A. A. Bhuiyan, "Enhancement of thermal and hydraulic performance of compact finned-tube heat exchanger using vortex generators (VGs): A parametric study," *International Journal of Thermal Sciences*, vol. 140, pp. 154–166, Jun. 2019, doi: 10.1016/J.IJTHERMALSCI.2019.02.041.

[4] A. J. Modi and M. K. Rathod, “Experimental investigation of heat transfer enhancement and pressure drop of fin-and-circular tube heat exchangers with modified rectangular winglet vortex generator,” *Int J Heat Mass Transf*, vol. 189, p. 122742, Jun. 2022, doi: 10.1016/J.IJHEATMASSTRANSFER.2022.122742.

[5] Y. L. He, P. Chu, W. Q. Tao, Y. W. Zhang, and T. Xie, “Analysis of heat transfer and pressure drop for fin-and-tube heat exchangers with rectangular winglet-type vortex generators,” *Appl Therm Eng*, vol. 61, no. 2, pp. 770–783, Nov. 2013, doi: 10.1016/J.APPLTHERMALENG.2012.02.040.

[6] M. Pranita Hendraswari, M. S. Tony, and M. F. Soetanto, “Heat Transfer Enhancement inside Rectangular Channel by Means of Vortex Generated by Perforated Concave Rectangular Winglets,” 2021, doi: 10.3390/fluids6010043.

[7] Syaiful, A. R. Siwi, T. S. Utomo, Yurianto, and R. Wulandari, “Numerical analysis of heat and fluid flow characteristics of airflow inside rectangular channel with presence of perforated concave delta winglet vortex generators,” *International Journal of Heat and Technology*, vol. 37, no. 4, pp. 1059–1070, 2019, doi: 10.18280/IJHT.370415.

[8] A. Sinha, H. Chattopadhyay, A. K. Iyengar, and G. Biswas, “Enhancement of heat transfer in a fin-tube heat exchanger using rectangular winglet type vortex generators,” *Int J Heat Mass Transf*, vol. 101, pp. 667–681, Oct. 2016, doi: 10.1016/J.IJHEATMASSTRANSFER.2016.05.032.

[9] A. Gupta, A. Roy, S. Gupta, and M. Gupta, “Numerical investigation towards implementation of punched winglet as vortex generator for performance improvement of a fin-and-tube heat exchanger,” *Int J Heat Mass Transf*, vol. 149, p. 119171, Mar. 2020, doi: 10.1016/J.IJHEATMASSTRANSFER.2019.119171.

[10] Y. Li, Z. Qian, and Q. Wang, “Numerical investigation of thermohydraulic performance on wake region in finned tube heat exchanger with section-streamlined tube,” *Case Studies in Thermal Engineering*, vol. 33, p. 101898, May 2022, doi: 10.1016/J.CSITE.2022.101898.

[11] M. W. Tian, S. Khorasani, H. Moria, S. Pourhedayat, and H. S. Dizaji, “Profit and efficiency boost of triangular vortex-generators by novel techniques,” *Int J Heat Mass Transf*, vol. 156, p. 119842, 2020, doi: 10.1016/j.ijheatmasstransfer.2020.119842.

[12] H. Naik and S. Tiwari, “Thermodynamic performance analysis of an inline fin-tube heat exchanger in presence of rectangular winglet pairs,” *Int J Mech Sci*, vol. 193, no. September 2020, p. 106148, 2021, doi: 10.1016/j.ijmecsci.2020.106148.

[13] L. O. Salviano, D. J. Dezan, and J. I. Yanagihara, “Thermal-hydraulic performance optimization of inline and staggered fin-tube compact heat exchangers applying longitudinal vortex generators,” *Appl Therm Eng*, vol. 95, pp. 311–329, Feb. 2016, doi: 10.1016/J.APPLTHERMALENG.2015.11.069.

Reviewer 2: This paper presented experimental results of the heat transfer, pressure drop and thermal performance characteristics of the perforated concave rectangular winglet pair vortex generators on plates in rectangular ducts to increase the heat transfer through the six heated tubes to the air stream. Perforated concave rectangular winglets were compared with perforated rectangular winglet pairs vortex generator mounted on rectangular plates. The subject of the article falls within the scope of the Results in Engineering. In my view, unless the paper is rewritten in a proper way, I think it is inadequate to be published in a scientific journal in its present state. I would like to provide the following comment:

1. There are many spelling and grammar mistakes in this paper, and many sentences are not easy to follow. The grammar and structure of sentences in this paper need to be modified carefully, such as the title of the article. The language of this paper need to be improved by a native English speaker.
   Thank you for your suggestion. To improve grammar and structure, I have sent this paper to elsevier service for proof reading.


ELSEVIER

Certificate of Elsevier
Language Editing Services

The following article was edited by Elsevier Language Editing Services:
"Perforated concave rectangular winglet pair vortex generators enhance the heat transfer of air flowing through heated tubes inside a channel"

Authored by:
oktarina heriyani

Date: 17-Sep-2022
Serial number: LEEX-19301-298A26F09925

2. The velocity ranges studied are given in the Abstract, whereas the Reynolds number ranges studied should be given.
   Thank you for your correction. In this experiment, the intake air velocity is in the range of 0.4 to 2 m/s at intervals of 0.2 m/s or in the Reynolds number range of 2.143 to 11.763. I have included the Reynolds number range in the abstract.

3. Please review the keywords and add a few, for instance **heat transfer, thermal performance**.

Thank you for your suggestion. The keywords for this study are vortex generators, heat transfer, thermal-hydraulic performance, economic benefit. I've added keywords in the paper.

4. The method section can be expanded.
   Thank you for your suggestion. I have improved this research method in the paper.

   Based on Fig. 1, the rectangular channel is equipped with a blower (50 Hz, Wipro with a rated voltage of 220V), an inverter (Mitsubishi Electric type FR-D700 with an accuracy of 0.01), straightener, hot wire anemometer (Lutron type AM-4204 with an accuracy of 0.1), wattmeter (Lutron DW-6060 with an accuracy ± 1.0), central processing unit (CPU), micromanometer, thermocouple (K type with a temperature interval of -200 –1250℃ and an accuracy ± 0.5) where one thermocouple was placed in the air inlet area, six thermocouples on the back surface of the tubes and 15 on the outlet side of the wire, data acquisition (Advantech USB-4718 type with an accuracy of 0.001) and heater regulator. The heater was connected to six tubes with a diameter of 19.05 mm and height of 65.8 mm, with each tube having the same power. Total heating power of 40 W was applied to the six tubes using a regulator. The heating air flowing through the tubes occurs via convection. Thus, the air at the outlet side becomes hotter than that at the inlet side.
   A pressure micromanometer (Fluke type 922, with an accuracy of ± 0.05) was used to monitor the flow pressure drop. Two pitot tubes, each set 26 cm ahead of the inlet of the test specimen and 2.5 cm behind it, were connected to a micromanometer to measure the pressure drop. The pressure drop measurements were recorded 30 times for 5 sekon at each speed variation. Furthermore, flow visualisation was performed by directing the smoke from vaporised fluid in the fluid vaporator into the mainflow.

5. The arrangement of vortex generators is given in Figure 2, but Figure 2 is not sufficient for a clear understanding of the construction of vortex generators. Additional figures should be drawn which clearly show the construction of vortex generators and the in-line and staggered arrangement.
   Thank you for your suggestion. The following shows the construction of vortex generators inline and staggered (figure 2, 4 and 5 in the paper).

Figure 2. Geometry of the VGs

For PRW and PCRW VGs in-line configurations with one, two, and three pairs are shown in Figures 4. For one pair, the VGs are placed on the left and right sides of the first row of tubes. VGs are placed on the first and third row tubes for two pairs. As for the three pairs, VGs are placed on the first, third, and fifth row tubes.

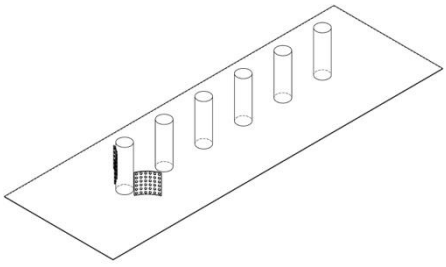

one pair PCRW inlline

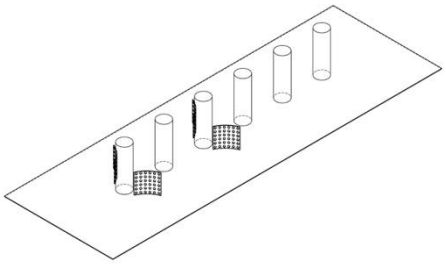

two pairs PCRW inline

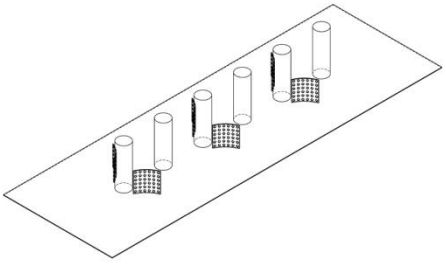

three pairs PCRW inline

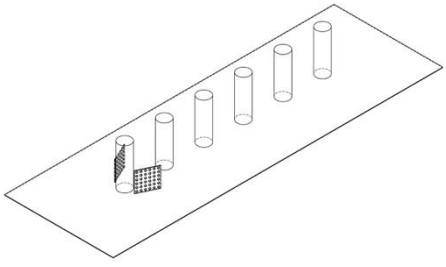

one pair PRW inline

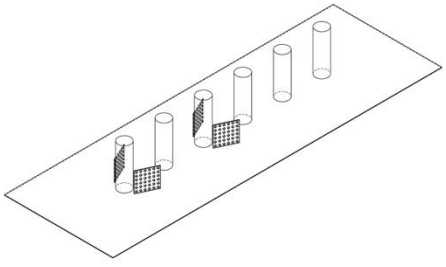

two pairs PRW inline

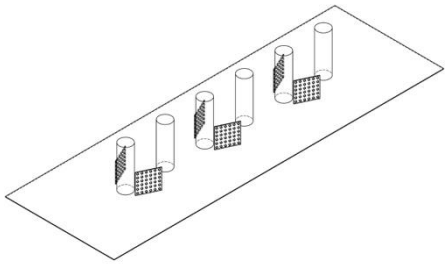

three pairs PRW inline

Figure 4. VGs pairs in-line configurations

For PRW and PCRW VGs staggered configurations with one, two, and three pairs are shown in Figures 5. For one pair, the VGs are placed on the right side of the first row tube and the left side of the second row tube. VGs are placed on the right side of the first, third row tubes and on the left side of the second and fourth tubes for two pairs. As for the three pairs, the VGs are placed on the right side of the first, third, fifth row of tubes and on the left side of the second, fourth and sixth tubes.

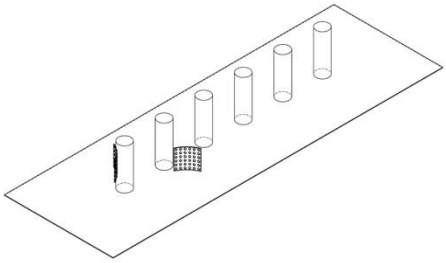

one pair PCRW staggered

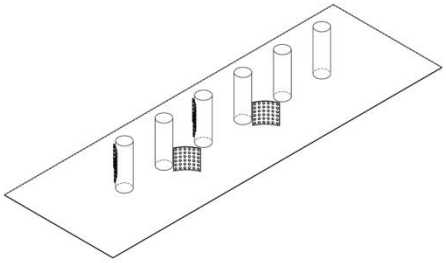

two pairs PCRW staggered

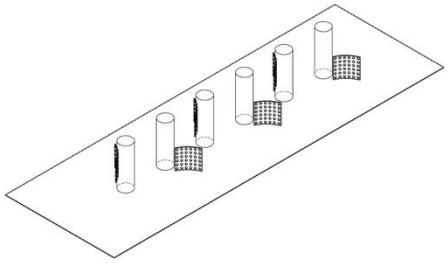

three pairs PCRW staggered

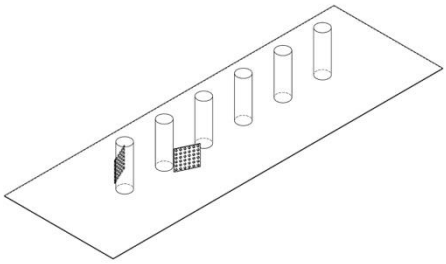

one pair PRW staggered

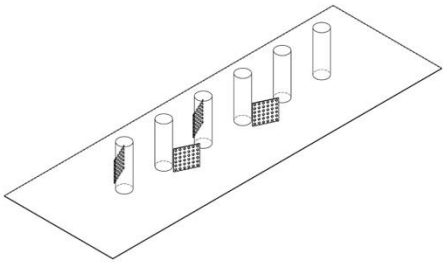

two pairs PRW staggered

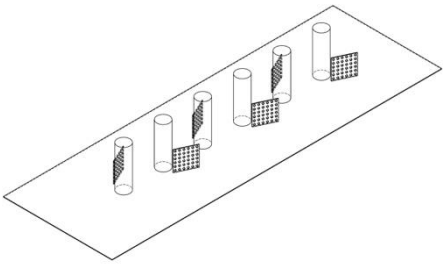

three pairs PRW staggered

Figure 5. VGs pairs staggered configurations

6. Thermal characteristics are given in terms of the convective heat transfer coefficient (*h*), friction characteristics are given in terms of pressure drop. Why are thermal characteristics not given in terms of Nusselt number (*Nu*) and friction characteristics in terms of coefficient of friction (*f)*?

   Thank you for your correction. *h* versus *Re* and *P* vs *Re* are used instead of *Nu* - *Re* and *f* - *Re* in this experiment because, in the TEF calculation, the value of *Nu* represents the value of *h* resulting from the equation in formula 3 (in the paper), thus

   $$h = \frac{N_u\, k}{D_h} \qquad (3)$$

   Figure 7 (in the paper) that *h* rises as *Re* rises shows that the *Nu* increases as *Re* rises, where *h* rises as *Re* rises [1]. While *f* in this experiment represents the ΔP as shown in the following formula

   $$f = \frac{2\,\Delta P\, D_h}{\rho\, V^2\, (L+6D)} \qquad (8)$$

   Formula 8 states that the friction factor *(f*) in the flow rate is determined by using the pressure drop (ΔP) characteristic where increasing the Reynolds number in figure 8 will decrease the friction factor [2].
   The following are examples of several studies that use *h* as a representative of *Nu* and (ΔP) as a representative of f.
   a. The experimental results of Yafid et al indicate that perforated VGs can increase the heat transfer rate and decrease the pressure drop using the parameters *h*, ΔP, and *TEF* as shown in the following graph[3].

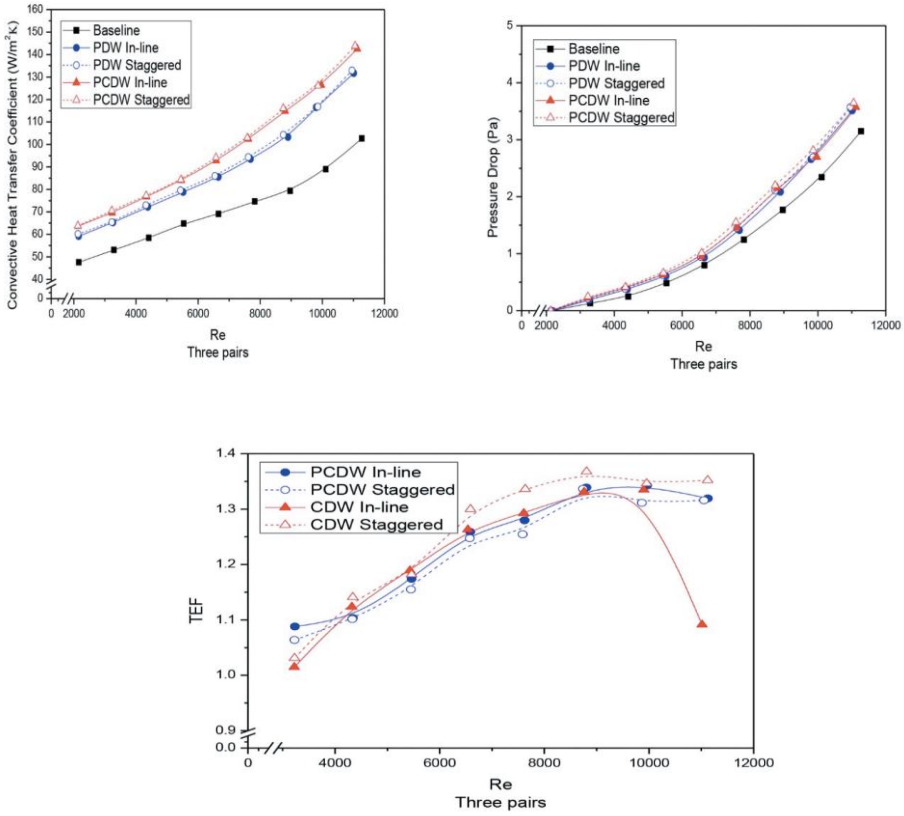

b. Al Asadi et al represents heat transfer coefficient and pressure drop to show the results of their investigation that the addition of span wise gap variations can increase heat transfer performance and reduce pressure drop [4], as shown in the figure below.

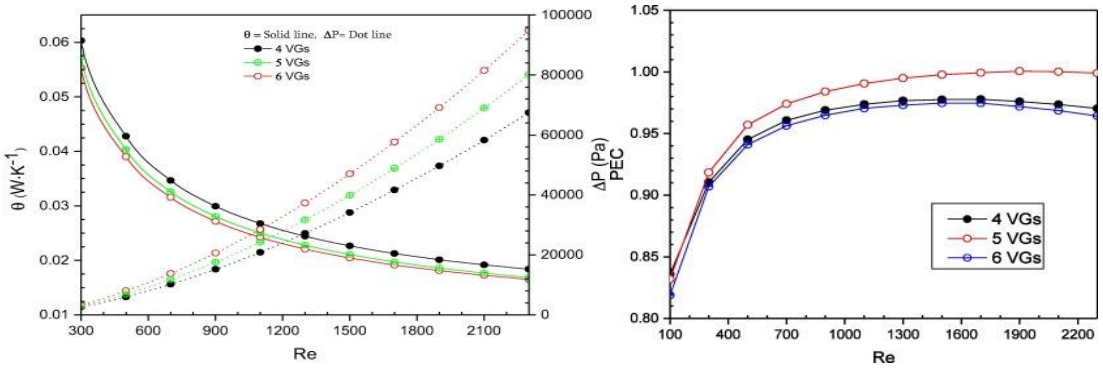

c. Increased heat transfer in heat sinks, Zhang et al described the micro gap by pairing more VGs which resulted in a larger heat transfer coefficient and a reduced pressure drop value [5], as shown in the figure below.

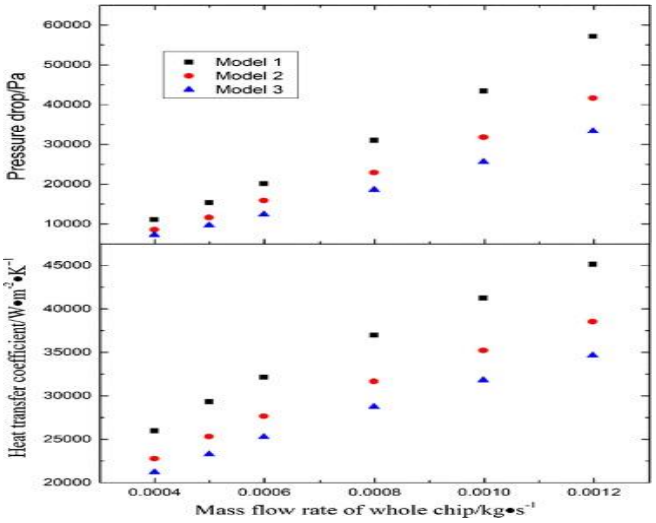

d. Hosseinirad et al showed that the increase in heat transfer coefficient and pressure drop vs. Reynold number had a tendency to increase with the increase in Re to evaluate heat transfer [6]. There is an increase in heat transfer with an increase in Re which is indicated by an increase in the heat transfer coefficient and an increase in pressure drop along with an increase in Re.

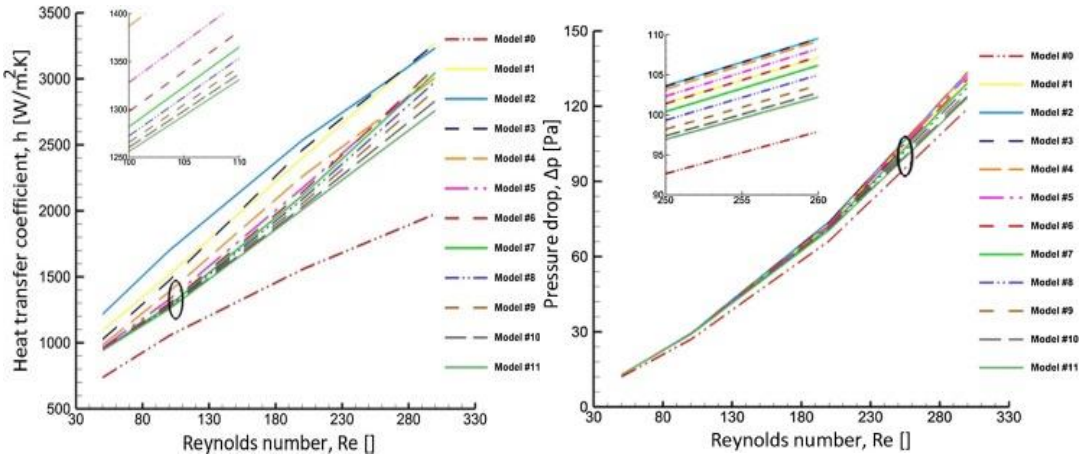

7. It is not specified how the hydraulic diameter (D_h) is calculated. How the Reynolds number (Re) was calculated is not specified.

Thank you for your corrections. The calculation of the hydraulic diameter in this experiment uses a rectangular air duct with a side length of a = 0.165 m and a side width of b = 0.064 m with the resulting D_h of 0.0106 from the following formula.

$$D_h = \frac{4A_c}{p} = \frac{4ab}{2(a+b)} = \frac{2ab}{a+b} \qquad (5)$$

The result of D_h is used to calculate *Re* with the formula

$$Re = \frac{\rho u_{in} D_h}{\mu} \qquad (7)$$

With u_{in} of 0.4 – 2 m/s with an interval of 0.2 m/s, on the physical properties of air at a pressure of 1 atm and is the viscosity of the fluid so that *Re* used in this experiment ranges from 2,143 – 11,763.

8. No correlation (Nu-Re), (f-Re) is given.

Thank you for the correction. In this experiment, Nu – Re and f – Re are not shown but use *h* vs *Re* and Δ*P* vs *Re* because the *Nu* value represents the value of *h* that arises in this experiment as in equation 4 (in the manuscript)

$$h = \frac{N_u\, k}{D_h} \qquad (3)$$

While *f* in this experiment represents the ΔP as shown in the following formula

$$f = \frac{2\,\Delta P\, D_h}{\rho\, V^2\, (L+6D)} \qquad (8)$$

The formula states that the friction factor *(f)* in the flow rate is determined by using the pressure drop (ΔP) characteristic where increasing the Reynolds number in figure 8 will decrease the friction factor [2].

9. Error analysis is given, but uncertainty analysis is not done.

Thank you for the correction. In the following, uncertainty analysis calculation data will be shown for the temperature at base line conditions with a velocity of 0.4 m/s as shown in Table 3 below.

Table 3 Base-line test temperature data at a speed of 0.4 m/s

T (Tube$_1$)	*T (Tube$_2$)*	*T (Tube$_3$)*	*T (Tube$_4$)*	*T (Tube$_5$)*	*T (Tube$_6$)*
49.19093	51.21368	48.32313	49.76915	47.80219	51.27142
49.1834	51.17728	48.3156	49.79053	47.7657	51.2639
49.14545	51.16826	48.30655	49.7526	47.7856	51.25489
49.12105	51.17277	48.28214	49.72821	47.76118	51.2594
49.15297	51.20465	48.28515	49.73122	47.73524	51.2624
49.09966	51.15141	48.28967	49.73573	47.76871	51.26691
49.09815	51.14991	48.23029	49.73423	47.73826	51.29428
49.08912	51.14089	48.25019	49.66739	47.72922	51.22751

From these data, it is found that $\overline{\boldsymbol{T}}_{\boldsymbol{Tube}}$ can be calculated by the equation as

$$\overline{\boldsymbol{T}}_{\boldsymbol{Tube}} = \frac{\overline{\boldsymbol{T}}_{\boldsymbol{Tube1}}+\overline{\boldsymbol{T}}_{\boldsymbol{Tube2}}+\overline{\boldsymbol{T}}_{\boldsymbol{Tube3}}+\overline{\boldsymbol{T}}_{\boldsymbol{Tube4}}+\overline{\boldsymbol{T}}_{\boldsymbol{Tube5}}+\overline{\boldsymbol{T}}_{\boldsymbol{Tube6}}}{\boldsymbol{6}} = \boldsymbol{49.56}℃ \quad (11)$$

Then, the average standard deviation is obtained by the following formula.

$$\boldsymbol{s}_{\boldsymbol{tube}} = \sqrt{\frac{\sum_{\boldsymbol{i=1}}^{\boldsymbol{N}}(\boldsymbol{T}_{\boldsymbol{tubei}}-\overline{\boldsymbol{T}}_{\boldsymbol{tube}})^{\boldsymbol{2}}}{\boldsymbol{N(N-1)}}} = \boldsymbol{0.029} \quad (12)$$

Therefore, the average T_{tube} can be written as 49.5 ± 0.029℃. $\overline{T}_{out}$ calculation results obtained 32.95℃. The average standard deviation was calculated using the following equation:

$$\boldsymbol{s}_{\boldsymbol{Tout}} = \sqrt{\frac{\sum_{\boldsymbol{i=1}}^{\boldsymbol{N}}(\boldsymbol{T}_{\boldsymbol{outi}}-\overline{\boldsymbol{T}}_{\boldsymbol{out}})^{\boldsymbol{2}}}{\boldsymbol{N(N-1)}}} = \boldsymbol{0,051} \quad (13)$$

Furthermore, the average value of T_{out} can be written as 32.95 ± 0.051℃. Using the same equation, the standard deviation of T_{in} was found to be 0.033. Thus, the average T_{in} value was 29.75 ± 0.016℃.

The value of q at a speed of 0.4 m/s was found to be 19.48 W. To determine of the standard deviation of q, the following equation was used:

$$RSS_q = \sqrt{\left(s(\Delta T_{out})\frac{\partial q}{\partial T_{out}}\right)^2 + \left(s(\Delta T_{in})\frac{\partial q}{\partial T_{in}}\right)^2} \quad (14)$$

$$\frac{\partial q}{\partial T_{out}} = \frac{\partial(m\cdot c_p\cdot T_{out} - m\cdot c_p\cdot T_{in})}{\partial T_{out}} = m\cdot c\cdot p$$

$$\frac{\partial q}{\partial T_{in}} = \frac{\partial(m\cdot c_p\cdot T_{out} - m\cdot c_p\cdot T_{in})}{\partial T_{in}} = -(m\cdot c\cdot p)$$

where $s(\Delta T_{out}) = 0.051$℃ and $s(\Delta T_{in}) = 0.033$℃, ensuring, that RSS_q= ± 0.290 W. Therefore, the heat transfer rate q becomes 19.48 ± 0.290 W. The value of ΔT_{lmtd} at a speed of 0.4 m/s was found to be 18.56℃. To determine the value of the standard deviation of ΔT_{lmtd} we used the following equation:

$$RSS_{\Delta T_{lmtd}} = \sqrt{\left(s(\Delta T_{tube})\frac{\partial(\Delta T_{lmtd})}{\partial T_{tube}}\right)^2 + \left(s(\Delta T_{out})\frac{\partial(\Delta T_{lmtd})}{\partial T_{out}}\right)^2 + \left(s(\Delta T_{in})\frac{\partial(\Delta T_{lmtd})}{\partial T_{in}}\right)^2} \quad (15)$$

$$\frac{\partial(\Delta T_{lmtd})}{\partial T_{tube}} = \frac{\partial\left(\dfrac{(T_{tube}-T_{out})-(T_{tube}-T_{in})}{\ln\dfrac{T_{tube}-T_{out}}{T_{tube}-T_{in}}}\right)}{\partial T_{tube}}$$

$$\frac{\partial(\Delta T_{lmtd})}{\partial T_{out}} = \frac{\partial\left(\frac{(T_{tube}-T_{out})-(T_{tube}-T_{in})}{\ln\frac{T_{tube}-T_{out}}{T_{tube}-T_{in}}}\right)}{\partial T_{out}}$$

$$\frac{\partial(\Delta T_{lmtd})}{\partial T_{in}} = \frac{\partial\left(\frac{(T_{tube}-T_{out})-(T_{tube}-T_{in})}{\ln\frac{T_{tube}-T_{out}}{T_{tube}-T_{in}}}\right)}{\partial T_{in}}$$

where $s(\Delta T_{tube}) = 0{,}029$℃, $s(\Delta T_{out}) = 0{,}051$℃ and $s(\Delta T_{in}) = 0{,}033$℃; we get $RSS_{\Delta T_{lmtd}}$ of ± 0.043, ensuring, that the obtained ΔT_{lmtd} is 8.56 ± 0.043.

The value of Nu at a speed of 0.4 m/s was found to be 155.31. The standard deviation of *Nu* was obtained using following equation

$$RSS_{Nu} = \sqrt{\left(s(q)\frac{\partial Nu}{\partial Q}\right)^2 + s(\Delta T_{lmtd})\frac{\partial Nu}{\partial \Delta T_{lmtd}}} \quad (16)$$

$$\frac{\partial Nu}{\partial q} = \frac{\partial\left(q \cdot D_h.At^{-1} \cdot {\Delta T_{lmtd}}^{-1} \cdot k^{-1}\right)}{\partial q} = \frac{D_h}{(At)(\Delta T_{lmtd})(k)}$$

$$\frac{\partial Nu}{\partial \Delta T_{lmtd}} = \frac{\partial\left(q \cdot D_h \cdot At^{-1} \cdot {\Delta T_{lmtd}}^{-1}.k^{-1}\right)}{\partial \Delta T_{lmtd}} = \frac{q.D_h}{(At)(\Delta T_{lmtd})^2(k)}$$

With the values of $s(q) = 0.290\ W$ and $s(\Delta T_{lmtd}) = 0.043$, the obtained RSS_{Nu} was ± 2.889 W/(m²°C). Therefore, the value of RSS_{Nu} is 155.31 ± 2.889 W/m²°C.

The value of h at a speed of 0.4 m/s was found to be 44.86. To determine the standard deviation of *Nu* the following equation is used

$$RSS_h = \sqrt{\left(s(Nu)\frac{\partial h}{Nu}\right)^2} \quad (17)$$

$$\frac{\partial h}{\partial Nu} = \frac{\partial(h.D_h.k^{-1})}{\partial h} = \frac{k}{D_h}$$

Furthermore, the value of D_h is 0.092 m and *k* at T_f = 40.24 is 0.026. So the value of h at a speed of 0.4 m/s is:

$$RSS_h = \sqrt{\left(s(Nu)\frac{\partial h}{Nu}\right)^2} = 0{,}83$$

Thus, the number *h* at a speed of 0.4 m/s is 44.86 ± 0.83. So, the error h for the baseline at a speed of 0.4 m/s is

$$Error = \frac{RSS_h}{h} \times 100 \quad (18)$$

$$Error = \frac{0.83}{44.86} \times 100 = 1.51\%$$

From the test in the baseline case with a speed of 2.0 m/s, the results of the pressure drop are listed in Table 4, which show that the average *P* can be calculated as follows:

$$\overline{\Delta P} = \frac{\Delta P_1 + \Delta P_2 + \Delta P_3 + \cdots + \Delta P_{30}}{30} = 3.51 \text{ Pa} \quad (19)$$

The average standard deviation of the pressure drop can then be calculated using the equation

$$s = \sqrt{\frac{\sum_{i=1}^{N} (\Delta P_i - \overline{\Delta P})^2}{N(N-1)}} = 8.9 \times 10^{-5} \quad (20)$$

Baseline case for the pressure drop value at a speed of 2.0 m/s is $3.51 \pm 8.9 \times 10^{-5}$Pa. Then, the error in the form of percentage can be calculated using the following equation:

$$\frac{8.9 \times 10^{-5}}{3.51} \times 100 = 0.71$$

Table 4 Baseline pressure drop data at a speed of 2.0 m/s

	ΔP (Pa)		
Data to	2.0 m/s	Data to	2.0 m/s
1	0.013	16	0.012
2	0.013	17	0.013
3	0.013	18	0.012
4	0.013	19	0.012
5	0.012	20	0.013
6	0.013	21	0.013
7	0.013	22	0.012
8	0.012	23	0.013
9	0.013	24	0.012
10	0.013	25	0.013
11	0.013	26	0.013
12	0.013	27	0.013
13	0.012	28	0.013
14	0.012	29	0.012
15	0.013	30	0.012

The equal calculation approach changed into used for all data. Therefore, the overall error outputs for the pressure-drop vortex generator with placement variations (in-line and staggered), *Re* and amount of VG sets (one, two and three) are listed in Table 5.

Table 5. Overall Pressure Drop (Δ*P*)

Vortex Generator Variations	*Overall Error P (perforated)*
1 PRWP *in-line*	2.94%
2 PRWP *in-line*	2.87%
3 PRWP *in-line*	1.98%
1 PRWP *staggered*	2.88%
2 PRWP *staggered*	2.34%
3 PRWP *staggered*	1.36%
1 PCRWP *in-line*	2.72%
2 PCRWP *in-line*	1.80%
3 PCRWP *in-line*	1.80%
1PCRWP*staggered*	2.43%
2PCRWP*staggered*	1.91%
3 PCRWP *staggered*	0.97%

The average TEF results from the experimental results can be calculated as follows.

$$\overline{TEF} = \frac{TEF_1+TEF_2+TEF_3+\cdots+TEF_{12}}{12} = 1.12 \quad (21)$$

Then, the average standard deviation of the TEF can be calculated with the equation

$$s = \sqrt{\frac{\sum_{i=1}^{N}(TEF_i-\overline{TEF})^2}{N(N-1)}} = 1.07 \quad (22)$$

Therefore, the TEF value was 1.12 ± 1.07. Then, the error in the form of percentage can be calculated using the following equation:

$$\frac{1.07}{1.12} \times 100 = 0.94\%$$

The overall error results for the TEF vortex generator with placement variations (in-line and staggered), *Re* and amount of VG sets (one, two and three) are are listed inTable 6.

Table 6. Overall error *TEF*

Variasi Vortex Generator	*Overall Error* TEF (Berlubang)
1 RWP *in-line*	0.47 %
2 RWP *in-line*	0.47%
3 RWP *in-line*	0.43%
1 RWP *staggered*	0.47%
2 RWP *staggered*	0.47%
3 RWP *staggered*	0.43%
1 CRWP *in-line*	0.45%
2 CRWP *in-line*	0.45%

3 CRWP *in-line*	0.42%
1 CRWP *staggered*	0.45%
2 CRWP *staggered*	0.45%
3 CRWP *staggered*	0.41%

First, find the average *CBR* of the experimental results with the following formula.

$$\overline{CBR} = \frac{CBR_1+CBR_2+CBR_3+\cdots+CBR_{12}}{12} = 2.14 \quad (23)$$

The average standard deviation of the pressure drop *CBR* can then be calculated using the following equation:

$$s = \sqrt{\frac{\sum_{i=1}^{N}(CBR_i-\overline{CBR})^2}{N(N-1)}} = 1.60 \quad (24)$$

The *CBR* value is 2.14 ± 1.60. Then the error in the form of percentage can be calculated using thefollowing equation:

$$\frac{1.60}{2.14} \times 100 = 0.63\%$$

The overall error results for the *CBR* vortex generator with placement variations (in-line and staggered), *Re* and amount of VG sets (one, two and three) are listed in Table 7

Table 7. Overall *error CBR*

Variasi Vortex Generator	*Overall Error* CBR (Berlubang)
1 RWP *in-line*	0.32%
2 RWP *in-line*	0.29%
3 RWP *in-line*	0.45%
1 RWP *staggered*	0.32%
2 RWP *staggered*	0.31%
3 RWP *staggered*	0.45%
1 CRWP *in-line*	0.4%
2 CRWP *in-line*	0.42%
3 CRWP *in-line*	0.56%
1 CRWP *staggered*	0.43%
2 CRWP *staggered*	0.42%
3 CRWP *staggered*	0.66%

Reference

[1] S. Caliskan, S. Şevik, and Ö. Özdilli, "Heat transfer enhancement by a sinusoidal wavy plate having punched triangular vortex generators," *International Journal of Thermal Sciences*, vol. 181, p. 107769, Nov. 2022, doi: 10.1016/J.IJTHERMALSCI.2022.107769.

[2] A. J. Modi and M. K. Rathod, "Comparative study of heat transfer enhancement and pressure drop for fin-and-circular tube compact heat exchangers with sinusoidal wavy and elliptical curved rectangular

winglet vortex generator," *Int J Heat Mass Transf*, vol. 141, pp. 310–326, Oct. 2019, doi: 10.1016/J.IJHEATMASSTRANSFER.2019.06.088.

[3] Y. Effendi, A. Prayogo, Syaiful, M. Djaeni, and E. Yohana, "Effect of perforated concave delta winglet vortex generators on heat transfer and flow resistance through the heated tubes in the channel," *Experimental Heat Transfer*, vol. 35, no. 5, pp. 553–576, 2022, doi: 10.1080/08916152.2021.1919245.

[4] M. T. Al-Asadi, F. S. Alkasmoul, and M. C. T. Wilson, "Benefits of spanwise gaps in cylindrical vortex generators for conjugate heat transfer enhancement in micro-channels," *Appl Therm Eng*, vol. 130, pp. 571–586, Feb. 2018, doi: 10.1016/J.APPLTHERMALENG.2017.10.157.

[5] J. F. Zhang, Y. K. Joshi, and W. Q. Tao, "Single phase laminar flow and heat transfer characteristics of microgaps with longitudinal vortex generator array," *Int J Heat Mass Transf*, vol. 111, pp. 484–494, Aug. 2017, doi: 10.1016/J.IJHEATMASSTRANSFER.2017.03.036.

[6] E. Hosseinirad, M. Khoshvaght-Aliabadi, and F. Hormozi, "Evaluation of heat transfer and pressure drop in a mini-channel using transverse rectangular vortex-generators with various non-uniform heights," *Appl Therm Eng*, vol. 161, p. 114196, Oct. 2019, doi: 10.1016/J.APPLTHERMALENG.2019.114196.

Reviewer 3: In connection with climate change and an increase in the average annual temperature on Earth, there is a new danger of the negative impact of high temperatures on human life.

In this case, the improvement of air conditioning systems, including the search for the best thermal enhancement factor, cost-benefit ratio, etc., takes on a new sense, which is one of the main targets of this article. The topic is timely and of great practical significance to environmental protection, enhancing safety, and people's life comfort.

The manuscript is well-structured and includes all necessary parts.

Two key strengths of the paper are a good introduction section and an analysis and discussion of the results. Both research objectives and content are clear. The key scientific issues to be solved are moderate. The research experimental method is reasonable.

There are also several shortages worthy to be mentioned:

1. Seriously revise the formulas
    a. If you use an italic font in formulas, use an italic font in their descriptions. For example, in formula (1), the Nusselt number (Nu) and friction factor (f); in formula (3), heat transfer coefficient (h). It may confuse the reader.

       Thank you for the corrections. For formula and description fonts, improvements have been made where all formula and description fonts are italicized consistently.

    b. The Nusselt numbers in formula (1) and formula (2) have different designations. It may confuse the reader.

       Thanks for the correction. Consistent improvements have been made to writing the *Nu* symbol on paper.

    c. What are Nusselt number and friction factor with subscript 0 in formula (1)?

       Thanks for the corrections. The subscript 0 for Nusselt number and friction factor is meant for the baseline condition. This additional explanation has been added to the paper. The following is an explanation of formula 1.

$$TEF = \frac{\left(\frac{Nu}{Nu_0}\right)}{\left(\frac{f}{f_0}\right)^{\frac{1}{3}}} \qquad (1)$$

       Di mana: Nu_0= Nusselt number pada kondisi baseline
       f_0 = friction factor pada kondisi baseline

d. In formula (5), a pressure drop is the lowercase letter Δp, but in formula (6), a pressure drop is uppercase ΔP. Are these different pressures?

Thank you for the corrections. I'm so sorry for the error in writing the pressure drop symbol which is inconsistent. Improvements in writing pressure drop have been made with uppercase *P* for the formula on the paper.

2. What is the error of pressure drop measurement with the Fluke 922 Airflow Micromanometer described in section "3.2 Effect of perforated vortex generators on pressure drop"? Did it cover the necessary range of pressures to be investigated? Could micromanometer error have affected the conclusions of the section? Because the pressure drop values of 4.58 Pa, 5 Pa and 5.4 Pa are close to each other.

Thanks for the question. Pressure measurement errors with the Fluke 922 Airflow Micromanometer are explained in the uncertainty analysis section with the calculation results as below.

From the test in the baseline case with a speed of 2.0 m/s, the results of the pressure drop are listed in Table 4, which show that the average *P* can be calculated as follows:

$$\overline{\Delta P} = \frac{\Delta P_1 + \Delta P_2 + \Delta P_3 + \cdots + \Delta P_{30}}{30} = 3.51 \text{ Pa} \quad (19)$$

The average standard deviation of the pressure drop can then be calculated using the equation

$$s = \sqrt{\frac{\sum_{i=1}^{N} (\Delta P_i - \overline{\Delta P})^2}{N(N-1)}} = 8.9 \times 10^{-5} \quad (20)$$

Baseline case for the pressure drop value at a speed of 2.0 m/s is $3.51 \pm 8.9 \times 10^{-5}$Pa. Then, the error in the form of percentage can be calculated using the following equation:

$$\frac{8.9 \times 10^{-5}}{3.51} \times 100 = 0.71$$

Table 4 Baseline pressure drop data at a speed of 2.0 m/s

	ΔP (Pa)		
Data to	2.0 m/s	Data to	2.0 m/s
1	0.013	16	0.012
2	0.013	17	0.013
3	0.013	18	0.012
4	0.013	19	0.012

5	0.012	20	0.013
6	0.013	21	0.013
7	0.013	22	0.012
8	0.012	23	0.013
9	0.013	24	0.012
10	0.013	25	0.013
11	0.013	26	0.013
12	0.013	27	0.013
13	0.012	28	0.013
14	0.012	29	0.012
15	0.013	30	0.012

The equal calculation approach changed into used for all data. Therefore, the overall error outputs for the pressure-drop vortex generator with placement variations (in-line and staggered), *Re* and amount of VG sets (one, two and three) are listed in Table 5.

Table 5. Overall Pressure Drop (ΔP)

Vortex Generator Variations	*Overall Error P (perforated)*
1 PRWP *in-line*	2.94%
2 PRWP *in-line*	2.87%
3 PRWP *in-line*	1.98%
1 PRWP *staggered*	2.88%
2 PRWP *staggered*	2.34%
3 PRWP *staggered*	1.36%
1 PCRWP *in-line*	2.72%
2 PCRWP *in-line*	1.80%
3 PCRWP *in-line*	1.80%
1 PCRWP *staggered*	2.43%
2 PCRWP *staggered*	1.91%
3 PCRWP *staggered*	0.97%

The results of the measurement error calculation are still below the maximum accuracy limit of the tool by 5% so that it does not affect the conclusion section.

3. The measurement error in the section "3.3 Effect of perforated VGs on thermal enhancement factor" and "Effects of perforated VGs on the cost-benefit ratio" is not clear. Can you show the error bar or describe it in the description?

   Thanks for the question. The measurement error for the thermal increase factor and the cost benefit ratio has been added to the explanation in the paper in the data uncertainty section, as follows.

   a. error bar TEF

   The average TEF results from the experimental results can be calculated as follows.

$$\overline{TEF} = \frac{TEF_1+TEF_2+TEF_3+\cdots+TEF_{12}}{12} = 1.12 \quad (21)$$

Then, the average standard deviation of the TEF can be calculated with the equation

$$s = \sqrt{\frac{\sum_{i=1}^{N}(TEF_i-\overline{TEF})^2}{N(N-1)}} = 1.07 \quad (22)$$

Therefore, the TEF value was 1.12 ± 1.07. Then, the error in the form of percentage can be calculated using the following equation:

$$\frac{1.07}{1.12} \times 100 = 0.94\%$$

The overall error results for the TEF vortex generator with placement variations (in-line and staggered), *Re* and amount of VG sets (one, two and three) are are listed inTable 6.

Table 6. Overall error *TEF*

Variasi Vortex Generator	*Overall Error* TEF (Berlubang)
1 RWP *in-line*	0.47 %
2 RWP *in-line*	0.47%
3 RWP *in-line*	0.43%
1 RWP *staggered*	0.47%
2 RWP *staggered*	0.47%
3 RWP *staggered*	0.43%
1 CRWP *in-line*	0.45%
2 CRWP *in-line*	0.45%
3 CRWP *in-line*	0.42%
1 CRWP *staggered*	0.45%
2 CRWP *staggered*	0.45%
3 CRWP *staggered*	0.41%

b error bar CBR

First, find the average *CBR* of the experimental results with the following formula.

$$\overline{CBR} = \frac{CBR_1+CBR_2+CBR_3+\cdots+CBR_{12}}{12} = 2.14 \quad (23)$$

The average standard deviation of the pressure drop *CBR* can then be calculated using the following equation:

$$s = \sqrt{\frac{\sum_{i=1}^{N}(CBR_i-\overline{CBR})^2}{N(N-1)}} = 1.60 \quad (24)$$

The *CBR* value is 2.14 ± 1.60. Then the error in the form of percentage can be calculated using thefollowing equation:

$$\frac{1.60}{2.14} \times 100 = 0.63\%$$

The overall error results for the *CBR* vortex generator with placement variations (in-line and staggered), *Re* and amount of VG sets (one, two and three) are listed in Table 7.

Table 7. Overall *error CBR*

Variasi Vortex Generator	*Overall Error CBR* (Berlubang)
1 RWP *in-line*	0.32%
2 RWP *in-line*	0.29%
3 RWP *in-line*	0.45%
1 RWP *staggered*	0.32%
2 RWP *staggered*	0.31%
3 RWP *staggered*	0.45%
1 CRWP *in-line*	0.4%
2 CRWP *in-line*	0.42%
3 CRWP *in-line*	0.56%
1 CRWP *staggered*	0.43%
2 CRWP *staggered*	0.42%
3 CRWP *staggered*	0.66%

4. In my humble opinion, the section "3.5 Flow visualisation" is better presented first in section "3. Results and Discussion".

   Thanks for the suggestions. The discussion of section 3.5 on visualization has been moved to the earlier section to 3.1 in the paper.

We tried our best to improve the manuscript and made some changes in the revised paper, and here we did not list the specific changes but marked in red in revised paper. We appreciate for Editors and Reviewrs' warm work earnestly, and hope that the correction will meet with approval. Once again, thank you very much for your comments and suggestions.

Yours Sincerely

Oktarina Heriyani